ASSESSMENT OF COLLATERALS IN ACUTE ISCHAEMIC STROKE USING CT IMAGING TECHNIQUES

Marta Guarisco

Submitted in partial fulfillment of the requirements for the Degree of Master of Science by Research

Institute of Neuroscience and Psychology
College of Medical, Veterinary and Life Sciences
University of Glasgow

March 2020

Contents

Abstract

There is growing evidence that the degree of collateral circulation in acute ischaemic stroke, and in particular of leptomeningeal collaterals, is a useful imaging marker that is correlated with various baseline and outcome clinical parameters. However, methods for assessing collaterals on acute ischaemic stroke are poorly standardized at present.

In the first part of this master thesis, an in-depth systematic review of methods for assessing collaterals published between 2009 and 2017 is presented. The review shows that although DSA is still used as gold standard, there has been a shift towards CT- and MR- based imaging modalities, which offer equal or higher sensitivity while being at the same time less invasive for the patient. In particular, CT seems to be a good candidate for replacing DSA as gold standard in the future and one scoring method proposed by Tan et al. has been widely adopted in recent studies. However, there has been zero or minimal progress towards a standardized method since previously published reviews.

In the second part of this thesis, a retrospective study conducted at the QEUH (Glasgow) to assess the reliability of collaterals on single-phase CTA is presented. CTA does not provide time-resolved information and this may lead to mislabeling of collaterals. The phase of acquisition of the scan should be taken into account when evaluating collaterals. From 4 past clinical trials, we identified patients with confirmed ICA or MCA occlusion. Three temporal-MIP images were reconstructed from CTP for each patient, each image corresponding to one of arterial, equilibrium and venous phase of contrast enhancement. Collateral scores were measured on both the temporal-MIP images and on single-phase CTA angiography and it was found

that there was substantial agreement between the scores if the CTA was acquired in the equilibrium phase but only moderate agreement if the CTA was acquired in the arterial or venous phase. This confirms that the arterial phase, despite being the preferred phase for assessing arterial occlusion and recanalization, is not the best phase for assessing collaterals and that a combination of CTA-CTP or a CTA scan employing a time-resolved protocol should be employed when evaluating collateral status in stroke patients.

List of Tables

List of Figures

Author's declaration

I declare that, except where explicit reference is made to the contribution of others, this thesis is the result of my own work and has not been submitted for any degree at the University of Glasgow or any other institution.

SIGNATURE:

List of abbreviations

ACA	Anterior cerebral artery
ACoA	Anterior communicating artery
AIS	Acute ischemic stroke
ASITN/SIR	American Society of Interventional and Therapeutic Neuroradiology/Society of Interventional Radiology
ASL	Arterial spin labeling
ASPECTS	Alberta Stroke Program Early CT Score
ATA	Arterial transit artifact
ATTEST	Alteplase-Tenecteplase Trial Evaluation for Stroke Thrombolysis
BA	Basilar artery
BTO	Balloon test occlusion
CBF	Cerebral blood flow
CBV	Cerebral blood volume
CE	Contrast-enhanced
CECT	Contrast-enhanced computed tomography
CF	Collateral flow
CIS	Capillary index score

CSF	Cerebrospinal fluid
CT	Computed tomography
CTA	Computed tomography angiography
CTP	Computed tomography perfusion
DCE T1-MRI	Dynamic contrast-enhanced T1-magnetic resonance imaging
DSA	Digital subtraction angiography
DSC-MRP	Dynamic susceptibility contrast-enhanced magnetic resonance perfusion
DWI	Diffusion-weighted imaging
ENI	Early neurological improvement
FLAIR	Fluid-attenuated inversion recovery
HT	Haemorrhagic transformation
HU	Hounsfield Unit
HV	Hyperdense vessel
HVS	Hyperdense vessel sign
IAT	Intra-arterial thrombolysis
ICA	Internal carotid artery
ICC	Inter-/Intra-class correlation coefficient
ICH	Intracranial hemorrhage
IV-FDCT	Intravenously enhanced flat-detector computed tomography
LCVF	Late phase cortical vein filling
LM	Leptomeningeal
LMC	Leptomeningeal collateral

LMF	Leptomeningeal flow
MASIS	Multicentre Acute Stroke Imaging Study
MCA	Middle cerebral artery
MIP	Maximum intensity projection
mp-CTA	Multi-phase computed tomography angiography
MPCT	Multiphasic perfusion computed tomography
MR	Magnetic resonance
MRA	Magnetic resonance angiography
MRI	Magnetic resonance imaging
MRP	Magnetic resonance perfusion
mRS	Modified Rankin Scale
mT-ASL	Multi-inversion arterial spin labeling
MTT	Mean transit time
NECT	Non-enhanced computed tomography
NIHSS	National Institutes of Health Stroke Scale
PCA	Posterior cerebral artery
pCASL	Pseudo-continuous arterial spin labeling
PCoA	Posterior communicating artery
POSH	POst Stroke Hyperglycaemia (study)
PSE	Perisylvian sulcal effacement
PWI	Perfusion-weighted imaging
QMRA	Quantitative magnetic resonance imaging
rFD	Relative filling time delay

rLMC	Regional leptomeningeal collateral
QEUH	Queen Elizabeth University Hospital
SCA	Superior cerebellar artery
SI	Source images
sp-CTA	Single-phase computed tomography angiography
TCD	Transcranial doppler
TIA	Transient ischaemic attack
TICI	Thrombolysis in cerebral infarction
TI-CTA	Time-invarant computed tomography angiography
TIMI	Thrombolysis in myocardial infarction
TI-MRI	Time-invariant magnetic resonance imaging
tMIP	Temporal maximum intensity projection
TOF-MRA	Time of flight magnetic resonance angiography
VA	Vertebral artery
VBA	Vertebro-basilar artery

Chapter 1

Introduction

1.1 Collaterals in acute ischaemic stroke

Stroke is a clinical syndrome given by an acute focal neurological deficit arising from a vascular problem. With about five and half million of deaths per year [8], stroke is the second leading cause of death worldwide [9] and the fourth in the UK (third in Scotland) [10].

Ischaemia is responsible for about 85% of all strokes in the UK [11]. Ischaemia is generally induced by a transient or permanent occlusion of a cerebral artery. The occlusion can be caused by a thrombus or embolus and can compromise the supply of a normal cerebral blood flow in the territory supplied by the affected vessel.

The phrase "time is brain" emphasizes the rapidity with which neurons are lost in the acute phase of ischaemic stroke, which is estimated to be around 1.9 million neurons/minute [12]. Due to the high demand for oxygen and glucose of cerebral tissues, a severe flow reduction quickly results into neurological death [13]. Normal cerebral blood flow (CBF) is around 50 to 60 mL/100 g tissue/min [14, 15]. If it drops under 10 mL/100g tissue/min, almost immediate damage is observed and infarcted tissue can appear within minutes. However, a reduced flow of 10-

20 mL/100g tissue/min has been shown to be sufficient to keep most neurons structurally intact, though not functional, for a limited period of time [15]. In the core of the ischaemic territory during acute stroke blood flow is often reduced to below 4-10% of normal levels. Thus, the core undergoes irreversible damage in the absence of prompt and adequate reperfusion. In the peripheral zones, instead, there is usually a certain amount of ischaemic but non infarcted tissue that is supported by collateral circulation and is potentially salvageable. This territory is commonly referred to as the ischaemic penumbra and its fate is determined by several factors, including the degree of ischemia and timing of reperfusion.

The main strategy for treating acute ischaemic stroke is revascularization, which is normally obtained via long-established intravenous thrombolysis (IVT) therapies with alteplase or more recent endovascular treatments such as intra-arterial thrombolysis and mechanical thrombectomy [16]. However, all the therapies so far available present different types of contraindications and are characterized by a loss of efficacy over time [17]. Administration of intravenous thrombolysis, for example, is recommended only up to 4.5 hours from symptoms onset and even with this precautionary requirement it does not always lead to successful revascularization and reperfusion [18, 19]. In their recent study, Bivard et al. showed that different factors, such as long onset to imaging time, large ischaemic core and lesion volume and symptomatic intracranial hemorrhage, are highly predictive of unacceptably poor outcome of thrombolysis treatment [19]. On the other hand recent trials have demonstrated the benefits of endovascular intra-arterial therapies (IAT) if performed within 6 hours from symptoms onset [16, 20]. In particular, the MR CLEAN study has shown improved clinical outcome of intra-arterial reperfusion therapies (IART) compared to the best medical care [21]. But IAT also has some pitfalls, such as the risk of complications secondary to endovascular manipulation [22]. Moreover, successful reperfusion following IAT might not automatically translate into improved outcome [23]. The risk of complications should always be balanced against the potential benefit on an individual case basis.

The best approach to endovascular treatment, including patient selection strategies, optimum device selection and outcome definitions are still being debated [24].

The availability of different therapeutic options makes it necessary to develop validated methods to help identifying when intravenous thrombolysis is likely to be futile but patients might benefit from newer more efficient treatments. When making decisions in acute ischaemic stroke (AIS) settings, clinicians have traditionally relied on clinical data such as the baseline National Institutes of Health Stroke Scale (NIHSS) score and time of symptoms onset. However, modern imaging technology now allows the inspection of extracranial arteries, extent of ischaemia and extent of infarcted core and penumbra, among other things. It is thus desirable to define imaging protocols which allow to evaluate neuroimaging markers with promptness, convenience, consistency and accuracy for diagnosis and prognosis in the acute stroke.

The extension of good collateral flow (CF) has been recently demonstrated to be an independent predictor of clinical outcome in acute ischaemic stroke [25, 26, 27]. Being often the only blood supply available to ischaemic territories, CF can be responsible for keeping the penumbra viable for a variable period of time. In particular, leptomeningeal (LM) collaterals have been shown to contribute to early neurological improvement (ENI) after stroke. Thus the signs of development of collateral on clinical images in the acute setting can help identify patients more likely to show ENI and be used to select patients for endovascular therapy [28].

Unfortunately there is not at present an optimal method for assessing collateral flow. The many grading systems reported in literature are poorly agreed [29] and they all require the subjective scoring by an experienced radiologist or stroke physician, which often results in a poor inter-observer agreement. Most of the proposed methods are restricted to the analysis of specific vessels or vascular territories. The majority of collaterals scoring system relies on time-consuming procedures and is therefore unsuitable for use in the clinical practice where time is critical.

There is a need to provide a collaterals scoring method that is, firstly, standardized and, secondly, automated, so as to enable a faster, more objective and more reliable assessment of collaterals in acute stroke decision making.

1.2 Assessment of collaterals with CT imaging techniques

Non-contrast computed tomography (CT) is the most widely available and used imaging modality for stroke patients because it is relatively fast to perform and allows to detect early ischaemic changes such a hypoattenuation, focal swelling and intracerebral haemorrhage [30]. However, non-contrast CT provides limited resolution in terms of vessel detection and is not suitable for assessing collaterals.

CT angiography (CTA) combines CT with an injection of contrast medium in the patient's circulatory system, therefore producing scans with enhanced blood vessels. CTA is also widely available in stroke centers, mostly due to the fact that it can be performed in combination with a CT scans without moving the patient and with minimal extra time [31].

CTA is normally performed with a volumetric helical scanner. A contrast medium is injected in the patient's circulatory system and the acquisition is timed such that the imaging either starts at a fixed time interval after the delivery of the bolus of contrast medium or is automatically triggered when the contrast concentration within a ROI reaches a pre-specified threshold. The ROI is generally centered around a point located in the ascending aorta.

One factor to keep in mind when performing CTA, is the phase of the scan. Once injected, the contrast medium is pumped into the circulatory system and flows through the arterial and venous apparatus. Depending on the starting time of acquisition, a CTA scan may be acquired in an arterial, a venous or an intermediate equilibrium phase wherein the amount of contrast in the arterial and venous vessels is comparable.

It is important in CTA that the scanning is performed while the vascular territory of interest exhibits the maximum enhancement. Often, CTA is performed in stroke patients to identify occlusions in major arterial branches or to assess reperfusion following thrombolytic therapy or thrombectomy and therefore it is configured to capture the arterial phase of the bolus flow cycle. However, some suggested that

since collaterals are measured in the affected hemisphere where it will be normal to have a slowed flow, they may be better assessed in the late venous phase, after the normal circulation is already washed out in the contralesional hemisphere [32]. A CTA scan acquired in an early arterial phase may show poor collaterals simply because the contrast medium has not reached the territory of interested yet.

Time-resolved imaging techniques enable analysis of the vasculature at multiple phases of contrast enhancement and therefore reduce the risk of mislabeling collaterals. Examples of time-resolved CT imaging techniques include multiphase CT angiography (mpCTA) and CT perfusion (CTP). Multiphase CTA is a variant of conventional CTA (hereinafter sometimes referred to as single-phase CTA or spCTA as opposed to mpCTA) in which three time-resolved three-dimensional images of the cerebral vasculature are provided. Each image captures a different phase of contrast enhancement: peak arterial phase, equilibrium/peak venous phase and late venous phase [33]. CT perfusion is a functional imaging technique which provides quantitative temporal information by acquiring multiple brain images in fast succession. The volume of interest is scanned repeatedly as the contrast medium flows through the vasculature thereby providing time resolved information about blood flow which can be used to reconstruct different types of perfusion maps. CTP clearly provide the most complete information however it requires post-processing and its interpretation is not as well understood as CT angiography. In contrast, CTA provides a fast and relatively easy to implement protocol but does not provide the temporal resolution of CTP and does not provide functional information.

1.3 Thesis objectives and contents

The Queen Elizabeth University Hospital (QEUH) is one of the main stroke centers in Scotland. At present, all patients arriving at the QEUH with suspected ischaemic stroke undergo CT examination and in some cases CTA, however time-resolved CT imaging or other time-resolved imaging are not included in the standard baseline assessment of stroke patients. Moreover, although collateral parameters have been

included in past research trials [34], they are not currently taken in consideration in the daily practice for the diagnosis/prognosis of stroke patients.

It would be desirable to provide a reliable tool for measuring collaterals, for use in the first instance in research trials but potentially also for future use in the daily clinical practice. However, there are two main hurdles to this task: the first one is that there isn't a standardized method for assessing collaterals. The second one is that at present time-resolved imaging is not part of the routine baseline triage/diagnosis of stroke patients at the QEUH and as seen above the phase of acquisition of CTA can play an important role in the assessment of collaterals.

Therefore the main objective of this thesis are:

- to conduct a systematic review of methods for assessing collateral vessels in acute ischaemic stroke;
- to evaluate the reliability of collaterals measured on single-phase CT angiography.

The remaining of this chapter is a brief overview of some scales used for assessing the clinical symptoms and outcome of patients affected by AIS which are mentioned in the following chapters. The second chapter is a systematic literature review of methods for assessing collaterals in AIS. The third chapter reports the methods and results of a retrospective study conducted by some members of the stroke team at the QEUH in order to assess the relation between collaterals measured in single-phase CTA and collaterals measure on MIP constructed from CT perfusion (CTP). The last chapter is a short commentary on the conclusions of this thesis and future work.

1.4 Overview of scales used in Stroke

This section is a very brief overview of some scales commonly used in the clinical practice in the assessment of stroke patients and to which reference will be made in the following chapters. More details on each scale are widely available in

literature.

The National Institute of Health Score (NIHSS) is the most commonly used baseline parameter to objectively quantify the impairment caused by a stroke. It comprises 11 grades that can be summarized as follows:

- 0: no stroke symptoms
- 1-4: minor stroke
- 5-15: moderate stroke
- 6-20: moderate to severe stroke
- 21-42: severe stroke.

The modified Ranking Scale (mRS) is the most commonly used parameter for assessing functional outcome and it relates to independence in the daily activities. It is mostly commonly assessed at 3 months after the stroke episode and it comprises 6 grades which can be summarized as

- 0-2: independent
- 3-6: dependent.

The Alberta stroke program early CT Score (ASPECTS) is a 10-point quantitative score measured on CT for middle cerebral artery stroke [35]. It is determined by segmenting the middle cerebral artery territory in 10 predefined regions and deducting 1 point from the initial score of 10 for each region involved. It is now well established that ASPECTS scores correlated with functional outcome at 3 months. In particular score ≤ 7 have been shown to predict worse outcomes.

The thrombolysis in myocardial ischemia (TIMI) score is a 4-point system for assessing vessel revascularization following arterial occlusion, each grade being defined as follows [36]:

- 0: no recanalization
- 1: minimal recanalization

- 2: partial recanalization
- 3: complete recanalization.

Lastly, the thrombolysis in cerebral ischemia (TICI) score is a 4-point system analogous to TIMI for assessing reperfusion following arterial occlusion [37]. The TICI scale is defined as follows:

- 0: no perfusion
- 1: penetration with minimal perfusion
- 2: partial perfusion
  - 2A: only partial filling of the entire vascular territory
  - 2B: complete filling of all the expected vascular territory but filling slower than normal
- 3: complete perfusion.

Chapter 2

Systematic literature review of methods for assessing collateral flow

2.1 Introduction

Collateral flow (CF) is the perfusion via alternative indirect pathways when the principal circulation of anterograde flow fails. In the first hours of an ischaemic stroke, collaterals can play a crucial role in determining the patient's outcome. The penumbral regions of the ischaemic territories are often supplied by a certain amount of collateral vessels whose quality strongly influences the rate at which the penumbra is converted into core. In presence of favorable collaterals, it is possible that the penumbra changes at a very slow rate, allowing in general for better clinical outcomes and for a potential extension of the therapeutical time-windows [25]. Many recent studies support the hypothesis of the aiding role of collaterals and demonstrated a significant correlation with outcome parameters. Among others, good collaterals have been linked to small-lesion volume on follow-up imaging and a favorable clinical outcome [1, 27], better response to intravenous thrombolysis [38] and reduced loss of penumbral tissue [39].

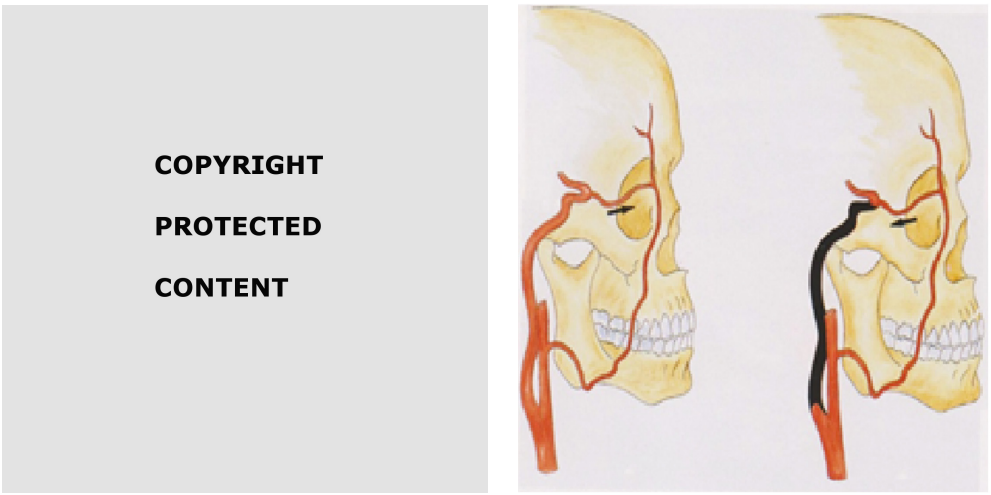

Figure 2.1: (a) Maximum intensity projection (MIP) magnetic resonance angiogram (MRA) showing collateral flow through the circle of Willis in a patient with right-sided ICA occlusions [4]. (b) Schematic representation of retrograde collateral flow from the ophthalmic branch of the external carotid artery after ICA occlusion [5], Copyright of Cambridge University Press 2016, reproduced with permission of The Licensor through PLSclear.

Figure 2.2: Axial (left) and coronal (right) MIP computer tomography angiography (CTA) showing leptomeningeal collateral blood flow from the posterior cerebral artery (arrows) to distal segments of the occluded middle cerebral artery [6].

There can be different sources of CF and depending on the location of the occlusion one or more of them may be recruited in acute ischaemic stroke. In a very basic classification we can distinguish between three main types of collaterals [40]: primary collaterals given by segments of the circle of Willis, large-artery communications between the extracranial and intracranial circulations and secondary CF through the leptomeningeal vessels. The circle of Willis (figure 2.1 (a)) consists of an anastomotic network connecting arteries from the anterior and posterior circulation as well as between the sides and therefore it represents a natural compensation mechanism in the presence of an occlusion in one of the parent vessels [41]. However, only $\sim 50\%$ of the individuals have been estimated to have a normal or complete configuration of the circle of Willis with both the posterior communicating arteries (PCoA) and an anterior communicating artery (ACA) [42]. The presence of any variant can compromise the ability of the circle of Willis to compensate for occluded vessels. The second class of collaterals includes the ophthalmic artery and the many branches that arise from the external carotid artery in the neck. These represent a potential source of CF in case of an occlusion of the internal carotid artery (ICA) [43] (figure 2.1 (b)). Finally, when primary CF flow through the circle of Willis or other large arteries has been exhausted or is not possible, e.g. in distal intracranial occlusions that are beyond the circle of Willis, leptomeningeal vessels might be recruited (figure 2.2). These are direct arteriole to arteriole connections of about 50-400 μm in diameter that join the terminal cortical branches of major cerebral arteries, such as ACA, middle cerebral artery (MCA) and posterior cerebral artery (PCA) forming a dense and very variable network in the leptomeninges [44, 41, 45]. Leptomeningeal collaterals allow for blood flow in both directions depending on the haemodynamic and metabolic need of the two territories that they connect and thus represent an important route for CF during a vascular occlusion [44].

Depending on the site of occlusion different collateral routes are recruited. For example in proximal ICA occlusion, i.e. occlusions which spare the carotid terminus, the circle of Willis offers potential for antegrade collateralization through the anterior and posterior communicating arteries, provided these are present and patent [45]. Alternatively, anastomoses between the extracranial arteries (ECA) and intracranial arteries can be recruited in proximal ICA occlusions, as mentioned

above. If the occlusion involves the carotid terminus instead the main channel for collateral supply, the circle of Willis, is cut off. In this case the ACA ipsilateral to the occlusion, if patent, can fill antegradely from the contralateral side, but there is no possibility of antegrade supply to the middle cerebral artery (MCA) territory. Leptomeningeal collaterals are the only resource for supplying the MCA territory through retrograde filling from the ipsilateral ACA or PCA. The same applies for occlusions of the M1 segment of the MCA or more distal segments, in which antegrade collateralization to the ischaemic territory is precluded. Quite interestingly, it has been shown that for MCA occlusions where only retrograde CF through leptomeningeal is possible, the more distal the MCA occlusion the more favorable the patient outcome [46]. This might be due to M1 occlusions also cutting out the lenticulostriate arteries, which are end arteries and thus can not be reached by retrograde collateral flow.

2.1.1 Leptomeningeal collaterals

Leptomeningeal collaterals are particularly interesting for researchers because unlike primary collaterals they are quite difficult to visualize and their properties are not completely understood yet. Many different studies suggested that leptomeningeal collateral flow (LMF) is highly predictive of better clinical and radiological outcomes after either intravenous or endovascular treatment of acute ischaemic stroke (table 2.1). Bang et al. showed that the state of pretreatment collaterals has a great impact on the recanalization rate after thrombolytic therapy. It was hypothesized that good collateral blood flow might allow thrombolytics to attack the thrombus from both sides. Moreover they showed that therapeutic revascularization did not result in better clinical outcome in patients with poor LMF [47]. Song et al. also showed that in patient with poor collaterals successful reperfusion was not significantly associated with favorable outcome and they inferred that time interval from imaging scan to reperfusion is particularly crucial in this group of patients. In fact collaterals affect the rate of penumbra loss and a rapid reperfusion might prove to be beneficial even in subjects with poor collaterals [48]. In another study, Christoforidis et al. showed that poor pial collaterals are associated with higher

incidence and size of hemorrhage following intra-arterial thrombolytic treatment [49].

LMF is therefore regarded by many as a good neuroimaging marker for decision making and collateral scores are being included in the imaging criteria for patient selection in an increasing number of studies. In the MR CLEAN trial [21] CF was the only imaging variable to significantly modify treatment response to endovascular therapy and in the ESCAPE trial [50] of endovascular thrombectomy it was one of the patient selection criteria. Moreover, recent findings on the role of CF in maintaining the penumbra during acute ischaemic stroke suggest that collateral flow enhancement might be considered as a therapeutic tool to support the reperfusion therapies in the treatment of acute stroke [51].

Yet the use of leptomeningeal collateral scoring in clinical practice and research trials is still very limited. We believe that one of the main limitations in the affirmation of collaterals as imaging marker is the fact that despite its now established importance there is not to date a standardized method for assessing LMF in acute stroke. The great variability in number, size and location makes it difficult to obtain consistent results from studies investigating the function of leptomeningeal vessels, with most works conducted on animals or post mortem [40]. Moreover, assessment of leptomeningeal vessels is not simple in humans since it can not rely on their direct visualization. Such small vessels are very difficult to capture on image and their assessment must rely on the indirect evaluation of the extent and rate of back-filling of pial arteries receiving blood flow from LMF [52] or on inference of their presence from surrogate markers such as modified blood flow velocity on transcranial doppler (TCD) [53].

Two recent systematic reviews of LM collaterals scoring systems have highlighted this issue [29] [54]. McVerry et al. [29] examined a total of 81 papers published up to 2009 and found 63 different scoring methods: 41 based on conventional digital subtraction angiography (DSA), 7 on computed tomography (CT), 9 on magnetic resonance (MR) and 6 on transcranial doppler imaging, with only 8 publications reporting inter- and/or intra-observer agreement. Martinon et al. [54] reported results from 48 publications up to 2013 (15 based on DSA , 14 on CT, 12 on MRI

Table 2.1: Main associations between collaterals and clinical outcome of acute stroke patients as reported in literature.

Better LPM collaterals	Poor LPM collaterals
Higher baseline ASPECTS score[55]	Higher and larger incidence of haemorrhage [46, 49]
Lower NIHSS score at presentation [27]	Large admission lesion size on MR-DWI [56]
Less infarct growth [57, 58, 27]	Infarct growth despite recanalization [57, 47]
Smaller final infarct volumes [59, 60, 61, 27]	Poor clinical outcome despite recanalization [57, 47, 62]
Improved patient outcomes [59, 58, 60, 61, 46, 55, 27]	Increased mortality [63, 64, 65]
Better recanalization [47] and reperfusion [66] after IAT	

and 3 on TCD) and concluded that at present dynamic CT angiography (CTA) seems to be the most appropriate method for collaterals evaluations, although MRI probably has a future due to its non-invasive quality, high sensitivity and continuous development of new techniques.

These two reviews offer a comprehensive picture of the main approaches up to 2013. However, with the constant advancements of imaging technologies and the new findings about the correlation of LMF with clinical outcome, we expected the number of publications now available discussing LMF assessment, whether using new or previously published scoring methods, to be significantly higher. We thus decided to perform an analogous systematic review to include publications between 2009-2016.

2.2 Materials and methods

2.2.1 Search strategy

The review was conducted on the Ovid online portal searching the MEDLINE database (with Revisions) from 1946 to April Week 2 2017 and the Embase database from 1996 to 2017 week 17. The search strategy (see Appendix 1) was devised in

order to match papers treating a combination of three macroareas: ischaemic stroke, collateral circulation and imaging. The keywords were selected by consulting the MeSH database and including all relevant synonyms.

All studies published in English, performed in adult humans and dated on or after 1 Jan 2009 were initially included . The target population included patients with acute stroke (<24 h from onset) or patients with cerebrovascular disease who had CF assessed at some point. Terms such as "pial/cortical anastomoses/collateral" were considered synonyms of leptomeningeal collaterals. The final search strategy was optimized to respect these inclusion criteria and run on MEDLINE and Embase on 12/04/17. The publications found on Ovid were then filtered based on relevance to the topic. In the first passage, the studies were discarded based on titles alone. The remaining papers were then inspected for relevant abstracts Finally, the last group of papers was filtered based on full-text review. Studies that did not describe the imaging assessment method were excluded. All publications which only evaluated primary collateral flow but not LMF (e.g. through the circle of Willis or via the ophthalmic artery) were also excluded from the analysis. All publications regarding Moyamoya disease were rejected since the leptomeningeal collateral flow observed in this condition is considered different from collaterals in stroke for development, recruitment and flow dynamics. Some additional publications were included following inspection of citations of all relevant articles in the initial search. Conference abstracts were not excluded a priori but eventually none was included for lack of complete information on the assessment method.

2.2.2 Data extraction

For each study we recorded

- site of occlusion: (if applicable)
- imaging modality: DSA, CT, MRI, TCD
- assessment criteria
- grading scale: number and definition of grades (if applicable)

- clinical setting: acute/non acute
- reliability: whether inter and intra-observer agreement was assessed
- prognostic value: correlation with outcome parameters.

Methods with similar imaging modalities but different grading scales were considered as different scoring methods. The clinical setting was considered acute if collaterals were assessed within 24 h from stroke/transient ischaemic attack (TIA) symptom onset, whereas non-stroke studies (e.g. chronic cerebrovascular disease) or AIS cases assessed >24 h from symptom onset were considered as non-acute. Papers stating that two or more raters were reaching an agreement by consensus or that reported independent scoring by two readers but did not indicate any inter-rater coefficient, were considered as not having reliability assessed (NS=not-stated). In studies with automated scoring methods reliability was marked as not applicable (NA). Similarly, when the outcome was not assessed because the study was focused on comparing different imaging modalities or on evaluating the correlation with other imaging parameters, the prognostic value was marked as not applicable, whereas if outcome was assessed but the correlation with collaterals was not indicated, it was marked as not stated (NS).

2.3 Results

2.3.1 Overview

MEDLINE and EMBASE searches yielded 9264 and 16199 publications respectively, for a total of 25463 publications. The results were imported in Endnote and after automated filtering for duplicates, 18253 items were inspected for the systematic review. After filtering titles, 1541 publications were retained for abstract review. After filtering abstract, 1225 further publications were discarded and 316 kept for full-text review. Among the discarded ones, 85 were excluded because they only discussed primary collaterals, 11 because it was not possible to retrieve the full-text, 12 because they scored collaterals without describing the scoring method and the

remaining ones because not relevant. After full-text inspection, 233 publications were retained for analysis. In addition, 15 papers from bibliographies of relevant publications were found to be relevant and included in the review. In total 248 papers and 93 different criteria for grading LMF were recorded (table 2.2).

Thirty-two of the publications discussed assessed collaterals on two (n=30) and three (n=2) different imaging modalities (DSA, CT, MRI, TCD). Fifty-two publications compared 2 or more assessment criteria/grading scales, either on the same imaging modality or different imaging modalities. No PET/SPECT based methods were recorded and only one TCD-based method was recorded, from a paper by Levi et al. [53]. In principle the presence, responsiveness and capacity of collaterals can be indirectly inferred also from flow or metabolic indices measured on PET/SPECT. In practice, the search yielded very few studies using TCD/PET/SPECT for LM assessment and none of these met the inclusion criteria apart from Levi's paper. TCD provides little information about CF and only at the circle of Willis. It is well suited for identifying collateralization in MCA occlusions where blood flow is diverted from the distal ICA to ACA. In this case there is usually a flow with higher velocity in the ipsilateral ACA as compared with the contralateral ACA. This difference can be measured on TCD and used as surrogate marker for presence of good collaterals [53]. By using this methods, Levi showed that the presence of ACA flow diversion (FD) detected on TCD is strongly associated with improved LMC and independently associated with 24 h infarct volume and modified Rankin Scale (mRS) at 3-months.

CT is the modality with the highest number of publications (n=128) and different methods (n=40) followed by conventional angiography and MRI. DSA is the modality with the highest standardization with "only" 27 methods in 108 publications, while MRI is the least standardized with 30 different methods in 46 publications.

It was not possible to determine excatly how many patients had collaterals assessed with each modality, because in some instance multiple papers discussed cases from the same study. However, publications assessing collaterals on DSA and CT generally had much higher number of cases per study. The total number of

patients who had collaterals assessed by DSA and CTA is 4-5 times higher than the number of patients who had collaterals assessed by using MR-based imaging modalities.

Almost all the studies assessed collaterals in acute stroke/TIA within 24 hours from symptom onset (n=219) while 9 studies looked at mixed acute/non acute cases, 5 studies did not state the time of measurement clearly, 1 had clinical setting NA and 14 studies looked at stroke/TIA cases >24 h after symptom onset or other pathologies. Eighty-one publications had reliability assessed for inter- and/or intra-observer agreement. In two cases reliability was not assessed because the scoring method was fully computational [67, 68] and in the remaining publications (n=165) the reliability was not assessed/reported. Over half of the studies (n=142) reported correlation of collaterals with clinical outcomes. Among the remaining publications, 19 failed to prove correlation between collaterals and outcomes, 1 showed mixed positive/negative correlation between collaterals and good outcomes, 27 did not state whether there was a correlation and 59 did not have outcomes available, since they were investigating other parameters or correlation between different modalities.

Details of each recorded method are reported in tables 2.3, 2.6, 2.9 for DSA, CT and MRI respectively and discussed below. Note that often two or more publications reported data regarding a common study and consequently the same patients, thus the numbers in the table are only indicative. It was not possible to determine which and how many patients had been assessed multiple times. In the studies that included both Moyamoya and non-Moyamoya patients ([69, 70]), only the non-Moyamoya have been considered towards the count. Among the assessed patients, 756 were control cases that were included for collateral analysis in three separate publications by Maas et al., 2009 [71] (235 control patients, CTA-based assessment), Qu et al, 2016 [72] (406 control cases, DSA-based assessment) and Zou et al.[73] (115 control cases, DSA-based assessment).

Table 2.2: Overview of the systematic review's results, showing for each modality how many methods were found, how many publications, how many patients were assessed by using each modality (see table footnote), how many publications dealt with studies performed in acute settings, how many assessed reliability and how many found a correlation between collaterals and clinical outcomes. Note that the line for "All" publications is not the sum of the above lines because many papers discussed ≥2 imaging modalities/scoring methods.

Imaging type	Methods	Publ.	N. of patients	Acute setting	Assessed reliability	Corr. w/ outcome
DSA	27	108	13001*	88	21	60
CT	40	128	16851*	121	50	79
MRI	30	46	3272*	35	20	21
TCD	1	1	53	0	0	1
All	93	248	30857*	219	81	142

*Estimate. In some instances multiple paper regarding the same studies have been identified and it is not possible to determine the correct number of overlapping cases.

2.3.2 Collaterals assessment with catheter angiography

DSA is still considered as the gold standard for measuring collaterals. A total of 108 publications had LM collaterals assessed by 27 different criteria using DSA. 88 assessed collaterals in acute stroke/TIA, 5 assessed a mix of acute/non acute stroke patients with ICA and/or MCA stenosis/occlusion [70, 74, 75, 76, 77], 3 studies did not report the time from symptom onset [78, 79, 72], 1 study assessed LM collaterals in patients undergoing balloon test occlusion (BTO) of ICA for aneurysm/dissection [80] and 11 assessed non-acute patients with minor symtomatic/asymptomatic TIA, retinal ischemia, atherosclerotic or non atherosclerotic intracranial stenosis in the ICA, MCA, vertebral artery (VA), basilar artery (BA) or vertebro-basilar artery (VBA) [81, 82, 83, 84, 85, 86, 87, 88, 67, 69, 89, 73].

Six publications reviewed collateral flow for posterior circulation occlusion only [90, 91, 82, 92, 93, 94], while the remaining assessed collaterals in anterior circulation alone or in both anterior and posterior circulation.

One method (n. 4, ASITN/SIR scale) had both inter/intra-rater agreement as-

sessed in one publication ([95], k_{inter}=0.872, k_{intra}=0.994) and only inter-observer agreement assessed in the rest of the studies where it was adopted (10 papers, [96, 47, 97, 39, 98, 79, 87, 99, 100, 73]). One method (8) had only intra-observer agreement assessed (2 publications, k=0.81 [49, 101]), 4 methods (n. 1, 6, 21, 27) had only inter-observer agreement assessed (5 publications, [102, 91, 103, 104, 105]) and the rest did not have reliability assessed. Where reported, the reliability was assessed using Cohen's kappa coefficient (k) and the resulting agreement was good (0.60<k<0.80) or very good (0.80<k<1). If not specified in the subscript, the k coefficient is always referred to inter-rater agreement (as opposed to intra-rater agreement).

The most commonly reported scoring method on DSA is the American Society of Interventional and Therapeutic Neuroradiology/Society of Interventional Radiology scale (ASITN/SIR), n. 4 in table 2.3, which appears in 56 publications. This scale consists of 5 grades assigned based on the number and rapidity of collaterals vessels [37]. The second most frequent scale, adopted in 8 publications, was proposed by Christoforidis et al. [61] and is based on the extent of retrograde contrast opacification of vessels within the occluded territory on delayed images. Arnold et al. (method 3), proposed a simpler classification with only poor and good collaterals, based on the extend of LM anastomoses in the occluded territory (more/less than half) [63, 46, 64, 65, 106, 107, 108]. None of the publications assessed reliability. One grading method (n. 22 table 2.3), first reported by Qureshi et al. and found in 5 publications, assigned scores based on the angiographic appearance of occlusion and incorporating both anatomic sites and collateral pathways to the affected region. None of the publications using this method and included in the systematic review assessed the reliability, although a study published before 2009 showed good inte-observer reliability (k=0.73), as reported in McVerry's systematic review [29]. Ali et al. proposed to divide the ischaemic area in 3 equal parts and score each with 0-1 depending on the capillary blush, then obtain a capillary index score (CIS) by summing the individual values [109, 110, 111, 112, 103]. The reliability for this method (n.1 in table 2.3) was tested only in one publication with 2 raters and resulted in an inter-rater agreement of k=0.73 [103].

All remaining methods were reported only in 3 or fewer publications. Among

these, 5 scoring systems classified collaterals only qualitatively, based on different criteria: patency of specific vessels (n. 36), good/poor visualization of filling in superior cerebellar artery (SCA) (n. 12), extent of cortical branches (n. 38), primary/secondary collaterals (n. 7) or antegrade/retrograde flow (n. 20). One paper reported a quantitative collateral measurement with no explicit grading based on the time that contrast agent takes to reach its peak value in the target downstream territory and the maximum contrast intensity within the duration of DSA acquisition (n. 37). The remaining methods proposed various scales, with number of grades varying from 3 to 6, based on either the absolute number of individual leptomeningeal vessels visualized at angiography, the anatomic extent and/or rapidity of vessel filling, or a combination of the two.

In 25 papers angiographically defined collaterals were compared with collaterals assessed on one or more other modality. Eight papers compared DSA with CT-methods [70, 113, 114, 91, 115, 58, 95, 87]. All papers reported good agreement between the different modalities, apart from two cases. Shin et al., compared DSA with both CTA-source images (CTA-SI) and dual-phase CTA and found that DSA-collaterals agreed well with those assessed on dual-phase CTA but less with those assessed on CTA [116]. Sung et al. found no significant correlation between DSA-defined collaterals and CTA-defined collaterals and showed the CTA defined collaterals were better associated with outcome [117]. Fifteen papers compared DSA with MR methods, of which 6 were looking at hyperdense vessel sign (HV sign or HVS) on fluid-attenuated inversion recovery (FLAIR)-MRI [118, 83, 74, 75, 79, 119] and 9 at other MR-based parameters, such as dynamic contrast enhanced (DCE) T1-MRI [70], dynamic susceptibility contrast enhanced MR perfusion (DSC-MRP) [32, 120], DSC diffusion-weighted imaging (DWI) [121], MR perfusion-weighted imaging (PWI) [99], contrast enhanced MR angiography (CE-MRA), time-of-flight MR angriography (TOF-MRA) [122], 3D pseudo-continuous arterial spin labeling (pCASL) [67], arterial transit artifact (ATA) from ASL-MR [69] (for patients with non atherosclerotic intracranial stenosis only) and 3D multi-inversion time ASL (mTI-ASL) [89]. One study [123] found that HV sign on FLAIR-MRI was associated with angiographic collaterals but the meaning differed depending on perysilvian sulcal effacement (PSE) status: if PSE was present, absence of HV was associated

with poor collaterals, while in absence of PSE, absence of HV was associated with good collaterals. In all these cases DSA compared well with the other modalities. In a study by Pop et al. [105] collaterals were assessed as HV on FLAIR imaging to select patients and then measured on DSA, but the two modalities were not compared. Three studies [124, 125, 94] used a mix of different modalities to assess collaterals based on what scans the patients had available, but did not compare them.

Table 2.3: DSA-based scoring methods for LM collaterals.

	Description	Grades	First author, year (Cases)	Acute/ Non acute	Reliability assessed	Prognostic value
1	Capillary blush in ischaemic area receiving retrograde flow through pial collaterals or very late antegrade flow	0-3, dichotomized in poor (0,1) vs favorable (2,3)	Ali, 2013 [109] (26)	Acute	No	Beneficial
			Ali, 2014 [110] (28)	Acute	No	Beneficial
			Ali, 2015 [111] (78)	Acute	No	Beneficial
			Fahed, 2016 [112] (62)	Acute	No	No effect
			Labeyrie, 2016 [103] (146)	Acute	Yes, k=0.73	Beneficial
2	Retrograde filling of BA and superior cerebellar artery and presence of bilateral anastomoses of cerebellar arteries or PCAs	Qualitative classification in 4 types, no scores	Alqadri, 2013 [90] (24)	Acute	No	Beneficial
3	LM anastomoses in the occluded territory filling by less/more than half	Poor vs Good	Arnold, 2014 [63] (389)	Acute	No	Beneficial
			Galimanis, 2012 [46] (623)	Acute	No	Beneficial
			Jung, 2012 [64] (24)	Acute	No	Beneficial
			Luedi, 2014 [65] (1000)	Acute	No	Beneficial
			Meyer, 2009 [106] (1000)	Acute	No	Beneficial
			Mono, 2012 [107] (567)	Acute	No	Beneficial
			Verma, 2014 [108] (33)	Acute	No	Beneficial
4	Rapidity and extent of retrograde collateral flow (ASITN/SIR)	0-4	Bang 2011, [96, 47] (222)	Acute	Yes, k=0.896	Beneficial
			Brekenfeld, 2009 [126] (12)	Acute	No	NA

– continues on next page –

Table 2.3 – continued from previous page

Description	Grades	First author	Acute/ Non acute	Reliability assessed	Prognostic value
		Chen, 2015 [113] (75)	Acute	No	Beneficial
		Cohen, 2013 [127] (31)	Acute	No	NS
		He, 2013 [82] (21)	Non acute	No	NA
		Hwang, 2015 [97] (207)	Acute	Yes, k-0.864	Beneficial
		Hwang, 2016 [128] (163)	Acute	No	Beneficial
		Imai, 2011 [129] (90)	Acute	No	No effect
		Jeong, 2014 [130] (141)	Acute	No	Beneficial
		Jeong, 2015 [131] (134)	Acute	No	Beneficial
		Jung, 2013 [39] (44)	Acute	Yes, k=0.636	Beneficial
		Khatri, 2014 [132] (240)	Acute	No	Beneficial
		Kim, 2009 [133] (41)	Acute	No	NA
		Kim, 2011 [134] (149)	Acute	No	NA
		Kim, 2011 [123] (96)	Acute	No	NA
		Kim, 2012 [95] (54)	Acute	Yes, k_{inter}=0.872, k_{intra}=0.994	NA
		Kim, 2014 [32] (134)	Acute	Yes, k=0.80	Beneficial
		Kurre, 2016 [135] (73)	Acute	No	NS
		Lau, 2012 [78] (69)	NS	No	Beneficial
		Lee, 2014 [98] (104)	Acute	Yes, k=0.821	NA
		Lee, 2015 [136] (98)	Acute	No	NA
		Lee, 2015 [120] (66)	Acute	No	Beneficial
		Liebeskind, 2011 [85] (287)	Non acute	No	NA
		Liebeskind, 2011 [86] (287)	Non acute	No	Beneficial

– continues on next page –

Table 2.3 – continued from previous page

Description	Grades	First author	Acute/ Non acute	Reliability assessed	Prognostic value
		Liebeskind, 2014 [66] (276)	Acute	No	Beneficial
		Liebeskind, 2014 [137] (119)	Acute	No	Beneficial
		Liebeskind, 2016 [138] (119)	Acute	No	NA
		Liu, 2014 [76] (103)	Mixed	No	No effect
		Liu, 2016 [79] (101)	NS	No	NS
		Liu, 2016 [87] (35)	Non acute	Yes, k=0.090	NS
		López-Cancio, 2014 [88] (136)	Non acute	No	NA
		Lyu, 2015 [67] (21)	Non acute	No	NA
		Marks, 2014 [139] (60)	Acute	No	Beneficial
		Nicoli, 2014 [99] (57)	Acute	No	Beneficial
		Olivot, 2014 [140] (56)	Acute	No	Beneficial
		Park, 2014 [77] (98)	Mixed	No	NS
		Park, 2015 [141] (37)	Acute	No	Beneficial
		Park, 2016 [142] (105)	Acute	No	NS
		Pereira, 2013 [143] (202)	Acute	No	Beneficial
		Potreck, 2017 [121] (47)	Acute	No	NS
		Sanossian, 2009 [119] (74)	Acute	No	NA
		Sanossian, 2011 [144] (102)	Acute	No	NA
		Seet, 2012 [125] (21)	Acute	No	Beneficial
		Sheth, 2016 [145] (117)	Acute	No	Beneficial
		Shi, 2010 [146] (159)	Acute	No	No
		Shimoyama, 2013 [100] (93)	Acute	Yes, k=0.817	Beneficial
		Shin, 2014 [116] (43)	Acute	No	Beneficial

– continues on next page –

Table 2.3 – continued from previous page

	Description	Grades	First author	Acute/ Non acute	Reliability assessed	Prognostic value
			Singer, 2015 [93] (124)	Acute	No	Beneficial
			Singer, 2015 [147] (160)	Acute	No	Beneficial
			Spiessberger, 2015 [148] (38)	Acute	No	NA
			Sung, 2015 [117] (30)	Acute	No	Beneficial
			Verma, 2015 [149] (74)	Acute	No	Beneficial
			Wen, 2016 [150] (18)	Acute	No	Beneficial
			Wu, 2016 [89] (25)	Non acute	No	NA
			Zou, 2013 [73] (211)	Non acute	Yes, k=0.4-1	NA
5	Extent of anterograde and retrograde vessel filling	Absent, minimal, moderate, maximal	Jung, 2011, [92] (106)	Acute	No	Beneficial
			Liebeskind, 2011 [85] (287)	Non acute	No	NA
6	Extension and stasis of retrograde reperfusion in cortical ACA-MCA territories	0-5	Consoli, 2016 [102] (103)	Acute	Yes, k=0.83	Beneficial
			Mangiafico, 2013 [151] (57)	Acute	No	Beneficial
			Mangiafico, 2014 [152] (103)	Acute	No	Beneficial
7	Qualitative classification in primary (AcoA, PCoA) and secondary (ophthalmic, LM)	Primary vs Secondary	Cheng, 2012 [81] (38)	Acute	No	NA
8	Extent of retrograde contrast opacification within occluded territory on delayed angiographic images	1-5	Christoforidis, 2009 [49] (104)	Acute	Yes, k_{intra}=0.81	Beneficial
			Christoforidis, 2010 [153] (67)	Acute	No	Beneficial
			Christoforidis, 2011 [101] (112)	Acute	Yes, k_{intra}=0.81	Beneficial
			Flores, 2015 [115] (81)	Acute	No	Beneficial
			Khatri, 2011 [154] (16)	Acute	No	NA
			Lazzaro, 2011 [155] (104)	Acute	No	NA
			Ribo, 2011 [156] (61)	Acute	No	Beneficial

– continues on next page –

Table 2.3 – continued from previous page

	Description	Grades	First author	Acute/ Non acute	Reliability assessed	Prognostic value
			Sargento, 2012 [157] (118)	Acute	No	Beneficial
9	Ratio between parenchyma supplied by collaterals and area that should be supplied by thrombosed vessel	Poor, fair, good	Cohen, 2012 [158] (17)	Acute	No	Beneficial
10	Leptomeningeal filling of MCA vasculature distal to the occlusion	0-3	Ernst, 2015[122] (44)	Acute	No	NA
11	Extent of retrograde contrast opacification within occluded territory on delayed angiographic images	1-4	Finistis, 2014 [22] (25)	Acute	No	No
12	Posterior circulation: visualization of filling of SCA; anterior circulation: extent of filling of occluded territory	Poor vs good	Qu, 2016 [72] (800)	NS	No	NA
13	Extent of collateral supply in occluded territory compared to contralateral side	Poor, moderate, good	Arnold, 2015 [159] (464)	Acute	No	Beneficial
			Gratz, 2014 [160] (226)	Acute	No	Beneficial
14	Contrast filling of ACoA, PCoA, or ophthalmic arteries	0-3	Sato, 2014 [80] (31)	NA	NA	NA
15	Extent of contrast filling in occluded territory	1-3	Drewer-Gutland, 2015 [161] (155)	Acute	No	No
			Hesselmann, 2012 [58] (31)	Acute	No	Beneficial
16	Retrograde contrast opacification of vessels within occluded territory on delayed angiographic images	1-3	Huang, 2012 [118] (29)	Acute	No	NS
17	Filling extent of at risk territory in 15 ASPECTS areas	0-3	Chen, 2015 [70] (7)	Mixed	No	NS
			Roach, 2016 [69] (11)	Non acute	No	NA
18	Extent of retrograde flow in MCA	Poor vs Good	Gasparotti, 2009 [162] (27)	Acute	No	NS

– continues on next page –

Table 2.3 – continued from previous page

	Description	Grades	First author	Acute/ Non acute	Reliability assessed	Prognostic value
19	Visual inspection of anterior circulation and LM collaterals	Poor, moderate, good	Lescher, 2015 [124] (39)	Acute	No	Beneficial
20	Provenience of flow on DSA	Antegrade, retrograde	Liu, 2011 [74] (233)	Mixed	No	NA
			Liu, 2012 [75] (11)	Mixed	No	NA
21	Retrograde opacification in 5 cortical regions	0-5	Pop, 2014 [104] (49)	Acute	Yes, k=0.77	Beneficial
			Pop, 2016 [105] (89)	Acute	Yes, k=0.77	Beneficial
22	Angiographic appearance of occlusion incorporating anatomic site and collateral pathway to affected region	0-5	Hassan, 2010 [163] (196)	Acute	No	NS
			Liebeskind, 2011 [85] (287)	Non acute	No	NA
			Qureshi, 2009 [164] (101)	Acute	No	NA
			Qureshi, 2015 [165] (150)	Acute	No	NA
			Shao, 2016 [166] (6)	Acute	No	NS
23	Pial collaterals from ACA	0-2	Rai, 2012 [167] (89)	Acute	No	Beneficial
24	Filling extent of at risk territory	None, partial, full	Liebeskind, 2011 [85] (287)	Non acute	No	NA
25	Qualitative evaluation based on patency of PCoA and anastomoses between PICA and SCA	N/A	Van Houwelingen2016 [94] (38)	Acute	No	No
26	Quantitative measurement based on density and time of contrast agent to reach peak value	N/A	Wen, 2016 [150] (105)	Acute	Yes, ICC=0.831 time, ICC=0.983 density	Beneficial
27	Presence of cortical branches from the contralateral ACA or from the PCA extending into the vascular territory of the stenoocclusive lesion	N/A	Kawashima, 2011 [83] (68)	Non acute	No	NA

Diagnostic/prognostic value of DSA-assessed collaterals

The prognostic value of DSA-assessed collaterals was discussed in 66 publications. All but 7 publications showed that collaterals have a beneficial impact, meanining that good collaterals are correlated with better outcome and/or poor collaterals are correlated with worse outcomes. Six publications ([112, 22, 129, 76, 146, 94]) found no correlations between collaterals and outcomes. Hwang et al. showed that excellent collaterals are associated with delayed re-occlusion[128]. Among the studies that did not assess the prognostic value of collaterals, 30 studies did not discuss outcomes (prognostic value NA), while 12 studies analyzed outcomes but did not state whether there was an association with collaterals (prognostic value NS).

A number of different outcome parameters have been associated with the grade of collaterals (see table 2.4 for a detailed list). The follow-up parameter most frequently adopted to assess the impact of collaterals was the modified-Rankin Scale score at 3 months: good collaterals were correlated with 3-month mRS$\leq$2 in 26 papers while 3 studies reported a correlation between poor collaterals and mRS=3-6. In addition, Lau et al. observed a correlation with mRS at 3 months and collateral score combined with antegrade score of blood flow through the clot ([78]). Lescher et al. found a trend but no statistical significance between good collaterals and mRS [124]. Two papers reported a correlation between good collaterals and mRS$\leq$2 at discharge. One paper did not specify the time at which mRS was assessed ([89]).

The second most commonly investigated follow-up parameter was mortality/survival (11 papers): 5 publications found correlations with good collaterals and survival while 6 reported correlation between poor collaterals and mortality. Good collaterals were also correlated with smaller final infarct volume (8 papers), smaller infarct growth (7 papers) and ratio of penumbra loss (1 paper). 12 publications reported a correlation with reperfusion or recanalization following treatment (either mechanical

Table 2.4: List of outcome parameters most frequently reported to have a correlation with DSA-assessed collaterals and corresponding publications.

Outcome parameter	Publications
mRS ≤2 at 3 months	29 papers: [109, 110, 111, 103, 46, 159, 97, 128, 132, 32, 66, 137, 141, 143, 125, 100], [116, 93, 147, 150, 102, 151, 152, 156, 58, 167], [89][1], [78], [124][2]
mRS≤2 at discharge	2 papers: [131, 145]
Survival/mortality	11 papers: [46, 32, 92, 102, 159]/[63, 64, 65, 107, 66, 167]
Final infarct volume	8 papers: [110, 145, 147, 149, 156, 157, 105, 104]
Infarct growth	7 papers: [47, 58, 32, 104, 120, 139, 145]
Recanalization as TICI 2b-3[3]	2 papers: [93, 156]
Recanalization as TIMI 2-3[3]	5 papers: [65, 47, 66, 99, 167]
Reperfusion (TICI)[3]	5 papers: [66, 137, 139, 147, 160]
Intracranial hemorrhage/HT	8 papers: [46, 65, 106, 137, 49, 153, 114, 96]
Favorable neurological improvement (NIHSS drop):	4 papers: [130, 101, 157, 32]
24 h ASPECTS	2 papers: [137, 152]
NIHSS at 7 days/discharge	3 papers: [137, 102, 156]
Ratio of penumbra loss	1 paper: [39]
Length of hospitalization	1 paper: [145]
Recurrency of TIA/stroke	1 paper: [78][4]
Infarct expansion in hyperglycemic patients	1 paper: [100]

[1] Does not specify time of mRS evaluation.
[2] Trend only.
[3] Following treatment (either by thrombolysis or mechanical intervention).
[4] Collateral score combined with antegrade flow score.

intervention or thrombolysis). The definition of follow-up recanalization was not homogeneous: 2 papers used a TICI score of 2b-3 to define good recanalization ([93, 156], while 5 papers reported good recanalization as a TIMI score of 2-3 [65, 47, 66, 99, 167]. Poor collaterals were correlated with intracranial hemorrhage and hemorrhagic transformation (HT) in 8 publications. Other less frequent correlations are listed in table 2.4.

Better/poorer DSA-assessed collaterals were also correlated with a number of baseline parameters, most importantly lower/higher NIHSS, higher/lower ASPECTS score and baseline DWI lesion volume (table 2.5). 7 of the studies that investigated collaterals found a correlation between good scores and presence of the HV sign. In particular one study by Kim et al. found that in presence of perysilvian sulcal effacement (PSE) the HV sign was predictive of good collaterals, but in absence of PSE a missing HV sign was indicative of good collaterals. Three papers reported a

correlation between the degree of collaterals and stroke subtype. Better collaterals were associated with intracranial large artery atherosclerotic stroke, while worse collaterals were associated with cardioembolic stroke [32, 134, 133]. Two papers reported opposite correlations with the degree of stenosis: Liebeskind et al. found that better collaterals were associated with higher degree of stenosis [85], while Liu et al. observed worse collaterals in patients with higher degree of stenosis [87]. 4 papers found a correlation between collaterals and the location of occlusion although there is discrepancy among the associations detected: in a study by Marks et al. better/worse collaterals were observed in patients with ICA/MCA occlusions respectively [139], while Mangiafico and Consoli observed more MCA occlusion and less ICA occlusion in their good collaterals group of patients [102, 152]. Labeyrie et al. investigate patients with M1 and M2 occlusion and found that patients with isolated occlusions are more likely to have better collaterals than patients with tandem M1-ICA or M2-ICA occlusions. Other less frequently observed correlations are listed in table 2.5.

2.3.3 Collaterals assessment with computed tomography

CT was the imaging modality with the highest number of publications (128), and different assessment criteria (40). 21 methods used single phase CT angiography (1, 6, 7, 9, 11, 12, 13, 14, 16, 19, 20, 22, 23, 25, 26, 27, 28, 30, 32) and/or multi-phase CTA (8, 17, 22, 40), 1 used time-invariant CTA (24), 1 used intravenously enhanced flat-detector CT (IV-FDCT) (n=34), 7 used dynamic CTA (2 3, 10, 15, 21, 29, 31), 5 used CTP (33, 35, 36, 37, 39), 1 used three-phasic contrast-enhance (CE) CT (38) and 3 used a combination of CTA and CT perfusion (4, 18) or CTA and non-enhanced CT (NECT)/CECT (5).

121 studies assessed collaterals in acute stroke/TIA while 4 studies assessed a mix of acute/non acute patients [70, 168, 169, 53] and 2 studies assessed LM collaterals in non-acute patients: Sundaram et al. looked at cases of TIA/stroke due to extracranial ICA occlusion within 3 weeks of symptom onset [170] and Liu et al. looked at cases of symptomatic anterior circulation intracranial stenosis with or without ischaemic stroke within 30 days after symptoms onset [87]. In one study

Table 2.5: List of baseline parameters most frequently reported to have a correlation with DSA-assessed collaterals and corresponding publications.

Baseline parameter	**Publications**
NIHSS	16 papers: [103, 97, 131, 32, 120, 139, 145, 102, 151, 152, 160, 167, 114, 89, 46]
ASPECTS	7 papers: [103, 97, 137, 149, 156, 105, 114, 108]
HV sign	7 papers: [123, 79, 119, 118, 83, 74, 75]
DWI lesion volume	5 papers: [32, 120, 140, 145, 114, 105]
PWI lesion volume	1 paper: [139]
PWI/DWI ratio	1 paper: [145]
Location of occlusion	4 papers: [139, 102, 152, 103]
Subtype of stroke	3 papers: [133, 32, 134]
Age	3 papers: [103, 157, 167]
Prestroke statin use	2 papers: [98, 157]
CTP parameters	2papers: [102, 87]
Degree of stenosis	2 papers: [85, 87]

OTHER CORRELATIONS:

Degree of stenosis [85], sex (collaterals more recurrent in women) [86], Tmax value on DSC-MRP maps [120], ALDH2 genotypes[72], rCVB on PWI [77], diabetes mellitus [87], history of hypertension [66], hyperlipidemia [100], history of congestive heart disease [66], elevated baseline blood glucose [137], elevated systolic blood pressure [137, 156], cerebrovascular reactivity [69], shorter time between symptom onset and arrival [138]

the time from symptom onset was not stated clearly [84].

Two studies reviewed collateral flow for posterior circulation occlusion only [91, 94], 20 studies looked at both anterior and posterior circulation ([161, 84, 169] and [144-160]) and the rest (106 publications) discussed collaterals in anterior circulation alone.

Six methods (n. 14, 18, 24, 27, 37, 40) had both intra- and inter-observer agreement assessed, while 15 (6-8, 13, 15-17, 19, 23, 25, 26, 29, 31, 35, 36) had only inter-rater agreement and the rest had no agreement assessed. In total the publications that discussed inter- and/or intra rater agreement for scoring method based on CT imaging were 50 out of 128. Where reported, the reliability was assessed using inter-/intra- class correlation coefficient (ICC) [171, 172, 52, 173, 174, 175, 60, 176], Kendall's W [168], K_α [177, 178, 179] or Cohen's k (all other publications). One study based on CTP that assessed collaterals based on the relative filling time delay (rFTD) in the Sylvian fissure, calculated inter-rater agreement as the average difference in rFTD assigned by the raters and found that it was good, $\Delta t<2$ sec [180]. Reliability assessment always resulted in good or very good inter-/intra-observer agreement, apart from 4 publications where it was fair for at least one of the collateral parameters assessed [181, 182, 177, 178].

A method proposed by Tan et al. [1] (n. 27 in table 2.6) was used in 54 of the reviewed publications and is by far the most frequently adopted. This method looks at the extent of filling in the occluded territory on CTA-MIP and assigns a score of 0 for absent collaterals, 1 for collaterals filling $\leq$50% of the occluded territory, 2 for collaterals filling >50% but less than 100% of the occluded territory and 3 for collateral filling equal to 100% of the occluded territory. This method had reliability assessed in multiple studies and a good inter-rater agreement has been reported. Among the remaining methods four have been used considerably more than the others. One (n.18 in table 2.6), reported in 17 publications, is a method proposed by Miteff et al. [27] for ICA/MCA complete occlusions and describes collaterals as good, moderate or poor based on the degree of retrograde reconstitution of the MCA up to the distal end of its occlusion. The second method (n. 13) is a 5-grade scale proposed by Maas et al. [71] and discussed in 16 papers that scores

collaterals in the sylvian fissure and LM convexity based on the comparison with the contralateral normal hemisphere. The third one (n.14, 14 publications) is a 20-point regional scoring system proposed by Menon et al. [52] that looks at the extent of contrast opacification in arteries distal to the occlusion with respect to contralateral hemisphere in the 6 ASPECTS cortical regions, Sylvian sulcus, ACA territory and basal ganglia. The last one (n. 26, 9 publications), proposed by Souza et al. [56], is a modification of the method used by Tan et al. with grading based upon 50% of 1 MCA division rather then the whole occluded territory: 0=absent collaterals in >50% of an MCA M2 branch territory, 1=diminished collaterals in >50% of an MCA M2 branch territory, 2=diminished collaterals in <50% of an MCA M2 branch territory, 3=collaterals equal to the contralateral hemisphere and 4=increased collaterals.

The rest of the CT-based methods appeared in 4 or fewer publications. Seven methods had no explicit grading: method n. 3 in table 2.6 simply looked at the presence/absence of delayed-late cortical vein filling as a sign of poor/good collaterals, n. 10 evaluated contrast peak density vs contrast peak time with respect to contralateral hemisphere on dynamic CTA with no explicit classification, n. 11 classified collaterals on CTA only anatomatically based on the origin of LM flow from ACA or PCA, n. 36 and 39 looked at continuous values of contrast arrival time on CTP, n. 38 looked at the ratio between the number of contrast enhancing MCA branches in the occluded and normal side on three-phasic CECT, n. 28 looked at the patency of posterior circulation vessels on CTA. The remaining had grading scales, ranging from 3 to 10 grades. Assessing criteria included origin, velocity, number and/or extent of contrast filling (either in the whole territory or only distal to the occlusion), difference in intensity/distribution of specific arteries/veins between the two hemispheres and K_{trans} values from CTP scans in ischaemic area.

One publication compared CT-assessed collaterals with HV sign on FLAIR-MR [183] and found a good correlation. Four studies (one discussed in three different publications) compared conventional single-phase CTA with time-invariant CTA [182], multi-phase CTA [171], dynamic CTA [184, 185, 186] and CTP [84], and found that the lack of temporal resolution is a shortage in collaterals assessment and that single-phase CTA is inferior to time-resolved modalities since sometimes

collaterals appear poor just because the contrast has not reached the vessels yet when single-CTA scans are acquired. Levi et al. [53] compared collaterals scored on CTA with ACA flow diversion on TCD and found that flow diversion was strongly associated with improved LM collaterals. Two studies [187, 188] used a mix of CTA and MRA scans to assess collaterals based on what scans the patients had available, but did not compare them. In addition, eight papers compared CT-scoring with DSA-scoring, as discussed in the previous section (2.3.2).

Table 2.6: CTA-based scoring methods for LM collaterals.

	Modality	Description	Grades	First author	Acute/ Non acute	Reliability assessed	Prognostic value
1	CTA	Presence of symmetrical density of signal intensity compared with opposite side	Inadequate vs adequate	Ali, 2016 [187] (380)	Acute	No	Beneficial
2	Dynamic CTA	Origin, velocity and extent of collateral filling	Ant/Post/Ind + velocity value + less/greater 50% extent	Beyer, 2015 [189] (116)	Acute	No	Beneficial
				Thierfelder, 2016 [190] (69)	Acute	No	No effect
3	Dynamic CTA	Delayed-late cortical vein filling as sign of poor collaterals	Presence or absence of LCVF	Bhaskar, 2017 [191] (117)	Acute	No	NA
				Bhaskar, 2017 [192] (119)	Acute	No	NA
4	CTA, CTP	Retrograde vessel filling distal to occlusion	Poor, moderate, good	Cheripelli, 2015 [34] (118)	Acute	No	Beneficial
5	NECT, CTA, CECT	ASPECTS on CT as predictor of collaterals	0-10	Choi, 2011 [114] (55)	Acute	No	Beneficial
6	CTA	Arterial contrast distal to the occlusion and reconstitution of veins in affected hemisphere	Class 1-4	Parthasarathy, 2015 [193] (81)	Acute	Yes, k=0.828	Benefcial

– continues on next page –

Table 2.6 – continued from previous page

	Modality	Description	Grades	First author	Acute/ Non acute	Reliability assessed	Prognostic value
7	CTA	Antegrade or retrograde contrast opacification of vessels within occluded territory in each of 6 segmental divisions of the posterior circulation arterial tree	6-1	Da Ros, 2016 [91] (15)	Acute	Yes	Beneficial
8	CTA, mp-CTA	Filling of MCA pial arterial circulation on single or multiphase CTA	Poor vs moderate-good	Doucet, 2016 [194] (31)	Acute	No	NA
				Goyal, 2015 [50] (315)	Acute	No	NA
				Kim, 2016 [195] (71)	Acute	Yes, k=0.728 mp-CTA, k=0.747 CTA	NA
				Muir, 2016 [196] (65)	Acute	No	NS
9	CTA	Extent of contrast filling in occluded territory	1-3	Drewer-Gutland, 2015 [161] (155)	Acute	No	No effect
				Hesselmann, 2012 [58] (31)	Acute	No	Beneficial
10	dynamic CTA	Regional evaluation of contrast peak density vs contrast peak time with respect to contralateral hemisphere	NA	Kawano, 2016 [197] (66)	Acute	No	Beneficial
11	CTA	Anatomical classification based on presence/of anastomoses between distal segments of ACA-MCA or PCA-MCA	None, one type or two types present	Keedy, 2012 [84] (135)	Acute	No	No effect
12	CTA	Visual inspection of anterior circulation and LM collaterals	Poor, moderate, good	Lescher, 2015 [124] (39)	Acute	No	Beneficial
13	CTA-SI	Comparison of collaterals in Sylvian fissure and LM convexity with	Absent, less than, equal to, greater than, exuberant	Agarwal, 2013 [198] (39)	Acute	Yes, k=0.73	No effect
				Arsava, 2014 [199] (70)	Acute	No	NA

– continues on next page –

Table 2.6 – continued from previous page

	Modality	Description	Grades	First author	Acute/ Non acute	Reliability assessed	Prognostic value
		contralateral hemispere		Beyer, 2015 [200] (136)	Acute	No	Beneficial
				Higazi, 2016 [201] (30)	Acute	No	NA
				Kamalian, 2013 [202] (45)	Acute	No	NS
				Lee, 2013 [203] (66)	Acute	No	Beneficial
				Lima, 2010 [55] (196)	Acute	No	Beneficial
				Lima, 2014 [204] (126)	Acute	No	Beneficial
				Maas, 2009 [71] (369)	Acute	No	Beneficial
				Malik, 2014 [205] (82)	Acute	No	NS
				Menon, 2015 [26] (185)	Acute	No	Beneficial
				Sundaram, 2017 [170] (65)	Acute	Yes, k=0.89	Beneficial
				Volny, 2016 [206] (86)	Acute	No	Beneficial
				Yeo, 2015 [207] (200)	Acute	Yes, k=0.82	Beneficial
				Yeo, 2016 [208] (100)	Acute	Yes, k=0.82	Beneficial
				Yeo, 2016 [209] (209)	Acute	Yes, k=0.82	Beneficial
14	CTA	rLMC: Regional assessment of opacification from LM vessel with respect to contralateral hemisphere	0-20	Beyer, 2015 [200] (136)	Acute	No	Beneficial
				Frölich, 2014 [171] (82)	Acute	Yes, ICC=0.81 spCTA, ICC=0.78 tMIP	Beneficial
				Gersing, 2017 [172] (115)	Acute	Yes, ICC_{inter}=0.87, ICC_{intra}=0.92	Beneficial
				Malik, 2014 [205] (82)	Acute	No	No effect
				Menon, 2011 [52] (138)	Acute	Yes, ICC=0.87	Beneficial
				Menon, 2013 [210] (206)	Acute	No	NS

– continues on next page –

Table 2.6 – continued from previous page

	Modality	Description	Grades	First author	Acute/ Non acute	Reliability assessed	Prognostic value
				Nambiar, 2014 [211] (84)	Acute	No	Beneficial
				Qazi, 2015 [212] (104)	Acute	No	NA
				Tan, 2016 [213] (283)	Acute	Yes, k=0.78 for ASPECT and insular ribbon regions, k=0.23 for others	Beneficial
				Thierfelder, 2016 [190] (69)	Acute	No	No effect
				von Baumgarten, 2016 [214] (103)	Acute	No	NS
				Yeo, 2015 [207] (200)	Acute	Yes, k=0.77	Beneficial
				Yeo, 2016 [208] (100)	Acute	Yes, k=0.77	Beneficial
				Yeo, 2016 [209] (209)	Acute	Yes, k=0.77	Beneficial
15	Dynamic CTA	Anatomical extent, prominence and flow velocity of pial arteries filling retrogradely from anterior/posterior circulation	Extent:0-2, Prominence: null/minimal, thin, same/more, Time: 0-2	Beyer, 2015 [189] (116)	Acute	No	Beneficial
				Menon, 2013 [181] (25)	Acute	Yes, k=0.73/0.88 extent, k=0.60/0.88 prominence, k=0.40/0.72 velocity	NS
16	sp-CTA	Extent and size of pial arteries backfilling frmo ACA/PCA beyond occlusion, as compared to contralateral hemisphere	Minimal, poor, fair, good, excellent	Flores, 2015 [115] (81)	Acute	No	Beneficial
				Menon, 2015 [26] (185)	Acute	No	Beneficial
				Menon, 2015 [33] (147)	Acute	Yes k=0.81	NA
				Vagal, 2015 [215] (53)	Acute	No	NA
17	mp-CTA	Pial arterial filling in the occluded	0-6	García-Tornel, 2016 [216] (108)	Acute	Yes, k=0.84	Beneficial

– continues on next page –

Table 2.6 – continued from previous page

	Modality	Description	Grades	First author	Acute/ Non acute	Reliability assessed	Prognostic value
		territory compared to similar arteries in contralateral hemisphere		Menon, 2015 [33] (147)	Acute	Yes, k=0.81	NA
				Seker, 2016 [217] (51)	Acute	No	NA
18	CTA, MIP, CTP	Retrograde filling of MCA	Poor, moderate, good	Bhaskar, 2017 [191] (117)	Acute	No	NA
				Bhaskar, 2017 [192] (119)	Acute	No	NA
				Bivard, 2017 [19] (1519)	Acute	No	Beneficial
				Kawano, 2016 [197] (66)	Acute	Yes, k=0.861	Beneficial
				Levi, 2012 [53] (53)	Mixed	No	Beneficial
				Mair, 2015 [177] (15)	Acute	Yes, α_{inter}=0.56, α_{intra}=0.72	NA
				Mair, 2017 [178] (135)	Acute	Yes, α=0.56	Beneficial
				Malik, 2014 [205] (82)	Acute	No	NS
				Miteff, 2009 [27] (92)	Acute	k=0.93	Beneficial
				Nordmeyer, 2017 [218] (87)	Acute	k=0.78	Beneficial
				Parthasarathy, 2013 [219] (39)	Acute	No	Beneficial
				Seet, 2012 [125] (21)	Acute	No	Beneficial
				Seker, 2016 [217] (30)	Acute	No	NA
				Yeo, 2015 [207] (200)	Acute	Yes, k=0.91	Beneficial
				Yeo, 2016 [208] (100)	Acute	Yes, k=0.91	Beneficial
				Yeo, 2016 [209] (209)	Acute	Yes, k=0.91	Beneficial
				Zareie, 2013 [220] (53)	Acute	No	NS
19	CTA	Difference in reconstitution of 4 given veins between the two hemispheres	0-2	Parthasarathy, 2013 [219] (39)	Acute	Yes, k=0.86	Beneficial

– continues on next page –

Table 2.6 – continued from previous page

	Modality	Description	Grades	First author	Acute/ Non acute	Reliability assessed	Prognostic value
20	CTA-MIP	Vessels distribution in Sylvian fissure and LM convexity	0-3	Seeta, 2014 [221] (87)	Acute	No	Beneficial
21	Dynamic CTA	ASITN/SIR collateral score applied to CTA	0-4	Seker, 2016 [217] (30)	Acute	No	NA
22	sp-CTA, dynamic CTA-MIP	Extent of retrograde contrast opacification of vessels in occluded territory on delayed angiographic images	1-5	Seker, 2016 [217] (30)	Acute	No	NA
23	CTA	Extent of vascularity at Sylvian fissure and at cerebral convexity.	0-8	Seyman, 2016 [179] (51)	Acute	Yes, α=0.96	Beneficial
24	TI-CTA	Extent of filling in territory of occluded vessel smaller/greater than 50% as compared to contralateral side	1-4	Kaschka, 2017 [222] (49)	Acute	No	NS
				Rohan, 2014 [223] (80)	Acute	Yes	NA
				Smit, 2013 [182] (40)	Acute	Yes, k_{inter}=0.68, k_{intra}=0.78	Beneficial
25	CTA-MIP	Extent of filling in MCA-M2 segment	0-3	Song, 2015 [48] (91)	Acute	Yes, k=0.697	Beneficial
26	CTA	Extent of filling in MCA-M2 segment	0-4	Elijovich, 2015 [224] (50)	Acute	No	Beneficial
				Giurgiutiu, 2015 [24] (73)	Acute	No	Beneficial
				Karadeli, 2016 [183] (39)	Acute	No	NA
				Rusanen, 2015 [173] (104)	Acute	Yes, k=0.68, ICC=0.87	Beneficial
				Rusanen, 2015 [174] (105)	Acute	Yes, k=0.68, ICC=0.87	Beneficial
				Saarinen, 2014 [175] (105)	Acute	Yes, k=0.68, ICC=0.87	Beneficial
				Sillanpää, 2015 [225] (105)	Acute	Yes, k=0.68, ICC=0.87	Beneficial

– continues on next page –

Table 2.6 – continued from previous page

	Modality	Description	Grades	First author	Acute/ Non acute	Reliability assessed	Prognostic value
				Souza, 2012 [56] (197)	Acute	Yes, k=0.76	Beneficial
				Timpone, 2015 [226] (55)	Acute	Yes, k=0.44	Beneficial
27	CTA	Extent of filling in territory of occluded vessel smaller/greater than 50% as compared to contralateral side	0-3, often dichotomized into poor(0-1) vs good (2-3)	Agarwal, 2013 [198] (39)	Acute	Yes, k=0.73	No effect
				Agarwal, 2015 [227] (53)	Acute	No	NS
				Angermaier, 2011 [228] (25)	Acute	Yes, k=0.71	Beneficial
				Angermaier, 2016 [229] (63)	Acute	No	No
				Aoki, 2014 [230] (56)	Acute	No	Beneficial
				Berkhemer, 2016 [231] (493)	Acute	Yes, k=0.60	Beneficial
				Beyer, 2015 [189] (116)	Acute	No	Beneficial
				Beyer, 2015 [200] (136)	Acute	No	Beneficial
				Brunner,2014 [232] (246)	Acute	Yes, k=1.0	Beneficial
				Chen, 2015 [113] (75)	Acute	No	Beneficial
				Cheng, 2015 [233] (76)	Acute	No	Beneficial
				Dehkharghani, 2015 [7] (47)	Acute	Yes, Pearson-k=0.85	No effect
				Dehkharghani, 2016 [234] (54)	Acute	No	No effect
				Dippel, 2016 [235] (233)	Acute	No	NS
				Eilaghi, 2013 [236] (114)	Acute	No	Beneficial
				Espinosa, 2015 [237] (150)	Acute	No	Beneficial
				Fanou, 2015 [238] (395)	Acute	No	Beneficial
				García-Tornel, 2016 [216] (108)	Acute	Yes, k=0.84	Beneficial
				Gerber, 2016 [168] (93)	Mixed	Yes, Kendall's W=0.752	Beneficial

– continues on next page –

Table 2.6 – continued from previous page

Modality Description	Grades	First author	Acute/ Non acute	Reliability assessed	Prognostic value
		Grech, 2014 [239] (55)	Acute	NS	Beneficial
		Higazi, 2016 [201] (30)	Acute	No	No effect
		Hom, 2011 [240] (32)	Acute	No	NA
		Huisa, 2014 [241] (165)	Acute	No	NS
		Kaschka, 2016 [222] (49)	Acute	No	NS
		Kawiorski, 2016 [242] (34)	Acute	No	NA
		Kheradmand, 2014 [169] (18)	Mixed	No	Beneficial
		Kim, 2010 [243] (68)	Acute	Yes, $k=_{intra}0.79$	Beneficial
		Kim, 2015 [244] (71)	Acute	No	Beneficial
		Lin, 2012 [245] (84)	Acute	No	Beneficial
		Malik, 2014 [205] (82)	Acute	No	No effect
		Man, 2015 [246] (97)	Acute	No	Beneficial
		Menon, 2015 [26] (185)	Acute	No	Beneficial
		Mortimer, 2013 [247] (15)	Acute	No	NA
		Nordmeyer, 2017 [218] (87)	Acute	Yes, k=0.93	Beneficial
		Ozkul, 2014 [248] (86)	Acute	No	Beneficial
		Pfaff, 2016 [188] (33)	Acute	No	NS
		Power, 2015 [45] (48)	Acute	No	NA
		Renú, 2017 [249] (146)	Acute	No	NS
		Shin, 2014 [116] (43)	Acute	Yes, k=0.475	Beneficial
		Smit, 2013 [182] (40)	Acute	Yes, $k_{inter}=0.57$, $k_{intra}=0.73$	Beneficial
		Soares, 2010 [250] (22)	Acute	No	Beneficial
		Sung, 2015 [117] (30)	Acute	No	Beneficial

– continues on next page –

Table 2.6 – continued from previous page

	Modality	Description	Grades	First author	Acute/ Non acute	Reliability assessed	Prognostic value
				Tan, 2009 [60] (85)	Acute	Yes, ICC=0.87	Beneficial
				Urra, 2014 [251] (78)	Acute	No	No effect
				van Seeters, 2015 [252] (1374)	Acute	No	Beneficial
				van Seeters, 2016 [253] (906)	Acute	No	Beneficial
				van Seeters, 2016 [254] (484)	Acute	No	Beneficial
				Van Den Wijngaard, 2015 [184] (70)	Acute	No	Beneficial
				Van Den Wijngaard, 2016 [185] (61)	Acute	No	Beneficial
				Van Den Wijngaard, 2016 [186] (88)	Acute	No	Beneficial
				Yeo, 2015 [207] (200)	Acute	Yes, k=0.93	No effect
				Zhu, 2013 [255] (165)	Acute	No	NS
				Zhu, 2013 [256] (165)	Acute	No	No effect
				Zhu, 2015 [257] (103)	Acute	No	No effect
28	CTA	Patency of vertebral arteries, PCoA and anastomosis between PICA and SCA	N/A	Van Houwelingen, 2016 [94] (38)	Acute	No	No effect
29	Dynamic CTA	Extent and filling velocity of vessels below and above caudate nuclesu	Good and fast, good and slow, poor and fast, poor and slow	Wijngaard, 2015 [184] (70)	Acute	Yes, k=0.86	Beneficial
				Wijngaard, 2016 [185] (61)	Acute	Yes, k=0.88	Beneficial
				Wijngaard, 2016 [186] (88)	Acute	No	Beneficial
30	CTA	Comparison of Sylvian collaterals with contralateral hemispere	0-2	Yoo, 2011 [258] (48)	Acute	No	NA

– continues on next page –

Table 2.6 – continued from previous page

	Modality	Description	Grades	First author	Acute/ Non acute	Reliability assessed	Prognostic value
31	4D CTA	rLMC on peak phase (rLMC-P) and tMIP (rLMC-M)	poor, intermediate, good	Zhang, 2016[176] (80)	Acute	Yes, ICC=0.85 rLMC-P, ICC=0.87 rLMC-M	Beneficial
32	CTA	Filling extent of at risk territory in 15 ASPECTS areas	0-3	Chen, 2015 [70] (7)	Mixed	No	NS
33	CTP	Arrival time of retrograde flow downstream from arterial region of interest	Poor, good	Ahn, 2015 [259] (39)	Acute	No	Beneficial
34	IV FDCT	Extent of retrograde contrast opacification of vessels within occluded territory	1-5	Blanc, 2012 [260] (14)	Acute	No	NS
35	CTP-SI, MTT maps	Extent of cortical arteries in hypoperfused MCA territory as defined by MTT maps	0-3	Calleja, 2013 [38] (54)	Acute	Yes, k=0.724	Beneficial
				Cortijo, 2014 [261] (68)	Acute	Yes, k=0.724	NS
				Liu, 2016 [87] (35)	Non acute	Yes, k=0.794	NA
36	CTP-SI	Relative filling time delay (rFTD) in the Sylvian fissure	N/A	Cao, 2014 [180] (60)	Acute	Yes, $\Delta t<2$	Beneficial
				Kaschka, 2016 [262] (121)	Acute	No	No effect
37	CTP	Mean K_{trans} values in ischaemic cerebral area	1-4	Chen, 2015 [113] (75)	Acute	Yes, k_{inter}=0.905, k_{intra}=0.934	Beneficial
38	Three-phasic CECT	Ratio between number of contrast enhancing MCA branches on occlusion and contralateral side	N/A	Jung, 2011 [263] (11)	Acute	No	NA
39	CTP	Functional assessment based on delayed arrival of intravenous contrast to brain parenchyma	N/A	Keedy, 2012 [84] (135)	Non acute	No	Beneficial

– continues on next page –

Table 2.6 – continued from previous page

	Modality	Description	Grades	First author	Acute/ Non acute	Reliability assessed	Prognostic value
40	MPCT	Number and rapidity of collateral vessels filling	ASITN/SIR scale (0-3)	Kim, 2012 [95] (54)	Acute	Yes, k_{inter}=0.813, k_{intra}=0.852	NA
				Shin, 2014 [116] (43)	Acute	Yes, k=0.776	Beneficial

Diagnostic/prognostic value of CT-assessed collaterals

The prognostic value of CT-assessed collaterals was discussed in 89 publications. 10 of these ([198, 229, 234, 161, 205, 190, 251, 94, 256, 262]) failed to demonstrate a correlation between collaterals and outcomes, while the remaining proved that collaterals are associated with a number of different parameters, such as mRS at 3 months/discharge, infarction volume, recanalization, recurrency of TIA/stroke, mortality, intracranial haemorrhage, NIHSS and ASPECTS. Among the studies that did not assess the prognostic value of collaterals, 21 studies did not discuss outcomes (NA), while 18 studies analyzed outcomes but did not state whether there was an association with collaterals (NS).

Table 2.7 lists the outcome parameters that have been associated with the grade of collaterals.

The follow-up parameter most frequently adopted to assess the impact of collaterals was again the modified-Rankin Scale score at 3 months: good collaterals were correlated with 3-month mRSleq2 in 42 papers while 3 studies reported a correlation betwwen poor collaterals and mRS=3-6 ([252, 254, 226]). Fanou et al. observed a correlation between good collaterals and mRS$\leq$2 at 3 months only in patients with no recanalization [238] while Souza et al. reported the correlation only for untreated patients [56]. Three papers reported a correlation between good collaterals and mRS$\leq$2 at discharge or at 6 months.

Table 2.7: List of outcome parameters most frequently reported to have a correlation with CT-assessed collaterals and corresponding publications.

Outcome parameter	Publications
mRS $\leq$ 2 at 3 months	47 papers: [231, 113, 236, 237, 238][1], [216, 168, 239, 58, 26, 218, 116, 182, 117, 60, 184, 186, 207, 114, 91, 193, 38, 180, 222], [173, 174, 175, 48, 56][2], [176, 19, 171, 172, 203, 27, 52, 211, 219, 125, 221, 170, 213, 226, 252, 254, 208, 209][3]
mRS$\leq$ 2 at discharge	3 papers: [232, 179, 224]
$\leq$ 2 at 6 months	3 papers: [55, 204, 178]
Death or discharge to facility other than home	1 paper: [187]
Final infarct volume	14 papers: [228, 189, 200, 238, 169, 116, 60, 253, 185, 197, 224, 113, 115, 56]
Infarct volume at 24 h	2 papers: [216, 193]
Infarct growth	6 papers: [58, 246, 218, 176, 27, 211]
Survival/mortality	8 papers: [232, 180]/[243, 218, 55, 204, 208, 209][3]
ICH / HT	7 papers: [232, 218, 208, 209, 245, 248, 176]
Malignant brain edem	2 papers: [244, 206]
Reperfusion (TICI)[4]	2 papers: [113, 250][5]
Recanalization (TIMI 2-3)[4]	1 paper: [228]
Early recanalization[4]	1 paper: [259]
Early neurological improvement (ENI)	1 paper: [38]
Recurrency of TIA/stroke	1 paper: [84]
NIHSS at 7 days/discharge	2 papers: [216, 117]
24 h NIHSS	3 papers: [218, 174, 175]
24 h ASPECTS	3 papers: [180, 173, 175]
follow-up ASPECTS	1 paper: [52]

[1] Correlation observed only for patients with no recanalization.
[2] Correlation observed only for untreated patients.
[3] Correlation observed only in univariable analysis.
[4] Following treatment (either by thrombolysis or mechanical intervention).
[5] Correlation with reperfusion in patients with no recanalization.

The second most commonly investigated follow-up parameter was final infarct volume (14 papers): 11 publications found that better collaterals were correlated with smaller final infarct volume and 3 reported that poor collaterals were correlated with larger infarct volume. Good/poor collaterals were also correlated with survival/mortality (2/6 papers respectively) and correlations between poor collaterals and intra-cranial haemorrhage and haemorrhagic transformation was observed in 4 and 3 papers respectively. Other less frequent correlations are listed in the table 2.7.

Better/poorer collaterals assessed with CT imaging were also correlated with a number of baseline imaging and clinical parameters (table 2.8).

The baseline parameters most frequenlty observed to have a correlation with

collaterals were NIHSS scores (17 papers) and ASPECTS scores (14 papers). Of the 14 publications that reported a correlation with ASPECTS scores, all but two used ASPECTS score measured on CTA. Rusanen et al. derived two ASPECTS score from cerebral blood volume (CBV) and mean transit time (MTT) perfusion maps, while Lee et al. used CBV-ASPECTS alone [174, 203]. Other baseline perfusion parameters were found to have a correlation with the quality of collaterals in six different publications.

After NIHSS and ASPECTS scores the baseline parameters which were most frequently correlated with collaterals were infarct volume and penumbra, age and perfusion/lesion mismatch. Interestingly, one group reported in 3 publications that poor and good collaterals are associated with shorter and longer onset to treatment time respectively, supporting the hypothesis that at least in some patients the longer the lack of perfusion the more the amount of collaterals to compensate for it [173, 174, 175].

Other less frequently observed correlations with baseline parameters are listed in table 2.8.

2.3.4 Collaterals assessment with magnetic resonance imaging

Collaterals were assessed with MRI in 46 publications using 30 different methods. 11 methods used MRA (1, 5, 6, 7, 9, 11, 12, 15, 26, 27, 30), 9 FLAIR-MRI (8, 11, 12, 13, 16, 17, 20, 23, 28), 7 PWI-MR (2, 9, 14, 21, 22, 24, 25), 4 ASL-MRI (4, 18, 19, 29) and 2 CE T1-MRI (3, 10).

35 studies assessed collaterals in acute stroke/TIA, while 4 looked at a mix of acute/non acute patients [264, 70, 74, 75], 6 looked at non-acute patients [265, 83, 67, 69, 266, 89] and 1 had unclear acute/non acute setting [267].

Two studies assessed collateral flow for posterior circulation occlusion alone [268, 269], 7 looked at both anterior and posterior circulation [187, 270, 183, 68, 69, 119, 271] while the rest (37 publications) discussed collaterals in anterior circulation

Table 2.8: List of baseline parameters most frequently reported to have a correlation with CT-assessed collaterals and corresponding publications.

Baseline parameter	**Publications**
NIHSS score	17 papers: [232, 236, 238, 216, 201, 180, 179, 24, 174, 175, 56, 176, 199, 172, 27, 52, 170]
ASPECTS	14 papers: [232, 205, 116, 38, 263, 179, 174, 225, 48, 172, 203, 55, 210, 52]
Age	7 papers: [198, 216, 205, 116, 173, 199, 210]
Sex	2 papers: [232, 179]
Leukoaraiosis volume	2 papers: [24, 199]
Infarct volume	10 papers: [228, 233, 201, 197, 261, 217, 179, 27, 215, 113]
Penumbra/lesion mismatch	5 papers: [198, 217, 27, 215, 214]
Perfusion lesion volume	1 papers: [197]
DWI lesion volume	3 papers: [193, 56, 230]
Baeline and 24 perilesional hyperperfusion	2 papers: [192, 176]
Type of stroke	2 papers: [116, 125]
Location of occlusion	2 papers: [116, 173]
Presence of distal HV sign	1 paper[183]
Flow diversion	1 paper: [220]
Perfusion parameters	6 papers: [189, 7, 169, 60, 87, 261]
Late cortical vein filling	1 paper: [191]
Degree of stenosis	1 paper: [87]
Thrombus extent / clot burden score	3 papers: [60, 212, 52]
History of hypertension	4 papers: [199, 172, 55, 210]
Shorter onset to treatment time	3 papers: ([173, 174, 175])
OTHER CORRELATIONS (WITH POOR COLLATERALS): Diabetes mellitus ([216, 38]), statin use [205], incomplete posterior circle of Willis ([254]), elevated baseline blood glucose ([254, 24]), evelated systolic blood pressure ([173, 55]), metabolic syndrome ([210], raised serum uric acid ([210]).	

alone.

Three methods (14, 21, 30) had both intra- and inter-observer agreement assessed, while 11 (2, 4, 6, 8, 9, 11, 12, 17, 18, 22, 23,) had only inter-rater agreement assessed, 2 (13, 29) only intra-rater agreement and the rest had no reliability assessed. In total the publications that discussed inter- and/or intra-rater agreement for scoring methods based on MRI were 19 out of 46. Two methods (7, 24) did not have reliability assessment available because they were completely automated. Where reported, the reliability was assessed using inter-/intra-class correlation coefficient (ICC) [270, 268, 183, 272, 99, 264], Cohen's Kappa (k) [69, 122, 79, 32], [252-259] or Pearson's kappa coefficient ($k_{Pearson}$) [89]. Reliability assessment always resulted in good or very good inter-/intra-rater agreement, apart from 3 publications where it was fair [273, 274, 69].

The most commonly used approach to measure collaterals on MRI consists in detecting the presence of one or more distal hyperintense vessel sign(s) on FLAIR-MRI (n. 8 in table 2.9). HV signs are described as focal, tubular or serpentine hyperintensities in the subarachnoid space against the relative hypointensity of cerebrospinal fluid (CSF). As opposed to other vessel signs that are associated with arterial insufficiency, HV does not represent a thrombus but rather sluggish and disordered blood flow which is supposedly due to leptomeningeal collaterals. This hypothesis seems to be supported by the following consideration. It is generally accepted that in presence of MCA occlusions the recruitment of leptomeningeal collaterals is induced by a pressure gradient between the ACA or PCA territory and a territory distal to the MCA occlusion site and that leptomeningeal collaterals may decrease or disappear once the occluded MCA reopens and the pressure gradient normalizes. Several studies in patients with ICA or MCA occlusion reported that HV collateral signs on initial FLAIR MR imaging disappeared within several days after early spontaneous recanalization or successful revascularization via endovascular therapy, therefore strengthening the hypothesis that HV sign may be used as an imaging marker for collaterals [28].

This association was first described by Lee et al. [275] and was used to assess collateral flow in 10 of the publications analyzed by the review. Other scoring

methods used the same criteria but introduced different grading scales (11, 12, 13, 16, 17, 20, 23). The second most common approach consists in applying the ASITN/SIR scale to 4D angiograms or collateral flow maps obtained from MRP (n. 9, 14). The rest of MRI-based methods appeared in only 2 or 1 publications and used a number of different criteria, as described in table 2.9.

A number of publications compared MRI-assessed collaterals with other imaging modalities as described in the previous sections (2.3.2, 2.3.3). In addition to these, some papers reported a comparison or a combination of different methods both based on MRI. Chen et al. [70] compared collaterals assessed on ASL-MRI and collaterals assessed based on K_{trans} maps from DCE T1 MRI with gold standard DSA-collaterals and found good agreement for the second but poor for the first method. Ernst et al. [122] compared collaterals assessed on CE-MRA and TOF-MRA both visually and computationally with DSA-assessed collaterals and they found that visual scores of CE but not TOF-MRA were as reliable a predictor of outcome as DSA-collaterals, while in the computational approach both TOF- and CE-MRA were predictive of penumbral reperfusion. Forster et al. [268] and Gawlitza et al. [276] compared HV sign on FLAIR-MRI with collaterals measured on 4D angiograoms from PWI raw images and found that there was no correlations between the two methods, but that a combination of both parameters allows a better characterization of collateral flow.

Table 2.9: MRI-based scoring methods for LM collaterals.

	Modality	Description	Grades	First author	Acute/ Non acute	Reliability assessed	Prognostic value
1	MRA	Presence of symmetrical density of signal intensity compared with opposite side	Inadequate vs adequate	Ali, 2016 [187] (380)	Acute	No	Beneficial
2	4D angiograms from MRP	Flow appearing within arterial phase of perfusion	ASITN/SIR scale (0-4)	Campbell, 2013 [270] (74)	Acute	Yes, ICC=0.85	Beneficial
				Forster, 2014 [268] (38)	Acute	Yes, ICC=0.85	Beneficial
				Forster, 2015 [269] (28)	Acute	No	Beneficial

– continues on next page –

Table 2.9 – continued from previous page

	Modality	Description	Grades	First author	Acute/ Non acute	Reliability assessed	Prognostic value
				Gawlitza, 2017 [276] (39)	Acute	No	NA
3	DCE T1-MRI	Volume transfer constant (K_{trans}) values in ASPECTS regions	0-3	Chen, 2015 [70] (7)	Acute	No	NS
4	ASL-MRI	Perfusion with/without arterial transit artifact in ASPECTS regions	0-3	Chen, 2015 [70] (7)	Acute	No	NS
				Roach, 2016 [69] (11)	Non acute	Yes, 3 readers, $k_{1,2}$=0.31-0.36, $k_{2,3}$=0.48-0.56	NA
5	7T MRA	Vascular density of collateral microvessels around steno-occlusive MCA	N/A	Choi, 2013 [265] (9)	No	No	NA
6	CE-MRA, TOP-MRA	Visual inspection of abundance of MCA vascularity distal to occlusion with respect to normal hemisphere	None/poor, fair, good/normal	Ernst, 2015 [122] (44)	Acute	Yes, k=0.70 CE-MRA, k=0.71 TOF-MRA	Beneficial
7	CE-MRA, TOP-MRA	Automated Collateral Index (CI). Ratio between hemispheres of signal intensity of MCA vascular voxels distal to M1 calculated by using atlas from normal MRAs	range 0-1	Ernst, 2015 [122] (44)	Acute	NA	Beneficial
8	FLAIR-MRI	Presence of distal hyperintense vessel sign	N/A	Forster, 2014 [268] (38)	Acute	No	No effect
				Gawlitza, 2014 [277] (33)	Acute	No	No effect
				Gawlitza, 2017 [276] (39)	Acute	No	NA
				Haussen, 2013 [273] (49)	Acute	Yes, k=0.58	NA
				Huang, 2012 [118] (29)	Acute	No	Beneficial

– continues on next page –

Table 2.9 – continued from previous page

	Modality	Description	Grades	First author	Acute/ Non acute	Reliability assessed	Prognostic value
				Kim, 2011 [123] (139)	Acute	No	NA
				Lee, 2009 [275] (52)	Acute	No	NA
				Mourand, 2016 [278] (41)	Acute	No	NS
				Pop, 2016 [105] (89)	Acute	No	NA
				Sanossian, 2009 [119] (74)	Acute	No	NA
				Kawashima, 2011 [83] (68)	Non acute	No	NA
9	Dynamic MRA, subtracted dynamic MRP-SI	Number and rapidity of collateral vessels filling	ASITN/SIR scale (0-4)	Hernández-Pérez, 2015 [279] (25)	Acute	Yes, k=0.93	NA
				Villringer, 2016 [274] (132)	Acute	Yes, k=0.58	Beneficial
10	CE T1-MRI	Comparison of pial and arachnoid enhancement between hemispheres	Mild, equivalent, prominent	Hong, 2015 [267] (31)	NA	No	NS
11	FLAIR-MRI, 3D TOF-MRA	Prominence of PCA laterality on TOF-MRA and HV sign on FLAIR as marker of collaterals	NA	Chang, 2016 [264] (87)	Mixed	Yes, ICC=0.924 PCA laterality, ICC=0.964 HV sign	NA
				Ichijo, 2013 [280] (50)	Acute	No	NA
12	FLAIR-MRI, 3D TOF-MRA	Prominence of PCA laterality on TOF-MRA and HV sign on FLAIR as marker of collaterals	PCA laterality:present/absent, positive/negative. HV sign: 0-12	Ichijo, 2015 [28] (48)	Acute	Yes, k=0.917 PCA laterality, k=0.772 HV	Beneficial
13	FLAIR-MRI	Score based on number, location and prominence of HV signs	0-2	Karadeli, 2016 [183] (39)	Acute	Yes, intra-rater ICC=0.74	NA
14	DSC-MRP	Manually and automatically generated CF maps from perfusion	ASITN/SIR scale (0-4)	Kim, 2014 [32] (134)	Acute	Yes, k_{inter}=0.82, k_{intra}=0.88	Beneficial
				Lee, 2015 [120] (66)	Acute	No	Beneficial

– continues on next page –

Table 2.9 – continued from previous page

	Modality	Description	Grades	First author	Acute/ Non acute	Reliability assessed	Prognostic value
				Son, 2017 [281] (73)	Acute	Yes, k_{inter}=0.82, k_{intra}=0.84	Beneficial
15	MRA	Visual inspection of anterior circulation and LM collaterals	Poor, moderate, good	Lescher, 2014 [124] (39)	Acute	No	Beneficial
16	FLAIR-MRI	Position of HV sign	N/A	Liu, 2011 [74] (233)	Mixed	No	NA
				Liu, 2012 [75] (11)	Mixed	No	NA
17	FLAIR-MRI	FHV extent and prominence in ASPECTS areas with (FHV-I) or without (FHV-O) infarction	N/A	Liu, 2016 [79] (101)	NS	Yes, k=0.72, FHV-Total, k=0.74 FHV-I, k=0.71 FHV-O	Beneficial
18	multi-delay 3D cASL	Presence of arterial transit artifact (ATA) on CBV maps in 10 different cortical regions	0-2	Lou, 2017 [282] (53)	Acute	Yes, k=0.83-0.92	Beneficial
19	3D-pCASL	Late arriving retrograde flow on CBF maps	N/A	Lyu, 2015 [67] (21)	Non acute	NA	NA
20	FLAIR-MRI	Location of HV sign closest to occlusion	1-5	Maurer, 2016 [283] (158)	Acute	No	No effect
21	MR-PWI	Ratio between critically and moderately hypoperfused area	Critical, moderate, total hypoperfused volume	Nicoli, 2013 [272] (64)	Acute	Yes, interrater-ICC=0.92/0.90/0.94, intrarater-ICC=0.85	Beneficial
22	MR-PWI + DWI	Volume of tissue with arterial delay time>6	N/A	Nicoli, 2014 [99]	Acute	Yes, ICC=0.994	Beneficial
23	7FLAIR-MRI	Presence of HV sign on 10 different horizontal slices starting from first M1-MCA appearance	Low, medium, high	Chang, 2016 [264]	Mixed	Yes, ICC=0.964	NA
				Olindo, 2012 [284] (105)	Acute	Yes, k=0.80	No effect
24	PWI-MR	Volume of tissue with Tmax delay > 12 s as marker or poor collaterals	Poor vs non-poor	Parsons, 2010 [68] (98)	Acute	NA	Beneficial

– continues on next page –

Table 2.9 – continued from previous page

	Modality	Description	Grades	First author	Acute/ Non acute	Reliability assessed	Prognostic value
25	DSC-PWI	Hypoperfusion intensity ration given by ratio of the Tmax>10s lesion over Tmax>6 s lesion volume	Poor, moderate, good	Potreck, 2017 [121] (47)	Acute	NA	Beneficial
26	quantitat. MRA (QMRA)	Asymetrically increased flow ipsilateral to a parent artery affected by steno-occlusive disease	N/A	Ruland, 2009 [266] (16)	Non acute	No	NA
27	MRA	rLMC: Regional assessment of LM vessel with respect to contralateral hemisphere in M1-M6 ASPECTS, basal ganglia and ACA regions	0-20	Wei, 2017 [285] (105)	Acute	No	NS
28	FLAIR-MRI, DWI, PWI	Hypoperfusion intensity ration given by ratio of the Tmax>10s lesion over Tmax>6 s lesion volume	Poor vs good	Wouters, 2016 [285] (141)	Acute	No	NA
29	3D multi-inversion time ASL	Regional CBF on ASL <0.82 as marker of poor collaterals	Poor vs good	Wu, 2016 [285] (25)	Non acute	Yes, intra-rater Pearson-k=0.871	NA
30	3D TOF MRA	Prolongation of ipsilateral PCA to the ischaemic side	NA	Yamamoto, 2015 [286] (76)	Acute	Yes, k_{inter}=0.92, k_{intra}=0.91	Beneficial

Table 2.10: List of outcome parameters most frequently reported to have a correlation with MR-assessed collaterals and corresponding publications.

Outcome parameter	Publications
mRS ≤2 at 3 months	12 papers: [118, 274, 28, 121, 32, 79, 282, 272, 284, 68, 271, 286]
mRS ≤2 at 6 months	1 paper: [280]
Death or discharge to facility other than home	1 paper: [187]
Final infarct volume	3 papers: [122, 118, 284]
Infarct growth	5 papers: [32, 270, 120, 281, 268]
Survival	1 paper: [32][1]
HT	1 paper: [79]
Recanalization TICI 2b-3)[2]	1 paper: [121]
Recanalization TIMI 2-3)[2]	4 papers: [99, 28, 280, 272]
Early improvement (NIHSS drop 24 h)	1 papers: [28]
Favorable neurological improvement	1 paper: [32][1]
NIHSS at 7 days/discharge	2 papers: [280, 28]
Follow-up ASPECTS	3 papers: [280, 28, 284]
Percentage of penumba saved	1 paper: [122]

[1]Following successful recanalization treatment.
[2] Following treatment (either by thrombolysis or mechanical intervention).

Diagnostic/prognostic value of MRI-assessed collaterals

The prognostic value of MRI-assessed collaterals was discussed in 22 publications. 3 of these found no correlation between collaterals and outcome ([277, 283, 284]) while the remaining ones found correlation with relative and absolute infarct growth, early neurological improvement, recanalization rate (TIMI score), NIHSS score at 24 h and 7 days, follow-up ASPECTS and long term functional outcome (mRS at 3 months). The two parameters that were most frequently associated with collaterals were once again the mRS at 3 months (12 papers) and infarct growth (5 papers).

Among the studies that did not assess the prognostic impact of collaterals, 19 were investigating correlation between other parameters (prognostic value N/A), while 5 analyzed outcomes but did not state whether there was an association with MR-assessed collaterals (NS) ([70, 267, 278, 188, 285]).

Better/poorer collaterals assessed with MRI were also correlated with a number of baseline imaging and clinical parameters (table 2.11). The baseline parameters most frequently reported to have a correlation with MR-assessed collaterals are baseline DWI lesion volume (9 papers), PWI lesion volume (5 papers) and PWI/DWI

Table 2.11: List of baseline parameters most frequently reported to have a correlation with MR-assessed collaterals and corresponding publications.

Baseline parameter	Publications
NIHSS	7 papers: [118, 274, 32, 120, 79, 99, 271]
DWI lesion volume	9 papers: [270, 268, 276, 279, 32, 120, 79, 272, 271]
PWI lesion volume	5 papers: [270, 276, 277, 279, 271]
PWI/DWI ratio	4 papers: [270, 268, 276, 277]
Presence of HV sign	5 papers: [277, 83, 123]*, [119, 74]**
Blood flow delay on MRP	1paper: [120]
rCBV on PWI	2 papers: [269, 268]
Stroke subtype	1paper: [32]
Cerebrovascular reserve impairment	1paper: [267]
Onset to treament time	1 paper: [281]
OTHER CORRELATIONS: Atrial fibrillation ([32]), dehydration ([264]), hyppocampal involvement ([269])	

*Depending on PSE
**Combined with degree of stenosis

volumes ratio (4 papers). Other baseline parameter frequently investigated and found to be correlated with MR-assessed collaterals were NIHSS score (7 papers) and the presence of HV sign (5 papers). Once again, one publication reported correlation between poor collaterals and shorter onset to treatment time ([281]). Other less frequently observed correlations are listed in table 2.11.

2.4 Discussion

Many studies have established that collaterals can help limit the extent of infarction prior to the restoration of reperfusion, that good LM collaterals are correlated with clinical outcome and in particular that they are associated with both smaller final infarct volume and mRS $\leq$2 at 3 months. Moreover collaterals have been correlated to a high number of baseline parameters, such as initial infarct size, NIHSS, ASPECTS and DWI/PWI mismatch.

Yet, this systematic review highlights how big the inconsistency in the assessment of LM collaterals still is, with at least 93 different methods reported in literature and no clear indication that over time the methods are becoming fewer and/or more standardized.

Three main imaging modalities are used for collateral assessment: DSA, CTA, MRI, with DSA and CTA being the most well established. TCD provides little information about CF and only at the circle of Willis and was found in only one publication. Although some of the publications reviewed presented assessment methods applicable to all vascular territories, the majority only looked at anterior circulation and in particular at MCA occlusions. A huge variety of grading scales was found, with lower numbers usually denoting bad collaterals and higher numbers indicating good collaterals, but grading criteria changing from one method to the other. Despite many scales having >3 grades, a lot of publications then used a dichotomized or trichotomized classification for the statistical analysis, since the final goal of the research is often to get a yes/no answer to whether a patient should be treated in a particular way or not. Less than half of the publications reported inter and/or intra rater agreement, but when present, the agreement was almost always good/very good, which makes it problematic to select an optimal assessment method.

DSA is still considered the gold standard for directly imaging blood vessels and it actually provides excellent temporal and spatial resolution. However it is time consuming, invasive and requires expert interventionists to perform it. CT angiographies have been proved to have really good specificity and sensitivity for the detection of proximal large vessel thrombus when compared with DSA, while requiring at the same time lower doses of contrast, having less risk of vascular complications and causing less patient discomfort than DSA. Therefore, CTA is gradually replacing conventional catheter angiography in clinical practice, especially in acute settings. This shift towards CTA is also aided by the fact that CTA is more widely available and has shorter scanning times. CTA is less expensive and easier to interpret also compared to MRA. It can reach acquisition speeds down to under 1 sec from arch to vertex [25], which is ideal for minimizing misrecording from breathing artifact and motion. In addition to these advantages, CTA poses itself as a fast natural extension of non contrast head CT, which in the majority of the stroke centers is already performed on all patients prior to thrombolytic treatment to exclude the presence of haemorrhages and large infarcts, which are contraindications for both thrombolysis and thrombectomy [11]. Thus rapid data

acquisition and postprocessing make CT-CTA a good candidate for assessment of collaterals.

CTA however has some limitations. For example, it can not provide information about flow direction. The capability of determining flow direction is a desirable feature in optimal imaging protocols for collateral assessment, since it may prevent from erroneously identifying residual anterograde flow through the occlusion as collateral flow. Moreover, conventional CTA is typically performed with single phase protocols which do not provide time resolved information and, although the time of acquisition with respect to bolus is typically quite accurate, delays in the arrival of the blood flow in the affected hemisphere may lead to mislabeling of collaterals.

The actual phase of acquisition of single-phase CTA is a crucial aspect for the correct interpretation of CTA-based collaterals. However there is disagreement regarding what is the optimal phase of contrast enhancement for collaterals assessment. It is generally agreed that the phase of peak arterial enhancement is often optimal to detect arterial occlusions stenoses and aneurysms, but may fail in capturing the arrival of delayed collateral contrast material. In line with this thinking, Kim et al. hypothesized that collaterals may be better assessed in the late venous phase [32], while Beyer et al. argued that the late venous phase may lead to an overstimation of collaterals due to concurrent enhancement of the venous vessels. Beer et al. compared different scoring systems based on both hypoattenuated volume detection and collateral vessels grading on multi-phase CTA and concluded that the degree of collateralization offers the best prognostic value when assessed during the arteriovenous phase rather than the peak arterial or late venous phase [200].

Some of the limitations of single-phase CTA may be overcome by the use of time-resolved CT imaging, such as CTP or multiphase CTA. CTP has been successfully used to assess collaterals and predict good response to intravenous thrombolysis treatment. However, it has the disadvantage of requiring longer acquisition times, additional radiation and time consuming post-processing. Moreover there is a lack of standardization in post-processing tools across vendors and there is no robust

evidence validating CTP use in identifying the penumbra [45, 287]. Tan et al. reported that CTA was better than combined CT-CTP for quantifying the degree of collateral circulation [1]. In this respect multiphase CTA might offer a simpler solution to the lack of time-resolved information in CTA and to determine flow direction and phase of contrast enhancement.

MRA is analogous to CTA, offers improved sensitivity and does not generally involve the use of ionizing radiation. Advanced MR techniques such as arterial spin labeling, can give quantitative assessment of flow velocity in addition to structural information. However, MR has the disadvantage of having more contraindications and longer acquisition times than CTA, which is undesirable in acute settings. MRA is not as readily available and easy to interpret as CTA. In general, there is a great potential for improving the feasibility and accuracy of MRI-based techniques to assess CF, but it is unlikely that MRI images will be obtained with the same efficiency as CT-based images in the very near future [288]. Moreover, from this systematic review it emerged that there is a larger variety in the assessment criteria for MRI-methods than for CT and DSA and the most commonly used methods consists in the detection of HV sign on FLAIR-MRI whose correlation with collaterals is still highly debated.

In conclusion, it is well established that collaterals influence the extension and fate of the ischaemic penumbra and that they may advance development of image-based treatments. However, assessment methods lack standardization and DSA is still used as gold-standard despite being invasive and of limited availability. In the future, noninvasive grading systems will be essential since many stroke patients do not undergo DSA and ideally even those undergoing endovascular therapy would be screened first with noninvasive imaging. It seems that time-resolved CT imaging would be an optimal candidate to replace DSA and provide whole-brain dynamic angiographic information.

Chapter 3

Quality of collateral scores on single-phase CTA

3.1 Introduction

This chapter presents the result of a retrospective study conducted at the Queen Elizabeth University Hospital in Glasgow. As previously mentioned, the use of collateral parameters in research clinical trials at the QEUH is still quite limited and is far from being implemented in the daily clinical practice. However, it is an objective of the Stroke Unit at the QEUH that collaterals parameter gradually become a part of routine assessment of stroke patients.

In order to do so, clear guidelines and faster and more reliable tools than currently available are needed. The low standardization of scoring methods and the increasingly large number of imaging modalities available make it harder to identify the optimal collateral scoring method, however some considerations can be made that narrow down the options available.

CT is the imaging modality currently available to all patients at the QEUH. CTP and/or multi-phase CTA, which provide time-resolved blood flow information, have the potential of giving more reliable collaterals assessment, but at present they are

not routinely performed on patients with suspected acute ischaemic stroke at the QEUH and their implementation in the daily practice would not be as immediate as for CTA. Baseline single-phase CTA, thanks to the lower costs, shorter acquisition time, higher availability of experienced staff and easier interpretation than CTP, is already performed on most stroke patients and is therefore the best candidate for assessing collateral vessels at the QEUH.

When measuring collaterals on single-phase CTA the timing/phase of acquisition must be taken into account. Although the automatic triggering of the scanner generally ensures that the image is acquired in the equilibrium phase, the finite resolution of the system as well as the unpredictable differences in the circulatory system of patients undergoing a stroke may cause off-time acquisitions.

With the above in mind, we decided to look at some recent stroke trials conducted at the QEUH and other centers with which the QEUH Stroke Unit has collaborated and that included both baseline single-phase CTA and time-resolved CT imaging. The aim of the study was to, firstly, investigate what the actual phase of contrast enhancement captured by the single-phase CTA scans is and, secondly, investigate how collaterals measured on single-phase CTA scans compare with collateral on time-resolved baseline imaging.

The clinical trials from which the scans were pooled were:

- the Multicentre Acute Stroke Imaging Study (MASIS) [289]
- POst Stroke Hyperglycaemia (POSH) study [290]
- the Alteplase-Tenecteplase Trial Evaluation for Stroke Thrombolysis (AT-TEST) [291]
- low-dose tenecteplase versus standard-does alteplase for acute ischaemic stroke study (Australian-TNK).

None of the above studies had multi-phase CTA imaging at baseline, however they had baseline CT perfusion. Therefore, we decided to compare single-phase CTA collaterals with collaterals measured on temporal MIP derived from CTP.

3.1.1 Clinical trials

MASIS was a multicentre prospective observational study conducted in Scotland between 2008 and 2010 and recruited 83 patients. Patients were enrolled if they had a clinical diagnosis of AIS, presented at <6 hours from symptom onset and were older than 18. Exclusions criteria included a non-AIS diagnosis prior to recruitment, inability to lie for the duration of the imaging procedures, intercurrent illness likely to cause death within 30 days, coma, chronic or acute renal failure and sensitivity to contrast for CTA or MRI imaging. Baseline imaging included either CT, CTA and CTP or MRI. The outcome was measured as mRS at 30 and 90 days.

POSH was an observational single-centre study conducted in Glasgow between 2009 and 2011 and recruited 111 patients. Patients were enrolled retrospectively after receiving routine care for acute stroke if they had undergone baseline CT, CTP and CTA. The inclusion criteria were a clinical diagnosis of AIS, age over 18 and <6 hours from symptom onset. Exclusion criteria were similar to the MASIS trial. Clinical outcome was measured as the mRS at 30 days.

The Australian-TNK study was a multicentre study conducted in three Australian stroke centres between 2008 and 2011 that recruited 75 patients, whereas ATTEST was a single centre study performed in Glasgow between 2011 and 2013 that recruited 105 patients.

Both the Australian-TNK and ATTEST trials were prospective, randomized, open-label, blinded endpoint studies that sought to compare the efficacy and safety of alteplase and tenecteplase. They recruited patients with supratentorial acute ischaemic stroke that were eligible for thrombolysis and used clinical and imaging biomarkers for outcome evaluation. The inclusion criteria were age >18, and time from symptom onset <4.5 hours for ATTEST and <6 hours for the Australian-TNK trial. Patients with major early ischaemic change on non-contrast CT were excluded.

Table 3.1: Classification of occlusions based on type and/or site of the occlusion.

Occlusion	Description
ICA	L- or T-shaped occlusion at the ICA-MCA bifurcation
PROX M1	Proximal M1 occlusion, defined as an occlusion in the first 10 mm of the M1 segment of the MCA
DIST M1	Distal M1 occlusion, defined as an occlusiono in the remaining portion of the M1 segment of the MCA
MCA-M2	Occlusion in the M2 portion of the MCA
PCA	Occlusion in the posterior cerebral artery
ACA	Occlusion in the anterior cerebral artery

3.2 Materials and methods

3.2.1 Site of occlusion

All the scans were assessed for the presence of occlusions by using the licensed imaging softare MIStar [292]. The scans were evaluated by looking at maxium intensty projection of variable thickness (5, 10, 15 and 20 mm). Each occlusion was classified according to the hemisphere, left or right. Each occlusion was further scored based on site and type of occlusion according to the classification reported in table 3.1.

All the scans were scored by consensus of at least two experienced stroke neurologists or neuroradiologists. Cases from POSH and MASIS were scored by Prof. Keith Muir (>10 years experience), Dr. Christopher Pollard (∼2 year experience) and Dr. Sin Yee Foo (∼2 year experience). For the cases of the ATTEST and Australian-TNK studies, previous scores were available and only scans with reported occlusions were analyzed. Two raters (K.M. and S.Y.F.) scored the site of occlusions by consensus. When the score was in disagreement with the previously reported score, the latest score was retained.

Table 3.2: CTA-based collateral scoring system proposed by Tan et al. [1].

Score	Description
0	Absent collaterals
1	Collaterals filling ≤50% of the occluded territory
2	Collaterals filling >50% but <100% of the occluded territory
3	Collaterals filling 100% of the occluded territory

3.2.2 Assessment of collaterals on single phase CTA

For all the scans that were found to have an occlusion, collaterals were assessed on single-phase CTA, by looking at MIPs of 20 mm thickness on the MIStar software. The collateral scores were determined by consensus of two raters (K.M. and S.Y.F.).

Collaterals were scored according to a method presented by Tan et al. and reported in table 3.2 [1]. This was selected based on the results of the systematic review presented in chapter 2 which showed it was the most used scale for assessment of collaterals on CTA angiography (reported in 54 publications). The raters were provided with an example image for each score prior to the assessment (figure 3.1).

3.2.3 Assessment of collaterals on tMIP from CTP

For each scan with ICA or MCA occlusion and with baseline CTP available, collaterals were scored using the scale proposed by Tan (table 3.2) on temporal MIPs. The processing of CTP scans and analysis of the temporal MIPs was done by radiologist S.Y.F. using the MIStar software and according to a method proposed by Smit et al. [182].

For each CTP scan 3 temporal MIPs were derived, corresponding to the arterial, equilibrium (or arteriovenous) and venous phase. Each temporal MIP was automatically reconstructed by taking for each pixel the the maximal enhancement over time relative to the selected time interval.

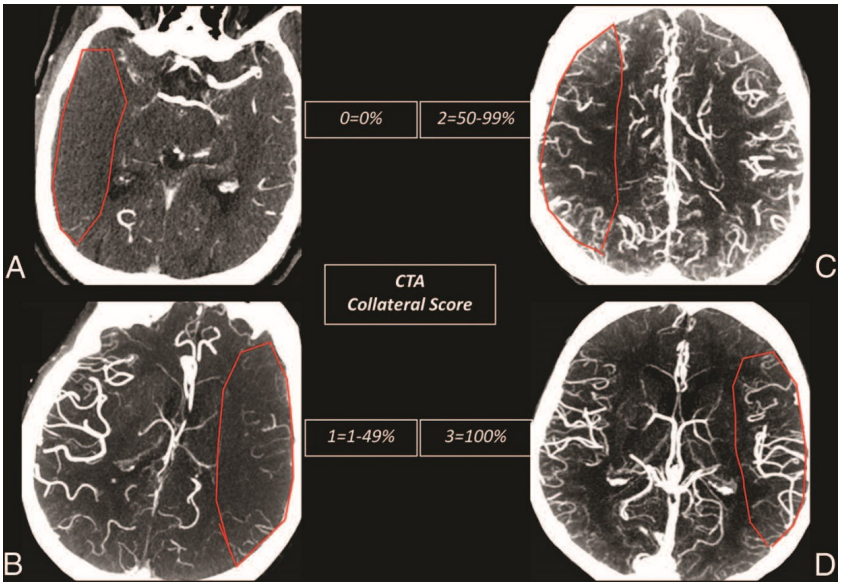

Figure 3.1: Axial 20-mm images illustrating the collateral scoring methodology proposed by Tan et al. (source of image: Dehkharghani et al., 2015[7]). The red ROI indicates a pathologic MCA territory.

For each phase of ecah scan, collaterals were then scored by using again the scale proposed by Tan et al. (table 3.2). Scores were determined independently by two radiologists (S.Y.F. and Dr. Amith Sitaram, $>$ 5 years experience) and agreement was reached by consensus in case of discrepancy.

3.2.4 Phase of acquisition of CTA scans

Each case for which temporal-MIP were reconstructed was then re-examined in order to determine the phase of acquisition of the single-phase CTA scan. The phases of scans from the POSH, MASIS and ATTEST studies were determined by M.G. and the phases of the Australian-TNK were determined by both M.G. and S.Y.F.

In order to calculate the phase we adopted a procedure proposed by Casault et al. [2]. The method as presented by Casault involves the following steps:

1. measure the maximum Hounsfield Unit (HU) in the intracranial portion of

Table 3.3: HU thresholds adopted to determine the phase of image acquisition of conventional (single-phase) CTA. [2].

Phase	Arterial HU	Venous HU
Early arterial	Higher than venous vasculature	≤200
Peak arterial	≥100 higher than venous vasculature	>200
Equilibrium	<100 higher or equal to venous vasculature	>200
Peak venous	>200	Higher than arterial vasculature
Late venous	≤200	Higher than arterial vasculature

the ICA and M1 portion of the MCA and calculate the average to obtain an arterial score;

2. measure the maximum HU in the sigmoid sinus, torcula and initial portion superior sagittal sinus and calculate the average to obtain the venous score;

3. compare the arterial and venous score and establish the phase of the scan based on the threshold reported in table 3.3.

Due to the low number of scans in our study, we chose to adopt a trichotomized score in our analysis, grouping early arterial and peak arterial into a single arterial phase and peak venous and late venous into a single venous phase.

In order to locate the maximum HU of the five vasculature territories a volume of interest (VOI) was manually segmented using the open-platform software 3D Slicer [293]. 3D Slicer supports user-customized modules and is therefore a very flexible tool. The choice of using the software was mostly dictated by the fact that it allows easy export of segmented volumes and various parameters as well as the possibility of developing Python-based scripts that can be run within the application

Each scan was opened in 3D Slicer and a segmentation was manually created, the segmentation containing 5 segments, one for each of the five vascular territories

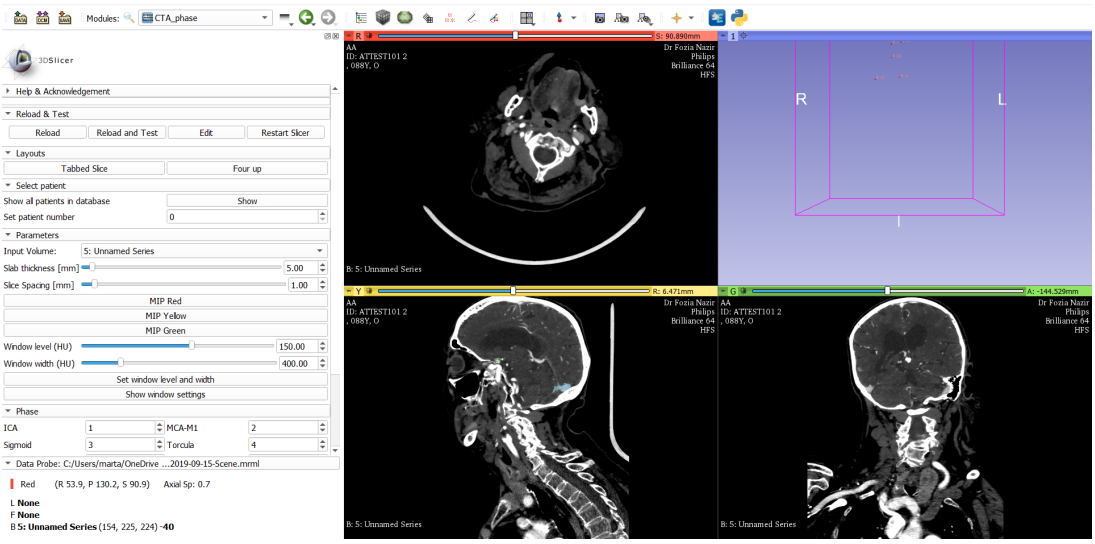

Figure 3.2: Example view of a scan being analyzed using the custome-written module in 3D Slicer.

listed above. A custom-written module was then used to automate the remaining steps. The code of the module is attached in Appendix B and was developed by using the built-in Scripted Loadable Module Python class provided by 3D Slicer. The module simply provides user-defined buttons which allow to:

- automatically locate the maximum HU within each segment;
- create a spherical ROI of unitary radius around this point;
- export the coordinates of the point with maximum HU, the volume array data of the ROI, minimum HU, average HU and maximum HU of each spherical ROI as a Python pickle object.

Figure 3.2 shows an example view of the custom built module used for the phase determination in 3D Slicer, with the module interface display in the grey panel on the left.

From the exported data the maximum HU can then be used to determine the phase as explained above either by using a simple Python script or in Excel. The rationale for using the above module was to retain segmentation data such that, if full automation of the phase calculation via machine learning is pursued in the

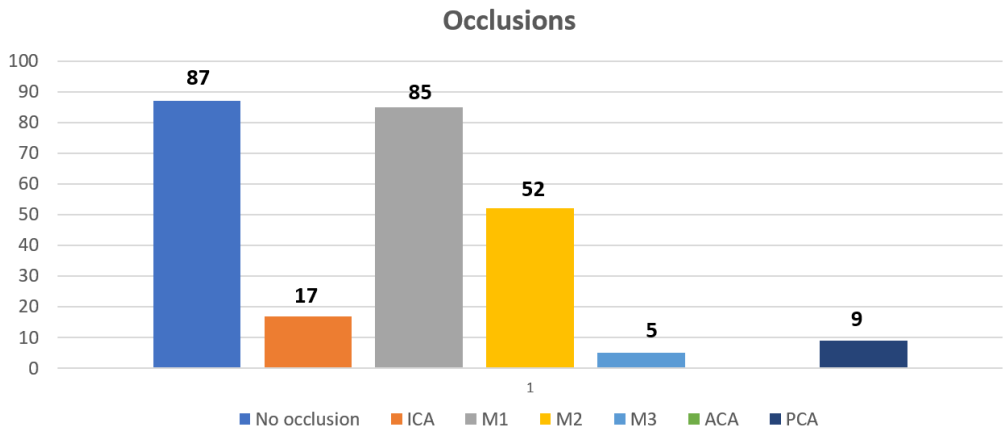

Figure 3.3: Classification of occlusions detected on the baseline CTA scans of the MASIS, POSH, ATTEST and Australian-TNK studies.

future, the segmented data may be used as training data for the algorithm.

Once the phase of each scan was estimated, CTA-based collateral scores were compared with the tMIP-based collateral score corresponding to the estimated phase. Agreement between the two score was assessed as Kappa value (analysis performed by S.Y. using SPSS [3]). K-values equal to 0.01-0.02 were rated as none to slight agreement, 0.21-0.40 as fair, 0.41-0.60 as moderate, 0.61-0.80 as substantial and 0.81-1.00 as almost perfect agreement.

3.3 Results

The total number of cases with baseline CTA retrieved from the 4 studies was 255: 38 from the MASIS study, 55 from the POSH study, 101 from the ATTEST and 61 from the Australian-TNK study. 168 of these were found to have an occlusion. The distribution of the occlusion site is illustrated in figure 3.3. No cases of ACA occlusions were detected. The majority of occlusions, as expected, was located in the MCA-M1 followed by MCA-M2 portion. Table 3.4 summarized the results of the collaterals assessment on single phase-CTA for each of the 168 cases with confirmed occlusion.

Table 3.4: Summary of collateral scores assessed on baseline single-phase CTA divided by occlusion type. One scan technically inadequate to assess collaterals. One scan had double occlusion on L/R side and could not be scored.

Score	ICA	M1	M2	M3	ACA	PCA	Total[1,2]
0	3	3	6	-	-	1	13
1	5	25	22	-	-	1	52
2	9	43	17	-	-	1	69
3	-	14	7	5	-	6	32

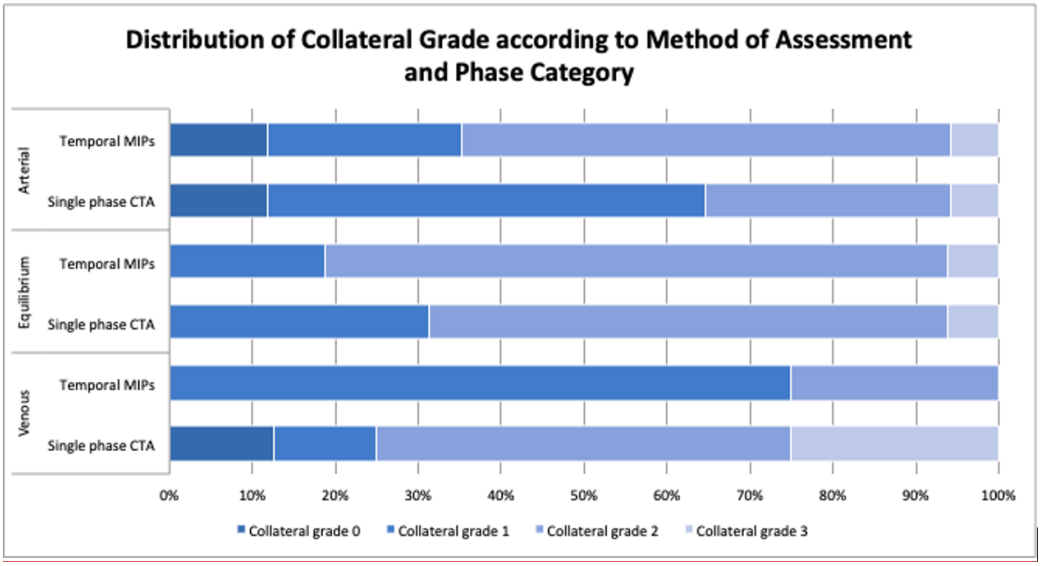

Figure 3.4: Collaterals grades by imaging modality and by phase.

Reconstruction of temporal MIPs and assessment of the acquisition phase of baseline CTA was performed only for 41 cases that had either ICA or M1 occlusions and baseline CTP available. Of these, 17 had baseline single-phase CTA acquired in arterial phase, 16 in the equilibrium phase and 8 in the venous phase. The collateral grading betweeen single phase CTA and temporal MIPs in each of the three phase is summarized in figure 3.4, whereas table 3.5 illustrates the agreement between collateral scores measured on single-phase CTA and collateral scores measured on the corresponding temporal MIP image reconstructed from CTP.

Table 3.5: Overview of the agreement between collateral scores (CS) measured on single-phase CTA and collateral scores measured on the corresponding tMIP derived from CTP, subdivided according to the phase of the single-phase CTA acquisitions. In the table, n is the number of cases recorded for each phase and K is the Kappa value. The numbers on the diagonal correspond to agreement between the two measurements, whereas the numbers off the diagonal correspond to disagreement [3].

ARTERIAL n=17

	CS	tMIP 0	1	2	3
C	0	**1**	1	0	0
	1	1	**2**	6	0
T	2	0	1	**3**	1
A	3	0	0	1	**0**

K = 0.242

EQUILIBRIUM n=16

	CS	tMIP 0	1	2	3
C	0	**0**	0	0	0
	1	0	**3**	2	0
T	2	0	0	**9**	1
A	3	0	0	1	**0**

K = 0.673

VENOUS n=8

	CS	tMIP 0	1	2	3
C	0	**0**	1	0	0
	1	0	**1**	0	0
T	2	0	4	**0**	0
A	3	0	0	2	**0**

K = 0.2

3.4 Discussion

From the above results and in particular from table 3.5, collateral scores assessed on single-phase CTA had substantial agreement with collateral score assessed on temporal MIPs in the equilibrium phase, however they only had fair agreement for CTA scans acquired in the arterial phase and none to slight agreement in the venous phase. This suggest that collaterals assessed in the equilibrium (arteriovenous) phase may be more reliable than collaterals assessed in the other phases. However more evidence and more cases should be assessed in order to confirm this hypothesis. CTA alone may not be sufficient to provide a complete assessment of recanalization (which is best done in arterial phase) and collateral status. A combination of CT, CTA and CTP or CT and multi-phase CTA would be desirable when the acquisition phase of the CTA is not known or is not in the equilibrium phase in order to provide more reliable collateral scores. Nevertheless, single-phase CTA still provide a valuable tool in assessing collaterals in acute ischaemic stroke, provided that the phase is assessed and taken into account in the interpretation of the score.

The phase assessment method described above to evaluate the actual phase of acquisition of the single-phase CTA is a time-consuming task and is not a suitable one for acute ischaemic stroke settings, where time is such as critical factor but future projects may investigate the development of an automated methods for assessing the phase and perhaps also for scoring collaterals. The main task in order to achieve automation would be providing an image processing algorithm, possibly based on machine learning or other classification techniques, that automatically identifies and segments the five vascular territories of interest for the phase calculation (ICA, M1, sigmoid sinus, torcula, superior sagittal sinus). Thereafter, it would be relatively straightforward to identify the area of maximum enhancement inside each segment and derive the phase score. This could then develop into being one step of a fully automated tool for assessment of collateral vessels on CTA, in which an algorithm determines a collateral score and the phase of the scan and the collateral score is adjusted by a correcting factor based on the phase of the scan.

Chapter 4

Conclusions

This master thesis was the result of a two year research experience at the Queen Elizabeth University Hospital in Glasgow.

The bulk of the thesis focused on the discussion of a systematic review of methods for assessing collaterals in acute ischaemic stroke. The review advances what was presented in previous reviews and shows that despite the growing acceptance of collaterals as useful imaging marker, their assessment is not yet standardized and there are no signs that suggest it will be in the near future.

The second part of the thesis reported the results of a retrospective study to which I contributed only in part and which sought to investigate the reliability of collaterals assessed on single-phase CTA as compared to collaterals measured with time-resolved imaging modalities and, in particular, with temporal-MIP reconstructed from CT perfusion.

As explained in details in the thesis, the phase of image acquisition in CT angiography has an impact on the reliability of the collateral score, since blood flow in the occluded hemisphere may be slowed down and arrive only when the contrast is already washed out in the unaffected hemisphere. Therefore, CTA-based collaterals scoring systems should take into account the phase of the scan and appropriate corrections should be applied if necessary. Our study showed that when CTA scans

are acquired in the equilibrium phase there is good agreement with collaterals score assessed on tMIP from CTP, however when CTA scans are acquired in the arterial or venous phase, there is only fair agreement. Despite the limited size of our study, this result may be seen as supporting the hypothesis that collaterals are best assessed in the arterioenous phase, as suggested by Beyer et al. [200]. However, different studies support a different hypothesis, i.e. that the best phase for collateral assessment is the late venous phase [32] indicating that there is a need for further investigation on larger sample sizes.

Although this project did not provide big research advancements, it may provide the basis for the development of an automated tool for the assessment of collaterals in acute ischaemic stroke. Automation may be achieved by a machine learning algorithm or other type of algorithm for which the data presented in the second part of the thesis may provide training datasets and the results produced by the systematic literature review may provide valuable information for selecting the best collateral scoring system.

Appendix A

Search strategy

Search strategy MEDLINE (1946 to April Week 1 2017) and EMBASE 1996 to 2017 week 17; the number in parenthesis are the results yielded by MEDLINE and EMBASE respectively:

1. exp Cerebrovascular Disorders/ (321813, 439332)

2. exp brain stem infarctions/ or exp lateral medullary syndrome/ or exp dementia, multiinfarct/ or exp vertebrobasilar insufficiency/ or exp carotidcavernous sinus fistula/ or exp moyamoya disease/ or exp cerebral small vessel diseases/ or exp cadasil/ or exp cerebral amyloid angiopathy, familial/ or exp fabry disease/ or exp melas syndrome/ or exp microscopic polyangiitis/ or exp stroke, lacunar/ or exp cerebrovascular trauma/ or exp carotid artery injuries/ or exp carotid artery, internal, dissection/ or exp vertebral artery dissection/ or exp dementia, vascular/ or exp intracranial aneurysm/ or exp intracranial arteriovenous malformations/ or exp "vein of galen malformations"/ or exp sinus thrombosis, intracranial/ or exp cavernous sinus thrombosis/ or exp lateral sinus thrombosis/ or exp sagittal sinus thrombosis/ or exp intracranial hemorrhages/ or exp cerebral hemorrhage/ or exp basal ganglia hemorrhage/ or exp putaminal hemorrhage/ or exp cerebral hemorrhage, traumatic/ or exp intracranial hemorrhage, hypertensive/ or exp intracranial hemorrhage, traumatic/ or exp brain hemorrhage, traumatic/ or exp brain stem hemorrhage, traumatic/ or exp hematoma, epidural, cranial/ or exp hematoma, subdural/ or exp hematoma, subdural, acute/ or exp hematoma, subdural, chronic/ or exp hematoma, subdural, intracranial/ or exp subarachnoid hemorrhage, traumatic/ or exp pituitary apoplexy/ or exp subarachnoid hemorrhage/ or exp leukomalacia, periventricular/ or exp sneddon syndrome/ or exp susac syndrome/ or exp vascular headaches/ or exp vasculitis, central nervous system/ or exp aids arteritis, central nervous system/ or exp giant cell arteritis/ or exp lupus vasculitis, central nervous system/ or exp vasospasm, intracranial/ (123210, 550204)

3. 1 not 2 (198697, 0)

4. exp Cerebrovascular Circulation/ (51286, 12269)

5. exp Cerebral Arteries/ (25086, 42851)

6. exp Arterial Occlusive Diseases/ (212912, 119518)

7. exp peripheral arterial disease/ or exp intermittent claudication/ or exp mesenteric vascular occlusion/ or exp moyamoya disease/ or exp renal artery obstruction/ or exp susac syndrome/ or exp stenosis, pulmonary artery/ or exp thromboangiitis obliterans/ (31985, 124189)

8. 6 not 7 (180927, 0)

9. exp Thrombosis/ (119951, 240323)

10. exp venous thrombosis/ or exp buddchiari syndrome/ or exp postthrombotic syndrome/ or exp retinal vein occlusion/ or exp thrombophlebitis/ or exp lemierre syndrome/ or exp upper extremity deep vein thrombosis/ (50773, 101200)

11. 9 not 10 (69178, 146123)

12. exp Constriction, Pathologic/ (28002, 397695)

13. 3 or 4 or 5 or 8 or 11 or 12 (486706, 554907)

14. ("stroke*" or "infarction*, brain" or "brain infarction*").mp (217311, 330753)

15. ("anterior cerebral circulation* infarction*" or "anterior circulation* brain infarction*" or "anterior circulation* infarction*, brain" or "brain infarction*, anterior circulation*" or "infarction*, anterior cerebral circulation*" or "infarction*, anterior cerebral circulation*, brain" or "infarction*, brain, anterior circulation*").mp (3, 6)

16. ("posterior cerebral circulation* infarction*" or "posterior circulation* brain infarction*" or "posterior circulation* infarction*, brain" or "brain infarction*, posterior circulation*" or "infarction*, posterior cerebral circulation*" or "infarction*, posterior cerebral circulation*, brain" or "infarction*, brain, posterior circulation*").mp (2, 3)

17. ("cerebrovascular accident*" or "accident*, cerebrovascular" or "cerebrovascular apoplex*" or "apoplex*, cerebrovascular" or "brain vascular accident*" or "vascular accident*, brain" or "cva").mp (6942, 164172)

18. ("cerebral infarction*" or "infarction*, cerebral" or "subcortical infarction*" or "infarction*, subcortical" or "anterior choroidal arter* infarction*" or "posterior choroidal arter* infarction*").mp (26832, 15669)

19. ("brain isch?emia*" or "isch?emic attack*" or "cerebral isch?emia*" or "encephalopath*, isch?emic" or "isch?emic encephalopath*" or "isch?emia*, brain" or "isch?emia*, cerebral" or "attack*, transient isch?emic" or "brain tia*" or "isch?emia*, transient cerebral" or "tia* transient isch?emic attack*" or "tia*, brain").mp (79208, 133095)

20. ("brain vascular disorder*" or "brain vascular disease*" or "cerebrovascular disease*" or "cerebrovascular disorder*" or "cerebrovascular insufficienc*" or "cerebrovascular occlusion*" or "disease*, cerebrovascular" or "insufficienc*, cerebrovascular" or "intracranial vascular disease*" or "intracranial vascular disorder*" or "occlusion*, cerebrovascular" or "vascular disease*, intracranial" or "vascular disorder*, intracranial" or "vascular disorder*, brain" or "vascular disease*, brain").mp (57210, 51761)

21. ("cerebrovascular circulation*" or "blood flow*, cerebral" or "cerebral blood flow*" or "cerebral circulation*" or "cerebral perfusion pressure*" or "circulation*, cerebral" or "circulation*, cerebrovascular" or "flow*, cerebral blood" or "perfusion pressure*, cerebral" or "pressure*, cerebral perfusion").mp (62395, 30662)

22. ("cerebral arter*" or "arter*, cerebral").mp (50991, 52469)

23. ("arter* narrowing*, carotid" or "arter* plaque*, carotid" or "arter* stenos*s, carotid" or "carotid arter* narrowing*" or "carotid arter* plaque*" or "carotid arter* stenos*s" or "carotid stenos*s" or "narrowing*, carotid arter*" or "plaque*, carotid arter*" or "stenos*s, carotid arter*").mp (16822, 13034)

24. ("carotid arter* thrombos*s" or "carotid thrombos*s" or "thrombos*s, carotid").mp (3294, 1558)

25. ("carotid arter* disease*" or "arter*disease*, carotid" or "arter* disease*, carotid" or "arter* disorder*, carotid" or "atherosclerotic disease*, carotid" or "carotid arter* disease*" or "carotid arter* disorder*" or "carotid atheroscleros*s" or "carotid atherosclerotic disease*" or "disorder*, carotid arter*").mp (22943, 15132)

26. ("arter* occlusive disease*" or "arter* obstructive disease*" or "disease*, arter* obstructive" or "disease*, arter* occlusive" or "occlusive disease*, arter*" or "obstructive disease*, arter*").mp (28694, 4407)

27. ("brain thrombos*s" or "brain thrombus" or "cerebral thrombos*s" or "cerebral thrombus" or "intracranial thrombos*s" or "intracranial thrombus" or "thrombos*s, brain" or "thrombos*s , cerebral" or "thrombos*s, intracranial" or "thrombus, brain" or "thrombus, cerebral" or "thrombus, intracranial").mp (5503, 830)

28. ("constriction* pathologic*" or "pathologic* constriction*" or "stenos*s" or "occlusion*").mp (317108, 334431)

29. ("infarction*, mca" or "embolus, mca" or "mca infarction*" or "mca circulation infarction*" or "mca embolic infarction*" or "mca embolus" or "mca infarction*" or "mca syndrome" or "mca thrombos*s" or "mca thrombotic infarction*" or "thrombos*s, mca" or "thrombotic infarction*, mca").mp (296, 513)

30. ("infarction*, middle cerebral arter*" or "embolus, middle cerebral arter*" or "middle cerebral arter* infarction*" or "middle cerebral arter* circulation infarction*" or "middle cerebral arter* embolic infarction*" or "middle cerebral arter* embolus" or "middle cerebral arter* infarction*"

or "middle cerebral arter* syndrome" or "middle cerebral arter* thrombos*s" or "middle cerebral arter* thrombotic infarction*" or "thrombos*s, middle cerebral arter*" or "thrombotic infarction*, middle cerebral arter*").mp (7192, 850)

31. ("infarction*, anterior cerebral arter*" or "embolus, anterior cerebral arter*" or "anterior cerebral arter* infarction*" or "anterior cerebral arter* circulation infarction*" or "anterior cerebral arter* embolic infarction*" or "anterior cerebral arter* embolus" or "anterior cerebral arter* infarction*" or "anterior cerebral arter* syndrome" or "anterior cerebral arter* thrombos*s" or "anterior cerebral arter* thrombotic infarction*" or "thrombos*s, anterior cerebral arter*" or "thrombotic infarction*, anterior cerebral arter*").mp (239, 52)

32. ("infarction*, posterior cerebral arter*" or "embolus, posterior cerebral arter*" or "posterior cerebral arter* infarction*" or "posterior cerebral arter* circulation infarction*" or "posterior cerebral arter* embolic infarction*" or "posterior cerebral arter* embolus" or "posterior cerebral arter* infarction*" or "posterior cerebral arter* syndrome" or "posterior cerebral arter* thrombos*s" or "posterior cerebral arter* thrombotic infarction*" or "thrombos*s, posterior cerebral arter*" or "thrombotic infarction*, posterior cerebral arter*").mp (291, 84)

33. ("infarction*, ica" or "embolus, ica" or "ica infarction*" or "ica circulation infarction*" or "ica embolic infarction*" or "ica embolus" or "ica infarction*" or "ica syndrome" or "ica thrombos*s" or "ica thrombotic infarction*" or "thrombos*s, ica" or "thrombotic infarction*, ica").mp (20, 30)

34. ("infarction*, pca" or "embolus, pca" or "pca infarction*" or "pca circulation infarction*" or "pca embolic infarction*" or "pca embolus" or "pca infarction*" or "pca syndrome" or "pca thrombos*s" or "pca thrombotic infarction*" or "thrombos*s, pca" or "thrombotic infarction*, pca").mp (37, 63)

35. 14 or 15 or 16 or 17 or 18 or 19 or 20 or 21 or 22 or 23 or 24 or 25 or 26 or 27 or 28 or 29 or 30 or 31 or 32 or 33 or 34 (675192, 758815)

36. 13 or 35 (845031, 1003439)

37. exp treatment outcome/ or exp response evaluation criteria in solid tumors/ or exp sustained virologic response/ or exp treatment failure/ or exp failure to rescue, health care/ (833128, 1245612)

38. exp response evaluation criteria in solid tumors/ or exp sustained virologic response/ (206, 1658)

39. 37 not 38 (832922, 1243954)

40. ("clinical outcome*" or "clinical effectiveness*" or "clinical efficacy" or "effectiveness*, clinical" or "efficacy, clinical" or "efficacy, treatment*" or "outcome*, treatment*" or "treatment*, effectiveness*" or "treatment* efficacy" or "treatment* outcome*").mp (920747, 1024796)

41. 39 or 40 (946087, 1472877)

42. 36 or 41 (1699411, 2317735)

43. exp Angiography/ (223904, 257778)

44. exp Magnetic Resonance Imaging/ (374612, 712411)

45. exp Tomography, XRay Computed/ (368009, 697158)

46. exp Ultrasonography, Doppler, Transcranial/ (6652, 466)

47. exp Contrast Media/ (106962, 119980)

48. ("angiograph*" or "arteriograph*" or "angiogram*").mp (265017, 254260)

49. ("magnetic resonance imaging" or "MR imaging" or "diffusion magnetic resonance" or "diffusion MR*" or "MR* diffusion weighted" or "magnetic resonance diffusion weighted" or "nuclear MRI" or "nuclear magnetic resonance imaging").mp (401710, 680466)

50. ("CT perfusion," or "comput* tomograph* perfusion" or "transmission comput* tomograph*" or "transmission CT").mp (1654, 3215)

51. ("xray* comput* tomograph*" or "xray* CT" or "x ray* comput* tomograph*" or "x ray CT").mp (4347, 8403)

52. ("tomograph*, xray* comput*" or "xray* tomograph*, comput*" or "comput* tomograph*, xray*" or "xray*, comput* tomograph*" or "comput*, xray* tomograph*" or "tomograph*, xray* comput*").mp (341442, 9963)

53. (“doppler transcranial *sonograph*" or "doppler *sonograph*, transcranial" or "*sonograph*, doppler transcranial" or "*sonograph*, transcranial doppler" or "transcranial doppler *sonograph*" or "transcranial *sonograph*, doppler").mp (1300, 1463)

54. “neurosonolog*".mp (162, 439)

55. (“contrast media" or "*contrast agent*" or "contrast material*").mp (90262, 41328)

56. 43 or 44 or 45 or 46 or 47 or 48 or 49 or 50 or 51 or 52 or 53 or 54 or 55 (994629, 1453919)

57. exp Cerebral Arteries/ (25086, 42851)

58. exp Cerebrovascular Circulation/ (51286, 12269)

59. exp Collateral Circulation/ (11720, 8316)

60. ("arteries, cerebral" or "artery, cerebral" or "cerebral arteries" or "cerebral artery").mp. (45095, 48771)

61. ("blood flow*, cerebral" or "cerebral blood flow*" or "cerebral circulation*" or "cerebral perfusion pressure*" or "cerebrovascular circulation*" or "circulation*, cerebral" or "circulation*, cerebrovascular" or "flow*, cerebral blood" or "perfusion pressure*, cerebral" or "pressure*, cerebral perfusion").mp (62395, 30662)

62. ("collateral circulation*" or "blood circulation*, collateral" or "blood collateral circulation*" or "circulation*, blood collateral" or "circulation*, collateral blood" or "circulation collateral" or "collateral blood circulation*" or "collateral circulation*, blood").mp (13932, 9939)

63. ("leptomeningeal collateral*" or "leptomeningeal vessel*" or "pial collateral*" or "pial vessel*").mp (763, 837)

64. ("collateral flow" or "collateral flows" or "collateral blood supply" or "collateral blood supplies").mp (2176, 2137)

65. ("collateral" or "collaterals").tw (33085, 30496)

66. ("recanali?ation" or "recanali? ation" or "recanali?e" or "recanali? e").mp (9229, 20476)

67. 57 or 58 or 59 or 60 or 61 or 62 or 63 or 64 or 65 or 66 (143189, 137630)

68. 42 and 56 and 67 (40226, 51456)

69. exp adult/ or exp aged/ or exp "aged, 80 and over"/ or exp frail elderly/ or exp middle aged/ or exp young adult/ (6410596, 4999208)

70. (adult* or aged or elderl*).mp (6980874, 5467682)

71. 69 or 70 (6980874, 5467710)

72. 68 and 71 (27985, 29940)

73. limit 72 to (english language and yr="2009 Current") (9357, 16487)

74. limit 73 to animals (152, 288)

75. limit 74 to humans (59, 0)

76. 74 and 75 (59, 0)

77. 74 not 76 (93, 288)

78. 73 not 77 (9264, 16199)

Appendix B

3D Slicer Module

```
import os
import vtk, qt, ctk, slicer
from slicer.ScriptedLoadableModule import *
import unittest
import logging
import numpy as np
import pickle as pkl
import SegmentStatistics
from pprint import pprint

dir = os.path.dirname(__file__)
exp_folder = os.path.join(dir, "../../../phase_HU/")

#
# CTA_phase
#
class CTA_phase(ScriptedLoadableModule):
    """Uses ScriptedLoadableModule base class"""

    def __init__(self, parent):
        ScriptedLoadableModule.__init__(self, parent)
        self.parent.title = "CTA_phase"
        self.parent.categories = ["Stroke"]
        self.parent.dependencies = []
```

```
25          self.parent.contributors = [
26            "Marta()"]
27          self.parent.helpText = """
28          For estimation of phase in CTA scans.)"""
29          self.parent.acknowledgementText = """ """
30
31  #
32  # CTA_phaseWidget
33  #
34  class CTA_phaseWidget(ScriptedLoadableModuleWidget):
35      """Uses ScriptedLoadableModuleWidget base class"""
36
37      def __init__(self, parent):
38          ScriptedLoadableModuleWidget.__init__(self, parent)
39
40      def setup(self):
41          ScriptedLoadableModuleWidget.setup(self)
42
43          self.grayscaleNode = None
44
45          # Instantiate and connect widgets ...
46
47          #
48          # Layout buttons
49          #
50          layoutsButton = ctk.ctkCollapsibleButton()
51          layoutsButton.text = "Layouts"
52          self.layout.addWidget(layoutsButton)
53          layoutsFormLayout = qt.QGridLayout(layoutsButton)
54
55          self.tabbedSliceButton= qt.QPushButton("Tabbed Slice")
56          self.tabbedSliceButton.toolTip = "Show Tabbed Slice layout "
57          self.tabbedSliceButton.enabled = True
58          layoutsFormLayout.addWidget(self.tabbedSliceButton, 0, 0)
59
60          self.fourUpButton= qt.QPushButton("Four up")
61          self.fourUpButton.toolTip = "Show Four Up Layout "
62          self.fourUpButton.enabled = True
63          layoutsFormLayout.addWidget(self.fourUpButton, 0, 1)
```

```
64
65          selectPatientCollapsibleButton = ctk.ctkCollapsibleButton()
66          selectPatientCollapsibleButton.text = "Select patient"
67          self.layout.addWidget(selectPatientCollapsibleButton)
68          selectPatientFormLayout = qt.QGridLayout(selectPatientCollapsibleButton)
69
70          #
71          # Patient Number Button
72          #
73          self.patientNumberButtonLabel = qt.QLabel("Show all patients in
                database")
74          self.patientNumberButton= qt.QPushButton("Show")
75          self.patientNumberButton.toolTip = "Prints patient numbers in your
                Slicer DICOM database"
76          self.patientNumberButton.enabled = True
77          selectPatientFormLayout.addWidget(self.patientNumberButtonLabel, 0, 0)
78          selectPatientFormLayout.addWidget(self.patientNumberButton, 0, 1)
79
80          self.patientSpinBoxLabel = qt.QLabel("Set patient number")
81          self.patientSpinBox = qt.QSpinBox()
82          self.patientSpinBox.setToolTip("Set number of patient under study")
83          self.patientSpinBox.setMinimum(0)
84          self.patientSpinBox.setMaximum(vtk.VTK_INT_MAX)
85          self.patientSpinBox.setValue(0)
86          selectPatientFormLayout.addWidget(self.patientSpinBoxLabel, 1, 0)
87          selectPatientFormLayout.addWidget(self.patientSpinBox, 1, 1)
88
89          #
90          # Parameters Area
91          #
92          parametersCollapsibleButton = ctk.ctkCollapsibleButton()
93          parametersCollapsibleButton.text = "Parameters"
94          self.layout.addWidget(parametersCollapsibleButton)
95          # Layout within the dummy collapsible button
96          self.parametersFormLayout = qt.QFormLayout(parametersCollapsibleButton)
97
98          #
99          # input volume selector
100         #
```

```
101         self.inputSelector = slicer.qMRMLNodeComboBox()
102         self.inputSelector.nodeTypes = ["vtkMRMLScalarVolumeNode"]
103         self.inputSelector.selectNodeUponCreation = True
104         self.inputSelector.addEnabled = False
105         self.inputSelector.removeEnabled = False
106         self.inputSelector.noneEnabled = False
107         self.inputSelector.showHidden = False
108         self.inputSelector.showChildNodeTypes = False
109         self.inputSelector.setMRMLScene( slicer.mrmlScene )
110         self.inputSelector.setToolTip( "Pick the input to the algorithm." )
111         self.parametersFormLayout.addRow("Input Volume: ", self.inputSelector)
112
113         #
114         # Slab thickness value
115         #
116         self.slabThicknessSliderWidget = ctk.ctkSliderWidget()
117         self.slabThicknessSliderWidget.singleStep = 1
118         self.slabThicknessSliderWidget.minimum = 1
119         self.slabThicknessSliderWidget.maximum = 100
120         self.slabThicknessSliderWidget.value = 5
121         self.slabThicknessSliderWidget.setToolTip("Set slab thickness value for
                computing MIP.")
122         self.parametersFormLayout.addRow("Slab thickness [mm]",
                self.slabThicknessSliderWidget)
123
124         #
125         # Slab slice spacing
126         #
127         self.slabSliceSpacingSliderWidget = ctk.ctkSliderWidget()
128         self.slabSliceSpacingSliderWidget.singleStep = 0.5
129         self.slabSliceSpacingSliderWidget.minimum = 0.5
130         self.slabSliceSpacingSliderWidget.maximum = 10
131         self.slabSliceSpacingSliderWidget.value = 1
132         self.slabSliceSpacingSliderWidget.setToolTip("Set slab slice spacing
                value for slice viewers.")
133         self.parametersFormLayout.addRow("Slice Spacing [mm]",
                self.slabSliceSpacingSliderWidget)
134
135         #
```

```
136         # Show MIP Button
137         #
138         self.showMIPRedButton = qt.QPushButton("MIP Red")
139         self.showMIPRedButton.toolTip = "Show MIP in red viewer"
140         self.showMIPRedButton.enabled = False
141         self.parametersFormLayout.addRow(self.showMIPRedButton)
142
143         self.showMIPYellowButton = qt.QPushButton("MIP Yellow")
144         self.showMIPYellowButton.toolTip = "Show MIP in yellow viewer"
145         self.showMIPYellowButton.enabled = False
146         self.parametersFormLayout.addRow(self.showMIPYellowButton)
147
148         self.showMIPGreenButton = qt.QPushButton("MIP Green")
149         self.showMIPGreenButton.toolTip = "Show MIP in green viewer"
150         self.showMIPGreenButton.enabled = False
151         self.parametersFormLayout.addRow(self.showMIPGreenButton)
152
153         #
154         # Window level value
155         #
156         self.windowLevelSliderWidget = ctk.ctkSliderWidget()
157         self.windowLevelSliderWidget.singleStep = 10
158         self.windowLevelSliderWidget.minimum = -1000
159         self.windowLevelSliderWidget.maximum = 1000
160         self.windowLevelSliderWidget.value = 150
161         self.windowLevelSliderWidget.setToolTip("Set window level (HU).")
162         self.parametersFormLayout.addRow("Window level (HU)",
                self.windowLevelSliderWidget)
163
164         #
165         # Window Width value
166         #
167         self.windowWidthSliderWidget = ctk.ctkSliderWidget()
168         self.windowWidthSliderWidget.singleStep = 20
169         self.windowWidthSliderWidget.minimum = 20
170         self.windowWidthSliderWidget.maximum = 2000
171         self.windowWidthSliderWidget.value = 400
172         self.windowWidthSliderWidget.setToolTip("Set window width (HU).")
173         self.parametersFormLayout.addRow("Window width (HU)",
```

```
            self.windowWidthSliderWidget)
174
175         #
176         # windowSettings Button
177         #
178         self.windowSettingsButton = qt.QPushButton("Set window level and width")
179         self.windowSettingsButton.toolTip = "Set window level and width. Fine
                adjustment with mouse."
180         self.windowSettingsButton.enabled = False
181         self.parametersFormLayout.addRow(self.windowSettingsButton)
182
183         self.getWinSettButton = qt.QPushButton('Show window settings')
184         self.getWinSettButton.toolTip = ""
185         self.getWinSettButton.enabled = True
186         self.parametersFormLayout.addRow(self.getWinSettButton)
187
188         #
189         # Add vertical spacer
190         #
191         self.layout.addStretch(1)
192
193         #
194         # Phase Arena
195         #
196         phaseCollapsibleButton = ctk.ctkCollapsibleButton()
197         phaseCollapsibleButton.text = "Phase"
198         self.layout.addWidget(phaseCollapsibleButton)
199         # Layout within the dummy collapsible button
200         phaseFormLayout = qt.QGridLayout(phaseCollapsibleButton)
201
202         #
203         # Fiducials list
204         #
205
206         #Display all fiducial points
207
208         # Set the 4 points
209         self.pOneSpinBoxLabel = qt.QLabel("ICA")
210         self.pOneSpinBox = qt.QSpinBox()
```

```
211         self.pOneSpinBox.setToolTip("Fiducial point in ICA")
212         self.pOneSpinBox.setMinimum(0)
213         self.pOneSpinBox.setMaximum(vtk.VTK_INT_MAX)
214         self.pOneSpinBox.setValue(1)
215         phaseFormLayout.addWidget(self.pOneSpinBoxLabel, 0, 0)
216         phaseFormLayout.addWidget(self.pOneSpinBox, 0, 1)
217
218         self.pTwoSpinBoxLabel = qt.QLabel("MCA-M1")
219         self.pTwoSpinBox = qt.QSpinBox()
220         self.pTwoSpinBox.setToolTip("Fiducial point in MCA-M1")
221         self.pTwoSpinBox.setMinimum(0)
222         self.pTwoSpinBox.setMaximum(vtk.VTK_INT_MAX)
223         self.pTwoSpinBox.setValue(2)
224         phaseFormLayout.addWidget(self.pTwoSpinBoxLabel, 0, 2)
225         phaseFormLayout.addWidget(self.pTwoSpinBox, 0, 3)
226
227         self.pThreeSpinBoxLabel = qt.QLabel("Sigmoid")
228         self.pThreeSpinBox = qt.QSpinBox()
229         self.pThreeSpinBox.setToolTip("Fiducial point in sigmoid sinus")
230         self.pThreeSpinBox.setMinimum(0)
231         self.pThreeSpinBox.setMaximum(vtk.VTK_INT_MAX)
232         self.pThreeSpinBox.setValue(3)
233         phaseFormLayout.addWidget(self.pThreeSpinBoxLabel, 1, 0)
234         phaseFormLayout.addWidget(self.pThreeSpinBox, 1, 1)
235
236         self.pFourSpinBoxLabel = qt.QLabel("Torcula")
237         self.pFourSpinBox = qt.QSpinBox()
238         self.pFourSpinBox.setToolTip("Fiducial point in sigmoid torcula")
239         self.pFourSpinBox.setMinimum(0)
240         self.pFourSpinBox.setMaximum(vtk.VTK_INT_MAX)
241         self.pFourSpinBox.setValue(4)
242         phaseFormLayout.addWidget(self.pFourSpinBoxLabel, 1, 2)
243         phaseFormLayout.addWidget(self.pFourSpinBox, 1, 3)
244
245         self.pFiveSpinBoxLabel = qt.QLabel("Sup Sag S")
246         self.pFiveSpinBox = qt.QSpinBox()
247         self.pFiveSpinBox.setToolTip("Superior sagittal sinus")
248         self.pFiveSpinBox.setMinimum(0)
249         self.pFiveSpinBox.setMaximum(vtk.VTK_INT_MAX)
```

```
250         self.pFiveSpinBox.setValue(5)
251         phaseFormLayout.addWidget(self.pFiveSpinBoxLabel, 2, 0)
252         phaseFormLayout.addWidget(self.pFiveSpinBox, 2, 1)
253 
254         self.radiusSpinBoxLabel = qt.QLabel("Radius of seed")
255         self.radiusSpinBox = qt.QSpinBox()
256         self.radiusSpinBox.setToolTip("Set radius of seed")
257         self.radiusSpinBox.setMinimum(0)
258         self.radiusSpinBox.setMaximum(vtk.VTK_INT_MAX)
259         self.radiusSpinBox.setValue(1)
260         phaseFormLayout.addWidget(self.radiusSpinBoxLabel, 2, 2)
261         phaseFormLayout.addWidget(self.radiusSpinBox, 2, 3)
262 
263         self.listFiducialsButton= qt.QPushButton("List points")
264         self.listFiducialsButton.toolTip = "Prints all fiducial points in the
                terminal"
265         self.listFiducialsButton.enabled = True
266         phaseFormLayout.addWidget(self.listFiducialsButton, 3, 1)
267 
268         self.getPhaseButton= qt.QPushButton("Get phase")
269         self.getPhaseButton.toolTip = "Prints all fiudcial points in the
                terminal"
270         self.getPhaseButton.enabled = True
271         phaseFormLayout.addWidget(self.getPhaseButton, 3, 3)
272 
273         # Output table selector
274         outputCollapsibleButton = ctk.ctkCollapsibleButton()
275         outputCollapsibleButton.text = "Output"
276         self.layout.addWidget(outputCollapsibleButton)
277         outputFormLayout = qt.QFormLayout(outputCollapsibleButton)
278 
279         self.outputTableSelector = slicer.qMRMLNodeComboBox()
280         self.outputTableSelector.nodeTypes = ["vtkMRMLTableNode"]
281         self.outputTableSelector.addEnabled = True
282         self.outputTableSelector.selectNodeUponCreation = True
283         self.outputTableSelector.renameEnabled = True
284         self.outputTableSelector.removeEnabled = True
285         self.outputTableSelector.noneEnabled = False
286         self.outputTableSelector.setMRMLScene( slicer.mrmlScene )
```

```
287         self.outputTableSelector.setToolTip( "Select the table where statistics
                will be saved into")
288         outputFormLayout.addRow("Output table:", self.outputTableSelector)
289
290         #
291         # Add vertical spacer
292         #
293         self.layout.addStretch(1)
294
295         #
296         # Reset view to default Button
297         #
298         self.undoMIPButton = qt.QPushButton("Default view")
299         self.undoMIPButton.toolTip = "Reset view to default mode"
300         self.undoMIPButton.enabled = False
301         self.layout.addWidget(self.undoMIPButton)
302
303         #
304         # Reset Scene Button
305         #
306         self.clearSceneButton = qt.QPushButton("Clear scene")
307         self.clearSceneButton.toolTip = "Clear the mrml scene"
308         self.clearSceneButton.enabled = True
309         self.layout.addWidget(self.clearSceneButton)
310
311         #
312         # Connections
313         #
314         self.showMIPRedButton.connect('clicked(bool)', self.onShowMIPRedButton)
315         self.showMIPYellowButton.connect('clicked(bool)',
                self.onShowMIPYellowButton)
316         self.showMIPGreenButton.connect('clicked(bool)',
                self.onShowMIPGreenButton)
317
318         self.getWinSettButton.connect('clicked(bool)', self.onGetWinSettButton)
319         self.windowSettingsButton.connect('clicked(bool)',
                self.onWindowSettingsButton)
320         self.inputSelector.connect("currentNodeChanged(vtkMRMLNode*)",
                self.onSelect)
```

```
321         self.patientNumberButton.connect('clicked(bool)',
                self.onPatientNumberButton)
322         self.tabbedSliceButton.connect('clicked(bool)',
                self.onTabbedSliceButton)
323         self.fourUpButton.connect('clicked(bool)', self.onFourUpButton)
324         self.listFiducialsButton.connect('clicked(bool)',
                self.onListFiducialsButton)
325         self.getPhaseButton.connect('clicked(bool)', self.onGetPhaseButton)
326         self.undoMIPButton.connect('clicked(bool)', self.onUndoMIPButton)
327         self.clearSceneButton.connect('clicked(bool)', self.onClearSceneButton)
328 
329         #
330         # Add vertical spacer
331         #
332         self.layout.addStretch(2)
333 
334         # Refresh drawMidLine button state
335         self.onSelect()
336 
337     def onSelect(self):
338         self.showMIPRedButton.enabled = self.inputSelector.currentNode()
339         self.showMIPYellowButton.enabled = self.inputSelector.currentNode()
340         self.showMIPGreenButton.enabled = self.inputSelector.currentNode()
341 
342         self.windowSettingsButton.enabled = self.inputSelector.currentNode()
343         self.listFiducialsButton.enabled = self.inputSelector.currentNode()
344         self.undoMIPButton.enabled = self.inputSelector.currentNode()
345 
346     def onPatientNumberButton(self):
347         logic = CTA_phaseLogic()
348         logic.showPatientNumbers()
349 
350     def onTabbedSliceButton(self):
351       logic = CTA_phaseLogic()
352       logic.selTabbedSliceLayout()
353 
354     def onFourUpButton(self):
355       logic = CTA_phaseLogic()
356       logic.selFourUpLayout()
```

```
357
358     def onShowMIPRedButton(self):
359         logic = CTA_phaseLogic()
360         patientNumber = self.patientSpinBox.value
361         slabThickness = self.slabThicknessSliderWidget.value
362         slabSliceSpacingFraction = self.slabSliceSpacingSliderWidget.value
363         logic.showMIPRed(self.inputSelector.currentNode(), slabThickness,
                slabSliceSpacingFraction, patientNumber)
364
365     def onShowMIPYellowButton(self):
366         logic = CTA_phaseLogic()
367         patientNumber = self.patientSpinBox.value
368         slabThickness = self.slabThicknessSliderWidget.value
369         slabSliceSpacingFraction = self.slabSliceSpacingSliderWidget.value
370         logic.showMIPYellow(self.inputSelector.currentNode(), slabThickness,
                slabSliceSpacingFraction, patientNumber)
371
372     def onShowMIPGreenButton(self):
373         logic = CTA_phaseLogic()
374         patientNumber = self.patientSpinBox.value
375         slabThickness = self.slabThicknessSliderWidget.value
376         slabSliceSpacingFraction = self.slabSliceSpacingSliderWidget.value
377         logic.showMIPGreen(self.inputSelector.currentNode(), slabThickness,
                slabSliceSpacingFraction, patientNumber)
378
379     def onWindowSettingsButton(self):
380         logic = CTA_phaseLogic()
381         windowWidth = self.windowWidthSliderWidget.value
382         windowLevel = self.windowLevelSliderWidget.value
383         logic.windowSettings(self.inputSelector.currentNode(), windowWidth,
                windowLevel)
384
385     def onGetWinSettButton(self):
386         logic = CTA_phaseLogic()
387         logic.getWindowSettings()
388
389     def onListFiducialsButton(self):
390         logic = CTA_phaseLogic()
391         logic.listFiducials(self.inputSelector.currentNode())
```

```
392
393     def onGetPhaseButton(self):
394
395         # Lock GUI
396         self.getPhaseButton.text = "Working..."
397         self.getPhaseButton.setEnabled(False)
398         slicer.app.processEvents()
399
400         logic = CTA_phaseLogic()
401
402         patientNumber = self.patientSpinBox.value
403         p1 = self.pOneSpinBox.value - 1
404         p2 = self.pTwoSpinBox.value - 1
405         p3 = self.pThreeSpinBox.value - 1
406         p4 = self.pFourSpinBox.value - 1
407         p5 = self.pFiveSpinBox.value - 1
408
409         radius = self.radiusSpinBox.value
410         logic.getPhase(self.inputSelector.currentNode(), patientNumber, p1, p2,
                p3, p4, p5, radius)
411
412         # Unlock GUI
413         self.getPhaseButton.setEnabled(True)
414         self.getPhaseButton.text = "Get phase"
415
416     def onUndoMIPButton(self):
417         logic = CTA_phaseLogic()
418         logic.MIPreset()
419
420     def onClearSceneButton(self):
421         slicer.mrmlScene.Clear(0)
422         CTA_phaseLogic().MIPreset()
423
424 #
425 # CTA_phaseLogic
426 #
427 class CTA_phaseLogic(ScriptedLoadableModuleLogic):
428     """This class should implements all the actual
429     computation done by the module."""
```

```
430
431     def selTabbedSliceLayout(self):
432   layoutManager = slicer.app.layoutManager()
433   layoutManager.setLayout(slicer.vtkMRMLLayoutNode.SlicerLayoutTabbedSliceView)
434
435     def selFourUpLayout(self):
436   layoutManager = slicer.app.layoutManager()
437   layoutManager.setLayout(slicer.vtkMRMLLayoutNode.SlicerLayoutFourUpView)
438
439     def showPatientNumbers(self):
440         # Print list of all patients in Slicer DICOM database so the user can
              see the number of each patient to access
441         # metadata
442         self.db = slicer.dicomDatabase
443         self.patientList = self.db.patients()
444         for i in range(len(self.patientList)):
445             patientID = self.getPatientID(i)
446             print 'PatientID', '=', patientID, ' -> Patient N.=', i
447         return
448
449     def getPatientID(self, patientNumber):
450         # Get patientID from metadata for a given patient in Slicer DICOM
              database
451         database = slicer.dicomDatabase
452         patList = database.patients()
453         stList = database.studiesForPatient(patList[patientNumber])
454         serList = database.seriesForStudy(stList[0])
455         flList = database.filesForSeries(serList[0])
456         patID = database.fileValue(flList[0], '0010,0020')
457         return patID
458
459     def getSliceThicknessAndSpacing(self, patientNumber):
460         """Get slice spacing and thickness from metadata in DICOM database for
              a given patient in Slicer DICOM database
461             """
462         self.db = slicer.dicomDatabase
463         self.patientList = self.db.patients()
464         self.studyList =
              self.db.studiesForPatient(self.patientList[patientNumber])
```

```
465         self.seriesList = self.db.seriesForStudy(self.studyList[0])
466         self.fileList = self.db.filesForSeries(self.seriesList[0])
467         sliceThickness = float(self.db.fileValue(self.fileList[0], '0018,0050'))
468         sliceSpacing = float(self.db.fileValue(self.fileList[0], '0018,0050'))
469 
470         # sliceSpacing = float(self.db.fileValue(self.fileList[0], '0018,0088'))
471         return sliceThickness, sliceSpacing
472 
473     def currentSliceInViewers(self, color):
474         """Get current slice in <color> view in RAS coordinate. In Slicer
                colors represent the different views:
475         axial (red), sagittal (yellow) and coronal (green)
476             """
477         lm = slicer.app.layoutManager()
478         sw = lm.sliceWidget(color)
479         sl = sw.sliceLogic()
480         current_slice = sl.GetSliceOffset()
481         return current_slice
482 
483     def convertRedSliceToIjk(self, inputVolume, sliceRAS):
484         """Convert a slice number given in RAS coordinate into slice number in
                IJK coordinates
485             """
486         current_slice_RAS = sliceRAS
487         rasToIjkMatrix = vtk.vtkMatrix4x4()
488         inputVolume.GetRASToIJKMatrix(rasToIjkMatrix)
489         current_sliceIJK = rasToIjkMatrix.MultiplyPoint([1, 1,
                current_slice_RAS, 1])[2]
490         return current_sliceIJK
491 
492     def convertPointToIjk(self, inputVolume, point_ras):
493         # Convert a point in ras coordinates into ijk coordinates
494         point_ras_coord = point_ras[:]
495         point_ras_coord.append(1)
496         rasToIjkMatrix = vtk.vtkMatrix4x4()
497         inputVolume.GetRASToIJKMatrix(rasToIjkMatrix)
498         point_ijk_coord = rasToIjkMatrix.MultiplyPoint(point_ras_coord)
499         return point_ijk_coord[0:3]
500 
```

```
501     def transformPoint(self, transf_matrix, point):
502         """Transform point to new coordinate system given transformation matrix
503             """
504         temp_point = point
505         temp_point.append(1)
506         transf_point = transf_matrix.MultiplyPoint(temp_point)
507         return transf_point[0:3]
508 
509     def MIPreset(self):
510         """ Reset slice viewers to default setting (no MIP).
511             """
512         print "Disabling MIP in the slice viewers"
513         sliceNode = None
514         sliceLogic = None
515         for slice_color in ["Green", "Red", "Yellow"]:
516             vtkMRMLSliceNode = 'vtkMRMLSliceNode' + slice_color
517             sliceNode = slicer.mrmlScene.GetNodeByID(vtkMRMLSliceNode)
518             if sliceNode:
519                 appLogic = slicer.app.applicationLogic()
520             if appLogic:
521                 sliceLogic = appLogic.GetSliceLogic(sliceNode)
522             if not sliceNode or not sliceLogic:
523                 print "Something is wrong, sliceNode or sliceLogic not found"
524                 return
525             sliceLayerLogic = sliceLogic.GetBackgroundLayer()
526             reslice = sliceLayerLogic.GetReslice()
527             reslice.SetSlabModeToMax()
528             reslice.SetSlabNumberOfSlices(1)
529             reslice.SetSlabSliceSpacingFraction(1)
530             sliceNode.Modified()
531         return
532 
533     def showMIPRed(self, inputVolume, slabThickness, slabSliceSpacingFraction,
        patientNumber):
534         """ Show maximum intensity projection in the 3 slice viewers. Does not
            change scalar volume, only modifies
535         viewing settings.
536             """
537 
```

```
538         print "\nShowing MIP in the axial view"
539         sliceNode = None
540         sliceLogic = None
541 
542         vtkMRMLSliceNode = 'vtkMRMLSliceNodeRed'
543         sliceNode = slicer.mrmlScene.GetNodeByID(vtkMRMLSliceNode)
544         if sliceNode:
545             appLogic = slicer.app.applicationLogic()
546         if appLogic:
547             sliceLogic = appLogic.GetSliceLogic(sliceNode)
548         if not sliceNode or not sliceLogic:
549             print "Something is wrong, sliceNode or sliceLogic not found"
550             return
551         sliceThickness, sliceSpacing =
                self.getSliceThicknessAndSpacing(patientNumber)
552         n_of_slices = int((slabThickness - sliceThickness) / sliceSpacing + 1)
553         spacing_fraction = slabSliceSpacingFraction
554         print "Slice thickness = ", sliceThickness, "mm"
555         print "Slice spacing = ", sliceSpacing, "mm"
556         print "Number of slices in MIP = ", n_of_slices
557         print "Actual slab thickness = ", sliceSpacing * (n_of_slices - 1) +
                sliceThickness, "mm \n"
558         sliceLayerLogic = sliceLogic.GetBackgroundLayer()
559         self.reslice = sliceLayerLogic.GetReslice()
560         self.reslice.SetSlabModeToMax()
561         self.reslice.SetSlabNumberOfSlices(n_of_slices)
562         self.reslice.SetSlabSliceSpacingFraction(spacing_fraction)
563         sliceNode.Modified()
564         return
565 
566     def showMIPYellow(self, inputVolume, slabThickness,
            slabSliceSpacingFraction, patientNumber):
567         """ Show maximum intensity projection in the 3 slice viewers. Does not
                change scalar volume, only modifies
568         viewing settings.
569         """
570 
571         print "\nShowing MIP in the sagittal view"
572         sliceNode = None
```

```
573         sliceLogic = None
574 
575         vtkMRMLSliceNode = 'vtkMRMLSliceNodeYellow'
576         sliceNode = slicer.mrmlScene.GetNodeByID(vtkMRMLSliceNode)
577         if sliceNode:
578             appLogic = slicer.app.applicationLogic()
579         if appLogic:
580             sliceLogic = appLogic.GetSliceLogic(sliceNode)
581         if not sliceNode or not sliceLogic:
582             print "Something is wrong, sliceNode or sliceLogic not found"
583             return
584         sliceThickness, sliceSpacing =
                self.getSliceThicknessAndSpacing(patientNumber)
585         n_of_slices = int((slabThickness - sliceThickness) / sliceSpacing + 1)
586         spacing_fraction = slabSliceSpacingFraction
587         print "Slice thickness = ", sliceThickness, "mm"
588         print "Slice spacing = ", sliceSpacing, "mm"
589         print "Number of slices in MIP = ", n_of_slices
590         print "Actual slab thickness = ", sliceSpacing * (n_of_slices - 1) +
                sliceThickness, "mm \n"
591         sliceLayerLogic = sliceLogic.GetBackgroundLayer()
592         self.reslice = sliceLayerLogic.GetReslice()
593         self.reslice.SetSlabModeToMax()
594         self.reslice.SetSlabNumberOfSlices(n_of_slices)
595         self.reslice.SetSlabSliceSpacingFraction(spacing_fraction)
596         sliceNode.Modified()
597         return
598 
599     def showMIPGreen(self, inputVolume, slabThickness,
            slabSliceSpacingFraction, patientNumber):
600         """ Show maximum intensity projection in the 3 slice viewers. Does not
                change scalar volume, only modifies
601         viewing settings.
602         """
603 
604         print "\nShowing MIP in the coronal view"
605         sliceNode = None
606         sliceLogic = None
607 
```

```
608         vtkMRMLSliceNode = 'vtkMRMLSliceNodeGreen'
609         sliceNode = slicer.mrmlScene.GetNodeByID(vtkMRMLSliceNode)
610         if sliceNode:
611             appLogic = slicer.app.applicationLogic()
612         if appLogic:
613             sliceLogic = appLogic.GetSliceLogic(sliceNode)
614         if not sliceNode or not sliceLogic:
615             print "Something is wrong, sliceNode or sliceLogic not found"
616             return
617         sliceThickness, sliceSpacing =
                self.getSliceThicknessAndSpacing(patientNumber)
618         n_of_slices = int((slabThickness - sliceThickness) / sliceSpacing + 1)
619         spacing_fraction = slabSliceSpacingFraction
620         print "Slice thickness = ", sliceThickness, "mm"
621         print "Slice spacing = ", sliceSpacing, "mm"
622         print "Number of slices in MIP = ", n_of_slices
623         print "Actual slab thickness = ", sliceSpacing * (n_of_slices - 1) +
                sliceThickness, "mm \n"
624         sliceLayerLogic = sliceLogic.GetBackgroundLayer()
625         self.reslice = sliceLayerLogic.GetReslice()
626         self.reslice.SetSlabModeToMax()
627         self.reslice.SetSlabNumberOfSlices(n_of_slices)
628         self.reslice.SetSlabSliceSpacingFraction(spacing_fraction)
629         sliceNode.Modified()
630         return
631
632     def windowSettings(self, inputVolume, windowWidth, windowLevel):
633         nodeID = inputVolume.GetID()
634         volumeNode = slicer.util.getNode(nodeID)
635         displayNode = volumeNode.GetDisplayNode()
636         displayNode.AutoWindowLevelOff()
637         displayNode.SetWindowLevel(windowWidth, windowLevel)
638
639     def getWindowSettings(self):
640         appLogic = slicer.app.applicationLogic()
641         sliceNode = slicer.mrmlScene.GetNodeByID('vtkMRMLSliceNodeRed')
642         sliceLogic = appLogic.GetSliceLogic(sliceNode)
643         window = vtk.mutable(0.0)
644         level = vtk.mutable(0.0)
```

```
645         high = vtk.mutable (0.0)
646         low = vtk.mutable(0.0)
647         sliceLogic.GetBackgroundWindowLevelAndRange(window, level, low, high)
648         print "Window = ", window
649         print "Level = ", level
650 
651     def listFiducials(self, inputVolume):
652         fidList = slicer.util.getNode('F')
653         numFids = fidList.GetNumberOfFiducials()
654         for i in range(numFids):
655             ras = [0, 0, 0]
656             fidList.GetNthFiducialPosition(i, ras)
657             print "Fid", i+1, ": RAS = ", ras, ", label = ",
                    fidList.GetNthFiducialLabel(i)
658         return
659 
660     def getPhase(self, inputVolume, patientNumber, p1, p2, p3, p4, p5, radius):
661         segmentationNode = slicer.vtkMRMLSegmentationNode()
662         slicer.mrmlScene.AddNode(segmentationNode)
663         segmentationNode.CreateDefaultDisplayNodes()
664         segmentationNode.SetReferenceImageGeometryParameterFromVolumeNode(
665             inputVolume)
666 
667         fidList = slicer.util.getNode('F')
668 
669         # For scans where superior sagittal sinus is out of scanned volume
670         if p5 == -1:
671             p = [p1, p2, p3, p4]
672             colours = ([1.0, 0.0, 0.0], [1.0, 0.5, 1.0], [0.0, 1.0, 0.0], [0.0,
                        0.0, 1.0])
673             segm_names = ('ICA', 'MCA-M1', 'SIGMOID', 'TORCULA')
674         else:
675             p = [p1, p2, p3, p4, p5]
676             colours = ([1.0, 0.0, 0.0], [1.0, 0.5, 1.0], [0.0, 1.0, 0.0], [0.0,
                        0.0, 1.0], [0.5, 0.0, 1.0])
677             segm_names = ('ICA', 'MCA-M1', 'SIGMOID', 'TORCULA', 'SUP SAG
                        SINUS')
678 
679         p_append = vtk.vtkAppendPolyData()
```

```
680         p_coords = []
681 
682         for i in range(len(p)):
683             ras = [0, 0, 0]
684             fidList.GetNthFiducialPosition(i, ras)
685             vess_seed = vtk.vtkSphereSource()
686             vess_seed.SetCenter(ras)
687             vess_seed.SetRadius(radius)
688             vess_seed.Update()
689             p_coords.append(ras)
690 
691             segmentID =
                    segmentationNode.AddSegmentFromClosedSurfaceRepresentation(
692                 vess_seed.GetOutput(), segm_names[i], colours[i])
693 
694         resultsTableNode = slicer.vtkMRMLTableNode()
695         slicer.mrmlScene.AddNode(resultsTableNode)
696 
697         statLogic = SegmentStatistics.SegmentStatisticsLogic()
698         statLogic.getParameterNode().SetParameter("Segmentation",
                segmentationNode.GetID())
699         statLogic.getParameterNode().SetParameter("ScalarVolume",
                inputVolume.GetID())
700         statLogic.computeStatistics()
701         statLogic.exportToTable(resultsTableNode)
702         statLogic.showTable(resultsTableNode)
703         stat = statLogic.getStatistics()
704 
705         del stat['MeasurementInfo']
706         patientID = self.getPatientID(patientNumber)
707 
708 
709         results_fileName = exp_folder + "phase_data.txt"
710         results_f = open(results_fileName, 'a+')
711         pickle_fileName = exp_folder + "pickle_data_" + patientID
712         pickle_f = open(pickle_fileName, 'wb+')
713         export_data = {}
714         header = 'PatientID'
715         lines = patientID
```

```
716
717         for segmID in segm_names:
718             segment_data = {
719                 segmID + '_ras' : p_coords[segm_names.index(segmID)],
720                 segmID + '_closedSurface_surf_mm2' : stat[(segmID,
                        'ClosedSurfaceSegmentStatisticsPlugin.surface_mm2')],
721                 segmID + '_closedSurface_vol_mm3' : stat[(segmID,
                        'ClosedSurfaceSegmentStatisticsPlugin.volume_mm3')],
722                 segmID + '_labelMap_volume_mm3' : stat[(segmID,
                        'LabelmapSegmentStatisticsPlugin.volume_mm3')],
723                 segmID + '_labelMap_voxelcount' : stat[(segmID,
                        'LabelmapSegmentStatisticsPlugin.voxel_count')],
724                 segmID + '_scalarVolume_max' : stat[(segmID,
                        'ScalarVolumeSegmentStatisticsPlugin.max')],
725                 segmID + '_scarVolume_min' : stat[(segmID,
                        'ScalarVolumeSegmentStatisticsPlugin.min')],
726                 segmID + '_scalarVolume_mean' : stat[(segmID,
                        'ScalarVolumeSegmentStatisticsPlugin.mean')],
727                 segmID + '_scalarVolume_stdev' : stat[(segmID,
                        'ScalarVolumeSegmentStatisticsPlugin.stdev')],
728                 segmID + '_scalarVolume_vol_mm3' : stat[(segmID,
                        'ScalarVolumeSegmentStatisticsPlugin.volume_mm3')],
729                 segmID + '_scalarVolume_voxelcount' : stat[(segmID,
                        'ScalarVolumeSegmentStatisticsPlugin.voxel_count')]
730                 }
731             export_data[segmID] = segment_data
732
733             keys = [segmID + '_ras',
734                     segmID + '_closedSurface_surf_mm2',
735                     segmID + '_closedSurface_vol_mm3',
736                     segmID + '_labelMap_volume_mm3',
737                     segmID + '_labelMap_voxelcount',
738                     segmID + '_scalarVolume_max',
739                     segmID + '_scarVolume_min',
740                     segmID + '_scalarVolume_mean',
741                     segmID + '_scalarVolume_stdev',
742                     segmID + '_scalarVolume_vol_mm3',
743                     segmID + '_scalarVolume_voxelcount']
744
```

```
745             values = [segment_data[segmID + '_ras']]
746
747             for i in keys[1:]:
748                 values.append('%.5f' % segment_data[i])
749
750             header += '\t' + '\t'.join(keys)
751             lines += '\t' + str(values[0]) + '\t' + '\t'.join(values[1:])
752
753         pprint (export_data)
754         pkl.dump(export_data, pickle_f)
755         pickle_f.close()
756
757         # results_f.seek(0)
758         # if (results_f.readline()==""):
759         #     results_f.write(header + '\n')
760         results_f.write(lines + '\n')
761
762         results_f.close()
763
764         return
765
766 #
767 # Slicer modules standard test code
768 #
769 class CTA_phaseTest(ScriptedLoadableModuleTest):
770     """ Tests"""
771
772     def setUp(self):
773         """ Do whatever is needed to reset the state - typically a scene clear
                will be enough.
774         """
775         slicer.mrmlScene.Clear(0)
776         sliceNode = None
777         sliceLogic = None
778
779         for slice_color in ["Green", "Red", "Yellow"]:
780             vtkMRMLSliceNode = 'vtkMRMLSliceNode' + slice_color
781             sliceNode = slicer.mrmlScene.GetNodeByID(vtkMRMLSliceNode)
782
```

```
783             if sliceNode:
784                 appLogic = slicer.app.applicationLogic()
785             if appLogic:
786                 sliceLogic = appLogic.GetSliceLogic(sliceNode)
787 
788             if not sliceNode or not sliceLogic:
789                 print "Something is wrong, sliceNode or sliceLogic not found"
790                 return
791 
792             sliceLayerLogic = sliceLogic.GetBackgroundLayer()
793             reslice = sliceLayerLogic.GetReslice()
794             reslice.SetSlabModeToMax()
795             reslice.SetSlabNumberOfSlices(1)
796             reslice.SetSlabSliceSpacingFraction(1)
797             sliceNode.Modified()
798 
799     def runTest(self):
800         self.delayDisplay("Starting the test")
801         self.setUp()
802         self.test_CTA_phase1()
803         self.delayDisplay('Test passed!')
804 
805     def test_CTA_phase1(self):
806         import urllib
807         downloads = (
808             ('http://slicer.kitware.com/midas3/download?items=5767', 'FA.nrrd',
                    slicer.util.loadVolume),
809             )
810 
811         for url,name,loader in downloads:
812             filePath = slicer.app.temporaryPath + '/' + name
813             if not os.path.exists(filePath) or os.stat(filePath).st_size == 0:
814                 logging.info('Requesting download %s from %s...\n' % (name, url))
815                 urllib.urlretrieve(url, filePath)
816             if loader:
817                 logging.info('Loading %s...' % (name,))
818                 loader(filePath)
819         self.delayDisplay('Finished with download and loading')
820 
```

```
821         volumeNode = slicer.util.getNode(pattern="FA")
822 
823         return
```

Bibliography

[1] J. C. Tan, W. P. Dillon, S. Liu, F. Adler, W. S. Smith, and M. Wintermark. Systematic comparison of perfusion-CT and CT-angiography in acute stroke patients. *Annals of Neurology*, 61(6):533–543, 2007.

[2] C. Casault, A.S. Al Sultan, A. Trivedi, S.I. Sohn, E. Qazi, M. Bokyo, M. Almekhlafi, C. d'Esterre, M. Goyal, A.M. Demchuk, et al. Collateral scoring on ct angiogram must evaluate phase and regional pattern. *Canadian Journal of Neurological Sciences*, 44(5):503–507, 2017.

[3] S.Y. Foo, M. Guarisco, A. Sitaram, and K. Muir. Agreement of collateral grade scoring between single phase CTA and temporal MIPs, 2019.

[4] M. J. Hartkamp, J. van der Grond, K. J. van Everdingen, B. Hillen, and W. P. T. M. Mali. Circle of willis collateral flow investigated by magnetic resonance angiography. *Stroke*, 30(12):2671–2678, 1999.

[5] M. Kaps. *Extracranial and intracranial collateral pathways* in Csiba, L. and Baracchini, C. (ed.) *Manual of Neurosonology*, chapter 11, pages 165–168. Cambridge University Press, 2016.

[6] D. S. Liebeskind. Collateral circulation. *Stroke*, 34(9):2279–2284, 2003.

[7] S. Dehkharghani, R. Bammer, M. Straka, L.S. Albin, O. Kass-Hout, J.W. Allen, S. Rangaraju, D. Qiu, M.J. Winningham, and F. Nahab. Performance and predictive value of a user-independent platform for ct perfusion analysis: threshold-derived automated systems outperform examiner-driven

approaches in outcome prediction of acute ischemic stroke. *American Journal of Neuroradiology*, 36(8):1419–1425, 2015.

[8] World Stroke Organization. Global stroke fact sheet, 2019. https://www.world-stroke.org/images/WSO_Global_Stroke_Fact_Sheet_final.pdf (accessed September 15, 2019).

[9] World Health Organization. The top 10 causes of death, 2016. https://www.who.int/news-room/fact-sheets/detail/the-top-10-causes-of-death (accessed September 15, 2019).

[10] Stroke Association. State of the nation - stroke statistics, 2018. stroke.org.uk (accessed September 15, 2019).

[11] Intercollegiate Stroke Working Party. National clinical guideline for stroke, 2016. https://www.strokeaudit.org/SupportFiles/Documents/Guidelines/2016-National-Clinical-Guideline-fir-Stroke-5t-(1).aspx (accessed September 15, 2019).

[12] J. L. Saver. Time is brain - quantified. *Stroke*, 37(1):263–266, 2005.

[13] F. C. Barone and G. Z. Feuerstein. Inflammatory mediators and stroke: New opportunities for novel therapeutics. *Journal of Cerebral Blood Flow and Metabolism*, 19(8):819–834, 1999.

[14] J. Astrup, B. K. Siesjö, and L. Symon. Thresholds in cerebral ischemia-the ischemic penumbra. *Stroke*, 12(6):723–725, 1981.

[15] J. Sobesky, O. Z. Weber, F.-G. Lehnhardt, V. Hesselmann, A. Thiel, C. Dohmen, A. Jacobs, et al. Which time-to-peak threshold best identifies penumbral flow? *Stroke*, 35(12):2843–2847, 2004.

[16] T. Peisker, B. Koznar, I. Stetkarova, and P. Widimsky. Acute stroke therapy: A review. *Trends in Cardiovascular Medicine*, 27(1):59 – 66, 2017.

[17] W. N. Whiteley, J. Emberson, K. R. Lees, L. Blackwell, G. Albers, E. Bluhmki, T. Brott, et al. Risk of intracerebral haemorrhage with alteplase after acute

ischaemic stroke: a secondary analysis of an individual patient data meta-analysis. *The Lancet Neurology*, 15(9):925 – 933, 2016.

[18] I. Christou, W. S. Burgin, A. V. Alexandrov, and J. C. Grotta. Arterial status after intravenous TPA therapy for ischaemic stroke. a need for further interventions. *International angiology*, 20(3):208, 2001.

[19] A. Bivard, C. Levi, L. Lin, X. Cheng, R. Aviv, N.J. Spratt, M. Lou, T. Kleinig, B. O'Brien, K. Butcher, et al. Validating a predictive model of acute advanced imaging biomarkers in ischemic stroke. *stroke*, 48(3):645–650, 2017.

[20] M. Goyal, B.K. Menon, W. H. Van Zwam, D. W. J. Dippel, P. J Mitchell, A. M. Demchuk, A. Davalos, et al. Endovascular thrombectomy after large-vessel ischaemic stroke: a meta-analysis of individual patient data from five randomised trials. *The Lancet*, 387(10029):1723 – 1731, 2016.

[21] O. A. Berkhemer, P. S.S. Fransen, D. Beumer, L. A. van den Berg, H. F. Lingsma, A. J. Yoo, W. J. Schonewille, et al. A randomized trial of intraarterial treatment for acute ischemic stroke. *New England Journal of Medicine*, 372(1):11–20, 2015. PMID: 25517348.

[22] . Finitsis, A. Kemmling, . Havemeister, S, G. Thomalla, J. Fiehler, and C. Brekenfeld. Stability of ischemic core volume during the initial hours of acute large vessel ischemic stroke in a subgroup of mechanically revascularized patients. *Neuroradiology*, 56(4):325–332, 2014.

[23] P.M. Meyers, H. C. Schumacher, E. Sander Connolly, E.J. Heyer, W. A. Gray, and R.T. Higashida. Current status of endovascular stroke treatment. *Circulation*, 123(22):2591–2601, 2011.

[24] D-V Giurgiutiu, A J Yoo, K Fitzpatrick, Z Chaudhry, T Leslie-Mazwi, L H Schwamm, and N S Rost. Severity of leukoaraiosis, leptomeningeal collaterals, and clinical outcomes after intra-arterial therapy in patients with acute ischemic stroke. *Journal of NeuroInterventional Surgery*, 7(5):326–330, 2015.

[25] R.G. Gonzalez, J.A. Hirsch, M.H. Lev, P.W. Schaefer, and Schwamm L.H. (Eds.). *Acute Ischemic Stroke*. Springer Berlin Heidelberg, 2 edition, 2011.

[26] B.K. Menon, E. Qazi, V. Nambiar, L.D. Foster, S.D. Yeatts, D. Liebeskind, T.G. Jovin, M. Goyal, M.D. Hill, T.A. Tomsick, et al. Differential effect of baseline computed tomographic angiography collaterals on clinical outcome in patients enrolled in the interventional management of stroke iii trial. *Stroke*, 46(5):1239–1244, 2015.

[27] F. Miteff, C.R. Levi, G.A. Bateman, N. Spratt, P. McElduff, and M.W. Parsons. The independent predictive utility of computed tomography angiographic collateral status in acute ischaemic stroke. *Brain*, 132(8):2231–2238, 2009.

[28] M. Ichijo, E. Iwasawa, Y. Numasawa, K. Miki, S. Ishibashi, M. Tomita, H. Tomimitsu, T. Kamata, H. Fujigasaki, S. Shintani, and H. Mizusawa. Significance of development and reversion of collaterals on mri in early neurologic improvement and long-term functional outcome after intravenous thrombolysis for ischemic stroke. *American Journal of Neuroradiology*, 36(10):1839–1845, 2015.

[29] F. McVerry, D. S. Liebeskind, and K. W. Muir. Systematic review of methods for assessing leptomeningeal collateral flow. *American Journal of Neuroradiology*, 33(3):576–582, 2012.

[30] K.W. Muir, J. Baird-Gunning, L. Walker, T. Baird, M. McCormick, and S.B. Coutts. Can the ischemic penumbra be identified on noncontrast ct of acute stroke? *Stroke*, 38(9):2485–2490, 2007.

[31] A. Srinivasan, M. Goyal, F.A.l. Azri, and C. Lum. State-of-the-art imaging of acute stroke. *Radiographics*, 26(suppl_1):S75–S95, 2006.

[32] S.J. Kim, J.P. Son, S. Ryoo, M.-J. Lee, J. Cha, K.H. Kim, G.-M. Kim, C.-S. Chung, K.H. Lee, P. Jeon, et al. A novel magnetic resonance imaging approach to collateral flow imaging in ischemic stroke. *Annals of neurology*, 76(3):356–369, 2014.

[33] B.K. Menon, C.D. d'Esterre, E.M. Qazi, M. Almekhlafi, L. Hahn, A.M. Demchuk, and M. Goyal. Multiphase ct angiography: a new tool for the

imaging triage of patients with acute ischemic stroke. *Radiology*, 275(2):510–520, 2015.

[34] B. K. Cheripelli, X. Huang, F. McVerry, and K. W. Muir. What is the relationship among penumbra volume, collaterals, and time since onset in the first 6 h after acute ischemic stroke? *International Journal of Stroke*, 11(3), 2016.

[35] J.H.W. Pexman, P.A. Barber, M.D. Hill, R.J. Sevick, A.M. Demchuk, M.E. Hudon, W.Y. Hu, and A.M. Buchan. Use of the alberta stroke program early ct score (aspects) for assessing ct scans in patients with acute stroke. *American Journal of Neuroradiology*, 22(8):1534–1542, 2001.

[36] TIMI Study Group*. The thrombolysis in myocardial infarction (timi) trial: phase i findings. *New England Journal of Medicine*, 312(14):932–936, 1985.

[37] Randall T. Higashida and Anthony J. Furlan. Trial design and reporting standards for intra-arterial cerebral thrombolysis for acute ischemic stroke. *Stroke*, 34(8):1923–1924, 2003.

[38] A.I. Calleja, E. Cortijo, P. García-Bermejo, R.D. Gómez, S. Pérez-Fernández, J.M. Del Monte, M.F. Munoz, R. Fernández-Herranz, and J.F. Arenillas. Collateral circulation on perfusion-computed tomography-source images predicts the response to stroke intravenous thrombolysis. *European journal of neurology*, 20(5):795–802, 2013.

[39] S. Jung, M. Gilgen, J. Slotboom, M. El-Koussy, C. Zubler, C. Kiefer, R. Luedi, M.-L. Mono, M.R. Heldner, A. Weck, et al. Factors that determine penumbral tissue loss in acute ischaemic stroke. *Brain*, 136(12):3554–3560, 2013.

[40] A. Shuaib, K. Butcher, A. A. Mohammad, M. Saqqur, and D. S. Liebeskind. Collateral blood vessels in acute ischaemic stroke: a potential therapeutic target. *The Lancet Neurology*, 10(10):909 – 921, 2011.

[41] R. H. C. Bisschops, C. J. M. Klijn, L. J. Kappelle, A. C. van Huffelen, and J. Van Der Grond. Collateral flow and ischemic brain lesions in patients with unilateral carotid artery occlusion. *Neurology*, 60(9):1435–1441, 2003.

[42] H. M. Vander Eecken. Morphological significance of leptomeningeal anastomoses confined to the territory of cerebral arteries. *Acta neurologica et psychiatrica Belgica*, 54(7):525, 1954.

[43] A. Krishnaswamy, J. P. Klein, and S. R. Kapadia. Clinical cerebrovascular anatomy. *Catheterization and Cardiovascular Interventions*, 75(4):530–539, 2010.

[44] M. Brozici, A. van der Zwan, and B. Hillen. Anatomy and functionality of leptomeningeal anastomoses. *Stroke*, 34(11):2750–2762, 2003.

[45] S. Power, S.H. McEvoy, Ja. Cunningham, J.P. Ti, S. Looby, A. O'Hare, D. Williams, P. Brennan, and J. Thornton. Value of ct angiography in anterior circulation large vessel occlusive stroke: Imaging findings, pearls, and pitfalls. *European journal of radiology*, 84(7):1333–1344, 2015.

[46] A. Galimanis, S. Jung, M.-L. Mono, U. Fischer, O. Findling, A. Weck, N. Meier, G.M. De Marchis, C. Brekenfeld, M. El-Koussy, et al. Endovascular therapy of 623 patients with anterior circulation stroke. *Stroke*, 43(4):1052–1057, 2012.

[47] O.Y. Bang, J.L. Saver, S.J. Kim, G.-M. Kim, C.-S. Chung, B. Ovbiagele, K.H. Lee, and D.S. Liebeskind. Collateral flow predicts response to endovascular therapy for acute ischemic stroke. *Stroke*, pages STROKEAHA–110, 2011.

[48] D. Song, K. Lee, E.H. Kim, Y.D. Kim, J. Kim, T.-J. Song, H.S. Lee, H.S. Nam, and J.H. Heo. Value of utilizing both ASPECTS and CT angiography collateral score for outcome prediction in acute ischemic stroke. *International Journal of Stroke*, 10(7):1018–1023, 2015.

[49] G.A. Christoforidis, C. Karakasis, Y. Mohammad, L.P. Caragine, M. Yang, and A.P. Slivka. Predictors of hemorrhage following intra-arterial thrombolysis for acute ischemic stroke: the role of pial collateral formation. *American Journal of Neuroradiology*, 30(1):165–170, 2009.

[50] M. Goyal, A.M. Demchuk, B.K. Menon, M. Eesa, J.L. Rempel, J. Thornton, D. Roy, and et al. Randomized assessment of rapid endovascular treatment

of ischemic stroke. *New England Journal of Medicine*, 372(11):1019–1030, 2015.

[51] A. Shuaib, N. M. Bornstein, H.-C. Diener, W. Dillon, M. Fisher, M. D. Hammer, C. A. Molina, et al. Partial aortic occlusion for cerebral perfusion augmentation. *Stroke*, 42(6):1680–1690, 2011.

[52] B.K. Menon, E.E. Smith, J. Modi, S.K. Patel, R. Bhatia, T.W.J. Watson, M.D. Hill, A.M. Demchuk, and M. Goyal. Regional leptomeningeal score on ct angiography predicts clinical and imaging outcomes in patients with acute anterior circulation occlusions. *American Journal of Neuroradiology*, 32(9):1640–1645, 2011.

[53] C. Levi, H. Zareie, and M. Parson. Transcranial doppler in acute stroke management - "a real-time" bed-side guide to reperfusion and collateral flow. *Perspectives in Medicine*, 1(1):185 – 193, 2012. New Trends in Neurosonology and Cerebral Hemodynamics - an Update.

[54] E. Martinon, P.H. Lefevre, P. Thouant, G.V. Osseby, F. Ricolfi, and A. Chavent. Collateral circulation in acute stroke: assessing methods and impact: a literature review. *Journal of neuroradiology*, 41(2):97–107, 2014.

[55] F.O. Lima, K.L. Furie, G.S. Silva, M.H. Lev, É.C.S. Camargo, A.B. Singhal, G.J. Harris, E.F. Halpern, W.J. Koroshetz, W.S. Smith, et al. The pattern of leptomeningeal collaterals on ct angiography is a strong predictor of long-term functional outcome in stroke patients with large vessel intracranial occlusion. *Stroke*, 41(10):2316–2322, 2010.

[56] L.C.S. Souza, A.J. Yoo, Z.A. Chaudhry, S. Payabvash, A. Kemmling, P.W. Schaefer, J.A. Hirsch, K.L. Furie, R.G. González, R.G. Nogueira, et al. Malignant CTA collateral profile is highly specific for large admission dwi infarct core and poor outcome in acute stroke. *American Journal of Neuroradiology*, 33(7):1331–1336, 2012.

[57] O. Y. Bang, J. L. Saver, B. H. Buck, J. R. Alger, S. Starkman, B. Ovbiagele, D. Kim, et al. Impact of collateral flow on tissue fate in acute ischaemic

stroke. *Journal of Neurology, Neurosurgery & Psychiatry*, 79(6):625–629, 2008.

[58] V. Hesselmann, T. Niederstadt, R. Dziewas, M. Ritter, A. Kemmling, D. Maintz, M. Koehler, H. Seifarth, A.H. Jacobs, E.B. Ringelstein, et al. Reperfusion by combined thrombolysis and mechanical thrombectomy in acute stroke: effect of collateralization, mismatch, and time to and grade of recanalization on clinical and tissue outcome. *American Journal of Neuroradiology*, 33(2):336–342, 2012.

[59] J. J. Kim, N. J. Fischbein, Y. Lu, D. Pham, and W. P. Dillon. Regional angiographic grading system for collateral flow. *Stroke*, 35(6):1340–1344, 2004.

[60] I.Y.L. Tan, A.M. Demchuk, J. Hopyan, L. Zhang, D. Gladstone, K. Wong, M. Martin, S.P. Symons, A.J. Fox, and R.I. Aviv. Ct angiography clot burden score and collateral score: correlation with clinical and radiologic outcomes in acute middle cerebral artery infarct. *American Journal of Neuroradiology*, 30(3):525–531, 2009.

[61] G. A. Christoforidis, Y. Mohammad, D. Kehagias, B. Avutu, and A. P. Slivka. Angiographic assessment of pial collaterals as a prognostic indicator following intra-arterial thrombolysis for acute ischemic stroke. *American Journal of Neuroradiology*, 26(7):1789–1797, 2005.

[62] H.-S. Song, C.-K. Kang, J. S. Kim, C.-A. Park, Y.-B. Kim, D. H. Lee, D.-W. Kang, et al. Assessment of pial branches using 7-tesla MRI in cerebral arterial disease. *Cerebrovascular Diseases*, 29(4):410–411, 2010.

[63] M. Arnold, S. Mattle, A. Galimanis, L. Kappeler, U. Fischer, S. Jung, G.M. De Marchis, J. Gralla, M.-L. Mono, C. Brekenfeld, et al. Impact of admission glucose and diabetes on recanalization and outcome after intra-arterial thrombolysis for ischaemic stroke. *International Journal of Stroke*, 9(8):985–991, 2014.

[64] S. Jung, K. Schindler, O. Findling, M.-L. Mono, U. Fischer, J. Gralla, M. El-Koussy, A. Weck, A. Galimanis, C. Brekenfeld, et al. Adverse effect of early epileptic seizures in patients receiving endovascular therapy for acute stroke. *Stroke*, 43(6):1584–1590, 2012.

[65] R. Luedi, K. Hsieh, A. Slezak, M. El-Koussy, U. Fischer, M.R. Heldner, J. Meisterernst, M.-L. Mono, C. Zubler, P. Mordasini, et al. Age dependency of safety and outcome of endovascular therapy for acute stroke. *Journal of neurology*, 261(8):1622–1627, 2014.

[66] D.S. Liebeskind, T.A. Tomsick, L.D. Foster, S.D. Yeatts, J. Carrozzella, A.M. Demchuk, T.G. Jovin, P. Khatri, R. von Kummer, R.M. Sugg, et al. Collaterals at angiography and outcomes in the interventional management of stroke (ims) iii trial. *Stroke*, 45(3):759–764, 2014.

[67] J. Lyu, N. Ma, D.S. Liebeskind, D.J.J. Wang, L. Ma, Y. Xu, T. Wang, Z. Miao, and X. Lou. Arterial spin labeling magnetic resonance imaging estimation of antegrade and collateral flow in unilateral middle cerebral artery stenosis. *Stroke*, 47(2):428–433, 2016.

[68] M.W. Parsons, S. Christensen, P. McElduff, C.R. Levi, K.S. Butcher, D.A. De Silva, M. Ebinger, P.A. Barber, C. Bladin, G.A. Donnan, et al. Pretreatment diffusion-and perfusion-mr lesion volumes have a crucial influence on clinical response to stroke thrombolysis. *Journal of Cerebral Blood Flow & Metabolism*, 30(6):1214–1225, 2010.

[69] B.A. Roach, M.J. Donahue, L.T. Davis, C.C. Faraco, D. Arteaga, S.-C. Chen, T.R. Ladner, A.O. Scott, and M.K. Strother. Interrogating the functional correlates of collateralization in patients with intracranial stenosis using multimodal hemodynamic imaging. *American Journal of Neuroradiology*, 37(6):1132–1138, 2016.

[70] H. Chen, B. Wu, G. Zhu, M. Wintermark, Xi. Wu, Z. Su, X. Xu, C. Tian, L. Ma, W. Zhang, et al. Permeability imaging as a biomarker of leptomeningeal collateral flow in patients with intracranial arterial stenosis. *Cell biochemistry and biophysics*, 71(3):1273–1279, 2015.

[71] M.B. Maas, M.H. Lev, H. Ay, A.B. Singhal, D.M. Greer, W.S. Smith, G.J. Harris, E. Halpern, A. Kemmling, W.J. Koroshetz, et al. Collateral vessels on ct angiography predict outcome in acute ischemic stroke. *Stroke*, 40(9):3001–3005, 2009.

[72] Y. Qu, H. Zhang, H. Li, L. Yu, and Y. Sun. Aldh2* 2 polymorphism is associated with an increased risk of extra cranial vascular stenosis and poor collateral vessels in ischemic stroke in han chinese. *Internationl Journal of Clinical and Experimental Medicine*, 9(10):19944–19952, 2016.

[73] W.X.Y. Zou, T.W. Leung, C.H. Simon, E.H.C. Wong, S.F. Leung, Y.O.Y. Soo, V.H.L. Ip, A.Y.Y. Chan, W.W.M. Lam, D.Y.W. Siu, et al. Angiographic features, collaterals, and infarct topography of symptomatic occlusive radiation vasculopathy. *Stroke*, 44(2):401–406, 2013.

[74] W. Liu, G. Xu, X. Yue, X. Wang, M. Ma, R. Zhang, H. Wang, C. Zhou, and X. Liu. Hyperintense vessels on flair: a useful non-invasive method for assessing intracerebral collaterals. *European journal of radiology*, 80(3):786–791, 2010.

[75] W. Liu, Q. Yin, L. Yao, S. Zhu, G. Xu, R. Zhang, K. Ke, and X. Liu. Decreased hyperintense vessels on flair images after endovascular recanalization of symptomatic internal carotid artery occlusion. *European journal of radiology*, 81(7):1595–1600, 2012.

[76] D. Liu, Y. Li, Z. Shi, S.M. Davis, K.S. Wong, T.W. Leung, B. Yan, Y. Xiong, W. Sun, G. Xu, et al. Presence of anterior temporal artery associates with good outcome in acute atherosclerotic m1-middle cerebral artery occlusion. *Neuroradiology*, 56(12):1023–1030, 2014.

[77] H.-S. Park, J.-K. Cha, D.-H. Kim, M.-J. Kang, J.-H. Choi, and J.-T. Huh. The rcbv ratio on perfusion-weighted imaging reveals the extent of blood flow on conventional angiography after acute ischemic stroke. *Clinical neurology and neurosurgery*, 122:54–58, 2014.

[78] Alexander YL Lau, Edward HC Wong, Adrian Wong, Vincent CT Mok, Thomas W Leung, and Ka-sing Lawrence Wong. Significance of good collateral compensation in symptomatic intracranial atherosclerosis. *Cerebrovascular diseases*, 33(6):517–524, 2012.

[79] D. Liu, F. Scalzo, N.M. Rao, J.D. Hinman, D. Kim, L.K. Ali, J.L. Saver, W. Sun, Q. Dai, X. Liu, et al. Fluid-attenuated inversion recovery vascular hyperintensity topography, novel imaging marker for revascularization in middle cerebral artery occlusion. *Stroke*, 47(11):2763–2769, 2016.

[80] K. Sato, H. Shimizu, T. Inoue, M. Fujimura, Y. Matsumoto, R. Kondo, H. Endo, Y. Sonoda, and T. Tominaga. Angiographic circulation time and cerebral blood flow during balloon test occlusion of the internal carotid artery. *Journal of Cerebral Blood Flow & Metabolism*, 34(1):136–143, 2014.

[81] X.-Q. Cheng, J.-M. Tian, C.-J. Zuo, J. Liu, Q. Zhang, and G.-M. Lu. Quantitative perfusion computed tomography measurements of cerebral hemodynamics: correlation with digital subtraction angiography identified primary and secondary cerebral collaterals in internal carotid artery occlusive disease. *European journal of radiology*, 81(6):1224–1230, 2012.

[82] Y. He, Z. Wang, T. Li, W.-J. Jiang, L. Zhu, J. Xue, W. Bai, and F. Hui. Preliminary findings of recanalization and stenting for symptomatic vertebrobasilar artery occlusion lasting more than 24h: a retrospective analysis of 21 cases. *European journal of radiology*, 82(9):1481–1486, 2013.

[83] M. Kawashima, T. Noguchi, Y. Yakushiji, Y. Takase, and T. Matsushima. Leptomeningeal collateral and cerebral hemodynamics in patients with ica and mca steno-occlusion. *Neurological research*, 33(3):307–313, 2011.

[84] A.W. Keedy, W.S. Fischette, B.P. Soares, S. Arora, B.C. Lau, R. Magge, J. Bredno, S.C. Cheng, and M. Wintermark. Contrast delay on perfusion ct as a predictor of new, incident infarct: a retrospective cohort study. *Stroke*, 43(5):1295–1301, 2012.

[85] D.S. Liebeskind, G.A. Cotsonis, J.L. Saver, M.J. Lynn, H.J. Cloft, M.I. Chimowitz, and Investigators For the Warfarin Aspirin Symptomatic Intracranial Disease (WASID). Collateral circulation in symptomatic intracranial atherosclerosis. *Journal of Cerebral Blood Flow & Metabolism*, 31(5):1293–1301, 2011.

[86] D.S. Liebeskind, G.A. Cotsonis, J.L. Saver, M.J. Lynn, T.N. Turan, H.J. Cloft, and M.I. Chimowitz. Collaterals dramatically alter stroke risk in intracranial atherosclerosis. *Annals of neurology*, 69(6):963–974, 2011.

[87] X. Liu, Y. Pu, Y. Pan, Y. Zhang, X. Dou, Y. Tan, L. Liu, and Y. Wang. Multi-mode ct in the evaluation of leptomeningeal collateral flow and the related factors: comparing with digital subtraction angiography. *Neurological research*, 38(6):504–509, 2016.

[88] E. López-Cancio, M.G. Matheus, J.G. Romano, D.S. Liebeskind, S. Prabhakaran, T.N. Turan, G.A. Cotsonis, M.J. Lynn, Z. Rumboldt, M.I. Chimowitz, et al. Infarct patterns, collaterals and likely causative mechanisms of stroke in symptomatic intracranial atherosclerosis. *Cerebrovascular Diseases*, 37(6):417–422, 2014.

[89] E.-Z. Wu, X. Liu, D. Dornbos, J. Pfeuffer, T.-Y. Qian, P.-G. Qiao, Y.-S. Pan, X. Dou, Z.-W. Zuo, L.-P. Liu, et al. Comparison of 3d multi-inversion time arterial spin labeling and digital subtraction angiography in the evaluation of cerebral collateral circulation. *CNS neuroscience & therapeutics*, 22(12):1009–1011, 2016.

[90] S. Alqadri, M.M. Adil, M. Watanabe, and A.I. Qureshi. Patterns of collateral formation in basilar artery steno-occlusive diseases. *Journal of vascular and interventional neurology*, 6(2):9, 2013.

[91] V. Da Ros, A. Meschini, R. Gandini, C. Del Giudice, F. Garaci, P. Stanzione, B. Rizzato, M. Diomedi, G. Simonetti, R. Floris, et al. Proposal for a vascular computed tomography-based grading system in posterior circulation stroke: a single-center experience. *Journal of Stroke and Cerebrovascular Diseases*, 25(2):368–377, 2016.

[92] S. Jung, M.-L. Mono, U. Fischer, A. Galimanis, O. Findling, G.M. De Marchis, A. Weck, K. Nedeltchev, G. Colucci, P. Mordasini, et al. Three-month and long-term outcomes and their predictors in acute basilar artery occlusion treated with intra-arterial thrombolysis. *Stroke*, 42(7):1946–1951, 2011.

[93] O.C. Singer, J. Berkefeld, C.H. Nolte, G. Bohner, H.-P. Haring, J. Trenkler, K. Gröschel, W. Müller-Forell, K. Niederkorn, H. Deutschmann, et al. Mechanical recanalization in basilar artery occlusion: the endostroke study. *Annals of neurology*, 77(3):415–424, 2015.

[94] R.C. van Houwelingen, G.-J. Luijckx, A. Mazuri, R.P.H. Bokkers, O.S. Eshghi, and M. Uyttenboogaart. Safety and outcome of intra-arterial treatment for basilar artery occlusion. *JAMA neurology*, 73(10):1225–1230, 2016.

[95] S.J. Kim, H.J. Noh, C.W. Yoon, K.H. Kim, P. Jeon, O.Y. Bang, G.M. Kim, Chung C.S., and K.H. Lee. Multiphasic perfusion computed tomography as a predictor of collateral flow in acute ischemic stroke: comparison with digital subtraction angiography. *Stroke*, 67(4):252–255, 2012.

[96] O.Y. Bang, J.L. Saver, S.J. Kim, G.-M. Kim, C.-S. Chung, B. Ovbiagele, K.H. Lee, D.S. Liebeskind, et al. Collateral flow averts hemorrhagic transformation after endovascular therapy for acute ischemic stroke. *Stroke*, 42(8):2235–2239, 2011.

[97] Y.-H. Hwang, D.-H. Kang, Y.-W. Kim, Y.-S. Kim, S.-P. Park, and D.S. Liebeskind. Impact of time-to-reperfusion on outcome in patients with poor collaterals. *American Journal of Neuroradiology*, 36(3):495–500, 2015.

[98] M.J. Lee, O.Y. Bang, S.J. Kim, G.M. Kim, C.S. Chung, K.H. Lee, B. Ovbiagele, D.S. Liebeskind, J.L. Saver, et al. Role of statin in atrial fibrillation-related stroke: an angiographic study for collateral flow. *Cerebrovascular Diseases*, 37(2):77–84, 2014.

[99] F. Nicoli, F. Scalzo, J.L. Saver, F. Pautot, A. Mitulescu, Y. Chaibi, N. Girard, N. Salamon, D.S. Liebeskind, UCLA Stroke Investigators, et al. The combination of baseline magnetic resonance perfusion-weighted imaging-derived tissue

volume with severely prolonged arterial-tissue delay and diffusion-weighted imaging lesion volume is predictive of mca-m1 recanalization in patients treated with endovascular thrombectomy. *Neuroradiology*, 56(2):117–127, 2014.

[100] T. Shimoyama, K. Shibazaki, K. Kimura, J. Uemura, T. Shiromoto, M. Watanabe, T. Inoue, Y. Iguchi, and S. Mochio. Admission hyperglycemia causes infarct volume expansion in patients with ica or mca occlusion: association of collateral grade on conventional angiography. *European journal of neurology*, 20(1):109–116, 2013.

[101] G. Christoforidis, Y.M. Mohammad, M. Khadir, M. Yang, and A.P. Slivka. Factors associated with rapid neurological improvement 24 h following intra-arterial thrombolytic treatment for acute ischemic stroke. *Journal of neurointerventional surgery*, pages neurintsurg–2011, 2011.

[102] A. Consoli, T. Andersson, A. Holmberg, L. Verganti, A. Saletti, S. Vallone, A. Zini, A. Cerase, D. Romano, S. Bracco, et al. Ct perfusion and angiographic assessment of pial collateral reperfusion in acute ischemic stroke: the capri study. *Journal of neurointerventional surgery*, 8(12):1211–1216, 2016.

[103] P-E. Labeyrie, H. Redjem, R. Blanc, M.-A. Labeyrie, B. Bartolini, G. Ciccio, T. Robert, B. Gilboa, R. Fahed, M. Abrivard, et al. The capillary index score before thrombectomy: an angiographic correlate of favorable outcome. *Journal of neurointerventional surgery*, 8(11):1119–1122, 2016.

[104] R. Pop, M. Manisor, R. Beaujeux, C. Marescaux, V. Wolff, and M. Simu. Regional angiographic evaluation of collateral circulation predicts infarction during endovascular procedures for middle cerebral artery stroke. *Romanian Journal of Neurology*, 13(3), 2014.

[105] R. Pop, M. Manisor, V. Wolff, G. Freys, M. Simu, C. Marescaux, and R. Beaujeux. Real-time estimation of core infarct in angiography using collateral flow. *Cerebrovascular Diseases*, 41(3-4):177–186, 2016.

[106] N. Meier, K. Nedeltchev, C. Brekenfeld, A. Galimanis, U. Fischer, O. Findling, L. Remonda, G. Schroth, H.P. Mattle, and M. Arnold. Prior statin use, intracranial hemorrhage, and outcome after intra-arterial thrombolysis for acute ischemic stroke. *Stroke*, 40(5):1729–1737, 2009.

[107] M.-L. Mono, L. Romagna, S. Jung, M. Arnold, A. Galimanis, U. Fischer, A. Kohler, P. Ballinari, C. Brekenfeld, J. Gralla, et al. Intra-arterial thrombolysis for acute ischemic stroke in octogenarians. *Cerebrovascular diseases*, 33(2):116–122, 2012.

[108] R.K. Verma, K. Hsieh, P.P. Gratz, A.C. Schankath, P. Mordasini, C. Zubler, F. Kellner-Weldon, S. Jung, G. Schroth, J. Gralla, et al. Leptomeningeal collateralization in acute ischemic stroke: impact on prominent cortical veins in susceptibility-weighted imaging. *European journal of radiology*, 83(8):1448–1454, 2014.

[109] F. Al-Ali, A. Jefferson, T. Barrow, T. Cree, S. Louis, K. Luke, K. Major, D. Nemeth, S. Smoker, and S. Walker. The capillary index score: rethinking the acute ischemic stroke treatment algorithm. results from the borgess medical center acute ischemic stroke registry. *Journal of neurointerventional surgery*, 5(2):139–143, 2013.

[110] F. Al-Ali, T.A. Tomsick, J.J. Connors, J.M. Gebel, J.J. Elias, G.Z. Markarian, Z. Al-Ali, and J.P. Broderick. Capillary index score in the interventional management of stroke trials i and ii. *Stroke*, 45(7):1999–2003, 2014.

[111] F. Al-Ali, J.J. Elias, T.A. Tomsick, D.S. Liebeskind, and J.P. Broderick. Relative influence of capillary index score, revascularization, and time on stroke outcomes from the interventional management of stroke iii trial. *Stroke*, 46(6):1590–1594, 2015.

[112] R. Fahed, H. Redjem, R. Blanc, J. Labreuche, T. Robert, G. Ciccio, D. Smadja, S. Smajda, and M. Piotin. Endovascular management of acute ischemic strokes with tandem occlusions. *Cerebrovascular Diseases*, 41(5-6):298–305, 2016.

[113] H. Chen, B. Wu, N. Liu, M. Wintermark, Z. Su, Y. Li, J. Hu, Y. Zhang, W. Zhang, and G. Zhu. Using standard first-pass perfusion computed tomographic data to evaluate collateral flow in acute ischemic stroke. *Stroke*, pages STROKEAHA–114, 2015.

[114] J.Y. Choi, E.J. Kim, J.M. Hong, S.E. Lee, J.S. Lee, Y.C. Lim, and H.S. Kim. Conventional enhancement ct: a valuable tool for evaluating pial collateral flow in acute ischemic stroke. *Cerebrovascular Diseases*, 31(4):346–352, 2011.

[115] A. Flores, M. Rubiera, M. Ribó, J. Pagola, D. Rodriguez-Luna, M. Muchada, S. Boned, L. Seró, E. Sanjuan, P. Meler, et al. Poor collateral circulation assessed by multiphase computed tomographic angiography predicts malignant middle cerebral artery evolution after reperfusion therapies. *Stroke*, 46(11):3149–3153, 2015.

[116] N.-Y. Shin, K.-e. Kim, M. Park, Y.D. Kim, D.J. Kim, S.J. Ahn, J.H. Heo, and S.-K. Lee. Dual-phase ct collateral score: a predictor of clinical outcome in patients with acute ischemic stroke. *PloS one*, 9(9):e107379, 2014.

[117] S.M. Sung, T.H. Lee, H.J. Cho, T.H. Kang, D.S. Jung, K.P. Park, M.K. Park, J.I. Lee, and J.K. Ko. Functional outcome after recanalization for acute pure m1 occlusion of the middle cerebral artery as assessed by collateral cta flow. *Clinical neurology and neurosurgery*, 131:72–76, 2015.

[118] X. Huang, W. Liu, W. Zhu, G. Ni, W. Sun, M. Ma, Z. Zhou, Q. Wang, G. Xu, and X. Liu. Distal hyperintense vessels on flair: a prognostic indicator of acute ischemic stroke. *European neurology*, 68(4):214–220, 2012.

[119] N Sanossian, JL Saver, JR Alger, D Kim, GR Duckwiler, R Jahan, F Vinuela, B Ovbiagele, and DS Liebeskind. Angiography reveals that fluid-attenuated inversion recovery vascular hyperintensities are due to slow flow, not thrombus. *American Journal of Neuroradiology*, 30(3):564–568, 2009.

[120] M.J. Lee, J.P. Son, S.J. Kim, S. Ryoo, S.-Y. Woo, J. Cha, G.-M. Kim, C.-S. Chung, K.H. Lee, and O.Y. Bang. Predicting collateral status with magnetic resonance perfusion parameters. *Stroke*, 46(10):2800–2807, 2015.

[121] A. Potreck, F. Seker, A. Hoffmann, J. Pfaff, S. Nagel, M. Bendszus, S. Heiland, and M. Pham. A novel method to assess pial collateralization from stroke perfusion mri: subdividing tmax into anatomical compartments. *European radiology*, 27(2):618–626, 2017.

[122] M. Ernst, N.D. Forkert, L. Brehmer, G. Thomalla, S. Siemonsen, J. Fiehler, and A. Kemmling. Prediction of infarction and reperfusion in stroke by flow-and volume-weighted collateral signal in mr angiography. *American Journal of Neuroradiology*, 36(2):275–282, 2015.

[123] S.J. Kim, Y.S. Ha, S. Ryoo, H.J. Noh, S.-Y. Ha, O.Y. Bang, G.-M. Kim, C.-S. Chung, and K.H. Lee. Sulcal effacement on fluid attenuation inversion recovery magnetic resonance imaging in hyperacute stroke. *Stroke*, 43(2):386–392, 2011.

[124] S. Lescher, K. Czeppan, L. Porto, O.C. Singer, and J. Berkefeld. Acute stroke and obstruction of the extracranial carotid artery combined with intracranial tandem occlusion: results of interventional revascularization. *Cardiovascular and interventional radiology*, 38(2):304–313, 2015.

[125] R.C.S. Seet, E.F.M. Wijdicks, and A.A. Rabinstein. Stroke from acute cervical internal carotid artery occlusion: treatment results and predictors of outcome. *Archives of neurology*, 69(12):1615–1620, 2012.

[126] C. Brekenfeld, G. Schroth, H.P. Mattle, D.-D. Do, L. Remonda, P. Mordasini, M. Arnold, K. Nedeltchev, N. Meier, and J. Gralla. Stent placement in acute cerebral artery occlusion. *Stroke*, 40(3):847–852, 2009.

[127] J.E. Cohen, A.A. Rabinstein, F. Ramirez-de Noriega, J.M. Gomori, E. Itshayek, R. Eichel, and R.R. Leker. Excellent rates of recanalization and good functional outcome after stent-based thrombectomy for acute middle cerebral artery occlusion. is it time for a paradigm shift? *Journal of Clinical Neuroscience*, 20(9):1219–1223, 2013.

[128] Y.-H. Hwang, Y.-W. Kim, D.-H. Kang, Y.-S. Kim, and D.S Liebeskind. Impact of target arterial residual stenosis on outcome after endovascular

revascularization. *Stroke*, 47(7):1850–1857, 2016.

[129] K. Imai, T. Mori, H. Izumoto, M. Watanabe, T. Kunieda, N. Takabatake, and S. Yamamoto. Mr imaging- based localized intra-arterial thrombolysis assisted by mechanical clot disruption for acute ischemic stroke due to middle cerebral artery occlusion. *American Journal of Neuroradiology*, 32(4):748–752, 2011.

[130] H.S. Jeong, H.-J. Kwon, C.W. Kang, H.-J. Song, H.S. Koh, S.M. Park, J.G. Lim, J.E. Shin, S.H. Lee, and J. Kim. Predictive factors for early clinical improvement after intra-arterial thrombolytic therapy in acute ischemic stroke. *Journal of Stroke and Cerebrovascular Diseases*, 23(4):e283–e289, 2014.

[131] H.S. Jeong, H.-J. Kwon, H.-J. Song, H.-S. Koh, Y.S. Kim, J.H. Lee, J.E. Shin, S.H. Lee, and J. Kim. Impacts of rapid recanalization and collateral circulation on clinical outcome after intraarterial thrombolysis. *Journal of stroke*, 17(1):76, 2015.

[132] P. Khatri, S.D. Yeatts, M. Mazighi, J.P. Broderick, D.S. Liebeskind, A.M. Demchuk, P. Amarenco, J. Carrozzella, J. Spilker, L.D. Foster, et al. Time to angiographic reperfusion and clinical outcome after acute ischaemic stroke: an analysis of data from the interventional management of stroke (ims iii) phase 3 trial. *The Lancet Neurology*, 13(6):567–574, 2014.

[133] S.J. Kim, J.M. Seok, O.Y. Bang, G.-M. Kim, K.H. Kim, P. Jeon, C.-S. Chung, K.H. Lee, J.R. Alger, and D.S. Liebeskind. Mr mismatch profiles in patients with intracranial atherosclerotic stroke: a comprehensive approach comparing stroke subtypes. *Journal of Cerebral Blood Flow & Metabolism*, 29(6):1138–1145, 2009.

[134] S.J. Kim, S. Ryoo, G.-M. Kim, C.-S. Chung, K.H. Lee, and O.Y. Bang. Clinical and radiological outcomes after intracranial atherosclerotic stroke: a comprehensive approach comparing stroke subtypes. *Cerebrovascular Diseases*, 31(5):427–434, 2011.

[135] W. Kurre, K. Bansemir, M.A. Pérez, R.M. Moreno, E. Schmid, H. Bäzner, and H. Henkes. Endovascular treatment of acute internal carotid artery dissections: technical considerations, clinical and angiographic outcome. *Neuroradiology*, 58(12):1167–1179, 2016.

[136] S.-J. Lee, J.M. Hong, M. Lee, K. Huh, J.W. Choi, and J.S. Lee. Cerebral arterial calcification is an imaging prognostic marker for revascularization treatment of acute middle cerebral arterial occlusion. *Journal of stroke*, 17(1):67, 2015.

[137] D.S. Liebeskind, R. Jahan, R.G. Nogueira, O.O. Zaidat, and J.L. Saver. Impact of collaterals on successful revascularization in solitaire fr with the intention for thrombectomy. *Stroke*, pages STROKEAHA–114, 2014.

[138] D.S. Liebeskind, R. Jahan, R.G. Nogueira, T.G. Jovin, H.L. Lutsep, and J.L. Saver. Early arrival at the emergency department is associated with better collaterals, smaller established infarcts and better clinical outcomes with endovascular stroke therapy: Swift study. *Journal of neurointerventional surgery*, 8(6):553–558, 2016.

[139] M.P. Marks, M.G. Lansberg, M. Mlynash, J.-M. Olivot, M. Straka, S. Kemp, R. McTaggart, M. Inoue, G. Zaharchuk, R. Bammer, et al. Effect of collateral blood flow on patients undergoing endovascular therapy for acute ischemic stroke. *Stroke*, 45(4):1035–1039, 2014.

[140] J.M. Olivot, M. Mlynash, M. Inoue, M.P. Marks, H.M. Wheeler, S. Kemp, M. Straka, G. Zaharchuk, R. Bammer, M.G. Lansberg, et al. Hypoperfusion intensity ratio predicts infarct progression and functional outcome in the defuse 2 cohort. *Stroke*, 45(4):1018–1023, 2014.

[141] J.H. Park, Y.M. Han, K.S. Jang, W.S. Yoon, D.K. Jang, and S.K. Park. Angiographic and clinical factors related with good functional outcome after mechanical thrombectomy in acute cerebral artery occlusion. *Journal of Korean Neurosurgical Society*, 58(3):192–196, 2015.

[142] M.-S. Park, W. Yoon, J.-T. Kim, K.-H. Choi, S.-H. Kang, B.C. Kim, S.-H. Lee, S.-M. Choi, M.-K. Kim, J.-S. Lee, et al. Drip, ship, and on-demand endovascular therapy for acute ischemic stroke. *PloS one*, 11(3):e0150668, 2016.

[143] V.M. Pereira, J. Gralla, A. Davalos, A. Bonafé, C. Castaño, R. Chapot, D.S. Liebeskind, R.G. Nogueira, M. Arnold, R. Sztajzel, et al. Prospective, multicenter, single-arm study of mechanical thrombectomy using solitaire flow restoration in acute ischemic stroke. *Stroke*, 44(10):2802–2807, 2013.

[144] N. Sanossian, B. Ovbiagele, J.L. Saver, J.R. Alger, S. Starkman, D. Kim, A.G. Ohanian, B.H. Buck, L.K. Ali, G.R. Duckwiler, et al. Leukoaraiosis and collaterals in acute ischemic stroke. *Journal of Neuroimaging*, 21(3):232–235, 2011.

[145] S.A. Sheth, N. Sanossian, Q. Hao, S. Starkman, L.K. Ali, D. Kim, N.R. Gonzalez, S. Tateshima, R. Jahan, G.R. Duckwiler, et al. Collateral flow as causative of good outcomes in endovascular stroke therapy. *Journal of neurointerventional surgery*, 8(1):2–7, 2016.

[146] Z.-S. Shi, D.S. Liebeskind, Y. Loh, J.L. Saver, S. Starkman, P.M. Vespa, N.R. Gonzalez, S. Tateshima, R. Jahan, L. Feng, et al. Predictors of subarachnoid hemorrhage in acute ischemic stroke with endovascular therapy. *Stroke*, 41(12):2775–2781, 2010.

[147] O.C. Singer, J. Berkefeld, C.H. Nolte, G. Bohner, A. Reich, M. Wiesmann, K. Groeschel, S. Boor, T. Neumann-Haefelin, E. Hofmann, et al. Collateral vessels in proximal middle cerebral artery occlusion: the endostroke study. *Radiology*, 274(3):851–858, 2014.

[148] A. Spiessberger, C. Federau, R. Guggenberger, and S. Kollias. Influence of leptomeningeal collateral pattern on the prognostic value of mismatch in acute anterior circulation stroke. *Journal of computer assisted tomography*, 39(2):213–216, 2015.

[149] R.K. Verma, J. Gralla, P.P. Klinger-Gratz, A. Schankath, S. Jung, P. Mordasini, C. Zubler, M. Arnold, M. Buehlmann, M.F. Lang, et al. Infarction distribution pattern in acute stroke may predict the extent of leptomeningeal collaterals. *PloS one*, 10(9):e0137292, 2015.

[150] W.-l. Wen, Y.-b. Fang, P.-f. Yang, Y.-w. Zhang, Y.-n. Wu, H. Shen, J.-j. Ge, Y. Xu, B. Hong, Q.-h. Huang, et al. Parametric digital subtraction angiography imaging for the objective grading of collateral flow in acute middle cerebral artery occlusion. *World neurosurgery*, 88:119–125, 2016.

[151] S. Mangiafico, A. Consoli, L. Renieri, A. Rosi, A. De Renzis, C. Vignoli, and L. Capaccioli. Semi-quantitative and qualitative evaluation of pial leptomeningeal collateral circulation in acute ischemic stroke of the anterior circulation: the careggi collateral score. *Italian Journal of anatomy and embriology*, 118(3), 2013.

[152] S. Mangiafico, V. Saia, P. Nencini, I. Romani, V. Palumbo, G. Pracucci, A. Consoli, A. Rosi, L. Renieri, S. Nappini, et al. Effect of the interaction between recanalization and collateral circulation on functional outcome in acute ischaemic stroke. *Interventional Neuroradiology*, 20(6):704–714, 2014.

[153] G.A. Christoforidis, A.P. Slivka, C. Karakasis, Y. Mohammad, B. Avutu, M. Yang, E.C. Bourekas, D.W. Chakeres, H.W. Slone, and W.T. Yuk. Hemorrhage rates and outcomes when using up to 100 mg intra-arterial t-pa for thrombolysis in acute ischemic stroke. *Interventional Neuroradiology*, 16(3):297–305, 2010.

[154] R. Khatri, G.J. Rodriguez, M.F.K. Suri, G. Vazquez, and M.A. Ezzeddine. Leptomeningeal collateral response and computed tomographic perfusion mismatch in acute middle cerebral artery occlusion. *Journal of vascular and interventional neurology*, 4(1):1, 2011.

[155] M.A. Lazzaro, M. Chen, G.A. Christoforidis, and Y. Mohammad. The impact of diabetes on the extent of pial collaterals in acute ischemic stroke patients. *Journal of neurointerventional surgery*, 3(3):242–245, 2011.

[156] M. Ribo, A. Flores, M. Rubiera, J. Pagola, J. Sargento-Freitas, D. Rodriguez-Luna, P. Coscojuela, O. Maisterra, S. Piñeiro, F.J. Romero, et al. Extending the time window for endovascular procedures according to collateral pial circulation. *Stroke*, 42(12):3465–3469, 2011.

[157] J. Sargento-Freitas, J. Pagola, M. Rubiera, A. Flores, F. Silva, D. Rodriguez-Luna, S. Pineiro, J. Alvarez-Sabín, C.A. Molina, and M. Ribo. Preferential effect of premorbid statins on atherothrombotic strokes through collateral circulation enhancement. *European neurology*, 68(3):171–176, 2012.

[158] J. E Cohen, J.M. Gomori, R.R. Leker, S. Moscovici, F. Ramirez-deNoriega, and E. Itshayek. Recanalization with stent-based mechanical thrombectomy in anterior circulation major ischemic stroke. *Journal of Clinical Neuroscience*, 19(1):39–43, 2012.

[159] M. Arnold, A. Slezak, M. El-Koussy, R. Lüdi, O. Findling, M.-L. Mono, M.R. Heldner, U. Fischer, P. Mordasini, G. Schroth, et al. Occlusion location of middle cerebral artery stroke and outcome after endovascular treatment. *European neurology*, 74(5-6):315–321, 2015.

[160] P.P. Gratz, S. Jung, G. Schroth, J. Gralla, P. Mordasini, K. Hsieh, M.R. Heldner, H.P. Mattle, M.-L. Mono, U. Fischer, et al. Outcome of standard and high-risk patients with acute anterior circulation stroke after stent retriever thrombectomy. *Stroke*, 45(1):152–158, 2014.

[161] F. Drewer-Gutland, A. Kemmling, S. Ligges, M. Ritter, R. Dziewas, E.B. Ringelstein, T.U. Niederstadt, W. Heindel, and V. Heßelmann. Ctp-based tissue outcome: promising tool to prove the beneficial effect of mechanical recanalization in acute ischemic stroke. In *RöFo-Fortschritte auf dem Gebiet der Röntgenstrahlen und der bildgebenden Verfahren*, volume 187, pages 459–466. © Georg Thieme Verlag KG, 2015.

[162] R. Gasparotti, M. Grassi, D. Mardighian, M. Frigerio, M. Pavia, R. Liserre, M. Magoni, L. Mascaro, A. Padovani, and A. Pezzini. Perfusion ct in patients with acute ischemic stroke treated with intra-arterial thrombolysis:

predictive value of infarct core size on clinical outcome. *American journal of Neuroradiology*, 30(4):722–727, 2009.

[163] A.E. Hassan, H. Zacharatos, G.J. Rodriguez, G. Vazquez, J.T. Miley, R.P. Tummala, M.F.K. Suri, R.A. Taylor, and A.I. Qureshi. A comparison of computed tomography perfusion-guided and time-guided endovascular treatments for patients with acute ischemic stroke. *Stroke*, 41(8):1673–1678, 2010.

[164] A.I. Qureshi, M.F.K. Suri, A.L. Georgiadis, G. Vazquez, and N.A. Janjua. Intra-arterial recanalization techniques for patients 80 years or older with acute ischemic stroke: pooled analysis from 4 prospective studies. *American Journal of Neuroradiology*, 30(6):1184–1189, 2009.

[165] A.I. Qureshi, M.H. Qureshi, F. Siddiq, D. Kainth, A.E. Hassan, and A. Maud. Preprocedure change in arterial occlusion in acute ischemic stroke patients undergoing endovascular treatment by computed tomographic angiography. *The American journal of emergency medicine*, 33(5):631–634, 2015.

[166] Q. Shao, L. Zhu, T. Li, Z. Wang, L. Li, W. Bai, and Y. He. Management of tandem internal carotid and middle cerebral arterial occlusions with endovascular multimodal reperfusion therapy. *International Journal of Neuroscience*, 126(12):1077–1083, 2016.

[167] A.T. Rai, Y. Jhadhav, J. Domico, and G.R. Hobbs. Procedural predictors of outcome in patients undergoing endovascular therapy for acute ischemic stroke. *Cardiovascular and interventional radiology*, 35(6):1332–1339, 2012.

[168] J.C. Gerber, M. Petrova, P. Krukowski, M. Kuhn, A. Abramyuk, U. Bodechtel, I. Dzialowski, K. Engellandt, H. Kitzler, L.-P. Pallesen, et al. Collateral state and the effect of endovascular reperfusion therapy on clinical outcome in ischemic stroke patients. *Brain and behavior*, 6(9), 2016.

[169] A. Kheradmand, M. Fisher, and D. Paydarfar. Ischemic stroke in evolution: predictive value of perfusion computed tomography. *Journal of Stroke and Cerebrovascular Diseases*, 23(5):836–843, 2014.

[170] S. Sundaram, S. Kannoth, B. Thomas, P.S. Sarma, and P.N. Sylaja. Collateral assessment by ct angiography as a predictor of outcome in symptomatic cervical internal carotid artery occlusion. *American Journal of Neuroradiology*, 38(1):52–57, 2017.

[171] A.M.J. Frölich, S.L. Wolff, M.N. Psychogios, E. Klotz, R. Schramm, K. Wasser, M. Knauth, and P. Schramm. Time-resolved assessment of collateral flow using 4d ct angiography in large-vessel occlusion stroke. *European radiology*, 24(2):390, 2014.

[172] A.S. Gersing, B.J. Schwaiger, J.F. Kleine, J. Kaesmacher, S. Wunderlich, B. Friedrich, S. Prothmann, C. Zimmer, and T. Boeckh-Behrens. Clinical outcome predicted by collaterals depends on technical success of mechanical thrombectomy in middle cerebral artery occlusion. *Journal of Stroke and Cerebrovascular Diseases*, 26(4):801 – 808, 2017.

[173] H. Rusanen, J.T. Saarinen, and N. Sillanpää. The association of blood pressure and collateral circulation in hyperacute ischemic stroke patients treated with intravenous thrombolysis. *Cerebrovascular Diseases*, 39(2):130–137, 2015.

[174] H. Rusanen, J.T. Saarinen, and N. Sillanpää. Collateral circulation predicts the size of the infarct core and the proportion of salvageable penumbra in hyperacute ischemic stroke patients treated with intravenous thrombolysis. *Cerebrovascular Diseases*, 40(3-4):182–190, 2015.

[175] J.T. Saarinen, H. Rusanen, and N. Sillanpää. Collateral score complements clot location in predicting the outcome of intravenous thrombolysis. *American Journal of Neuroradiology*, 35(10):1892–1896, 2014.

[176] S. Zhang, W. Chen, H. Tang, Q. Han, S. Yan, X. Zhang, Q. Chen, M. Parsons, S. Wang, and M. Lou. The prognostic value of a four-dimensional ct angiography-based collateral grading scale for reperfusion therapy in acute ischemic stroke patients. *PloS one*, 11(8):e0160502, 2016.

[177] G. Mair, R. von Kummer, A. Adami, P.M. White, M.E. Adams, B. Yan, A.M. Demchuk, A.J. Farrall, R.J. Sellar, R. Ramaswamy, et al. Observer reliability

of ct angiography in the assessment of acute ischaemic stroke: data from the third international stroke trial. *Neuroradiology*, 57(1):1–9, 2015.

[178] G. Mair, R. von Kummer, A. Adami, P.M. White, M.E. Adams, B. Yan, A.M. Demchuk, A.J. Farrall, R.J. Sellar, E. Sakka, et al. Arterial obstruction on computed tomographic or magnetic resonance angiography and response to intravenous thrombolytics in ischemic stroke. *Stroke*, 48(2):353–360, 2017.

[179] E. Seyman, H. Shaim, S. Shenhar-Tsarfaty, T. Jonash-Kimchi, N.M. Bornstein, and H. Hallevi. The collateral circulation determines cortical infarct volume in anterior circulation ischemic stroke. *BMC neurology*, 16(1):206, 2016.

[180] W. Cao, B.C.V. Campbell, Q. Dong, S.M. Davis, and B. Yan. Relative filling time delay based on ct perfusion source imaging: a simple method to predict outcome in acute ischemic stroke. *American Journal of Neuroradiology*, 35(9):1683–1687, 2014.

[181] B.K. Menon, B. O'brien, A. Bivard, N.J. Spratt, A.M. Demchuk, F. Miteff, X. Lu, C. Levi, and M.W. Parsons. Assessment of leptomeningeal collaterals using dynamic ct angiography in patients with acute ischemic stroke. *Journal of Cerebral Blood Flow & Metabolism*, 33(3):365–371, 2013.

[182] E.J. Smit, E.-J. Vonken, T. van Seeters, J.W. Dankbaar, I.C. van der Schaaf, L. J. Kappelle, B. van Ginneken, B.K. Velthuis, and M. Prokop. Timing-invariant imaging of collateral vessels in acute ischemic stroke. *Stroke*, 44(8):2194–2199, 2013.

[183] H.H. Karadeli, D.-V. Giurgiutiu, L. Cloonan, K. Fitzpatrick, A. Kanakis, M.E. Ozcan, L.H. Schwamm, and N.S. Rost. Flair vascular hyperintensity is a surrogate of collateral flow and leukoaraiosis in patients with acute stroke due to proximal artery occlusion. *Journal of Neuroimaging*, 26(2):219–223, 2016.

[184] I.R. Van Den Wijngaard, J. Boiten, G. Holswilder, A. Algra, D.W.J. Dippel, B.K. Velthuis, M.J.H. Wermer, and M.A.A. van Walderveen. Impact of collateral status evaluated by dynamic computed tomographic angiography on

clinical outcome in patients with ischemic stroke. *Stroke*, pages STROKEAHA–115, 2015.

[185] I.R. Van Den Wijngaard, G. Holswilder, M.J.H. Wermer, J. Boiten, A. Algra, D.W.J. Dippel, J.W. Dankbaar, B.K. Velthuis, A.M.M. Boers, C.B.L.M. Majoie, et al. Assessment of collateral status by dynamic ct angiography in acute mca stroke: timing of acquisition and relationship with final infarct volume. *American Journal of Neuroradiology*, 37(7):1231–1236, 2016.

[186] I.R. Van Den Wijngaard, M.J.H. Wermer, J. Boiten, A. Algra, G. Holswilder, F.J.A. Meijer, D.W.J. Dippel, B.K. Velthuis, C.B.L.M. Majoie, and M.A.A. Van Walderveen. Cortical venous filling on dynamic computed tomographic angiography. *Stroke*, 47(3):762–767, 2016.

[187] S.F. Ali, K. Siddiqui, H. Ay, S. Silverman, A. Singhal, A. Viswanathan, N. Rost, M. Lev, and L.H. Schwamm. Baseline predictors of poor outcome in patients too good to treat with intravenous thrombolysis. *Stroke*, 47(12):2986–2992, 2016.

[188] J. Pfaff, C. Herweh, M. Pham, S. Schönenberger, S. Nagel, P.A. Ringleb, M. Bendszus, and M. Möhlenbruch. Mechanical thrombectomy in patients with acute ischemic stroke and lower nihss scores: recanalization rates, periprocedural complications, and clinical outcome. *American Journal of Neuroradiology*, 37(11):2066–2071, 2016.

[189] S.E. Beyer, L. Von Baumgarten, K.M. Thierfelder, M. Rottenkolber, H. Janssen, M. Dichgans, T.R.C. Johnson, A. Straube, B. Ertl-Wagner, M.F. Reiser, et al. Predictive value of the velocity of collateral filling in patients with acute ischemic stroke. *Journal of Cerebral Blood Flow & Metabolism*, 35(2):206–212, 2015.

[190] K.M. Thierfelder, W.H. Sommer, B. Ertl-Wagner, S.E. Beyer, F.G. Meinel, W.G. Kunz, G. Buchholz, M.F. Reiser, and H. Janssen. Prediction of stent-retriever thrombectomy outcomes by dynamic multidetector ct angiography in patients with acute carotid t or mca occlusions. *American Journal of Neuroradiology*, 37(7):1296–1302, 2016.

[191] S. Bhaskar, A. Bivard, M. Parsons, M. Nilsson, J.R. Attia, P. Stanwell, and C. Levi. Delay of late-venous phase cortical vein filling in acute ischemic stroke patients: Associations with collateral status. *Journal of Cerebral Blood Flow & Metabolism*, 37(2):671–682, 2017.

[192] S. Bhaskar, A. Bivard, P. Stanwell, M. Parsons, J.R. Attia, M. Nilsson, and C. Levi. Baseline collateral status and infarct topography in post-ischaemic perilesional hyperperfusion: An arterial spin labelling study. *Journal of Cerebral Blood Flow & Metabolism*, 37(3):1148–1162, 2017.

[193] R. Parthasarathy, S.-II Sohn, T. Jeerakathil, M.P. Kate, S.M. Mishra, V.K. Nambiar, A. Ahmad, B.K. Menon, and A. Shuaib. A combined arterial and venous grading scale to predict outcome in anterior circulation ischemic stroke. *Journal of Neuroimaging*, 25(6):969–977, 2015.

[194] C. Doucet, F. Roncarolo, D. Tampieri, and M. del Pilar Cortes. Paradoxically decreased mean transit time in patients presenting with acute stroke. *Journal of computer assisted tomography*, 40(3):409–412, 2016.

[195] E.Y. Kim, D.H. Shin, Y. Noh, B.H. Goh, and Y.-B. Lee. Comparison of imaging selection criteria for intra-arterial thrombectomy in acute ischemic stroke with advanced ct. *European radiology*, 26(9):2974–2981, 2016.

[196] K.W. Muir, G.A. Ford, C.-M. Messow, I. Ford, A. Murray, A. Clifton, M.M. Brown, J. Madigan, R. Lenthall, F. Robertson, et al. Endovascular therapy for acute ischaemic stroke: the pragmatic ischaemic stroke thrombectomy evaluation (piste) randomised, controlled trial. *J Neurol Neurosurg Psychiatry*, pages jnnp–2016, 2016.

[197] H. Kawano, A. Bivard, L. Lin, N.J. Spratt, F. Miteff, M.W. Parsons, and C.R. Levi. Relationship between collateral status, contrast transit, and contrast density in acute ischemic stroke. *Stroke*, 47(3):742–749, 2016.

[198] S. Agarwal, D.J. Scoffings, P.S. Jones, S.T. Marrapu, P.J. Barry, E.W. O'brien, J.-C. Baron, and E.A. Warburton. Interaction of age with the ischaemic penumbra, leptomeningeal collateral circulation and haemodynamic variables

in acute stroke: a pilot study. *J Neurol Neurosurg Psychiatry*, 84(3):271–276, 2013.

[199] E.M. Arsava, A. Vural, E. Akpinar, R. Gocmen, S. Akcalar, K.K. Oguz, and M.A. Topcuoglu. The detrimental effect of aging on leptomeningeal collaterals in ischemic stroke. *Journal of Stroke and Cerebrovascular Diseases*, 23(3):421–426, 2014.

[200] S.E. Beyer, K.M. Thierfelder, L. Von Baumgarten, M. Rottenkolber, F.G. Meinel, H. Janssen, B. Ertl-Wagner, M.F. Reiser, and W.H. Sommer. Strategies of collateral blood flow assessment in ischemic stroke: prediction of the follow-up infarct volume in conventional and dynamic cta. *American Journal of Neuroradiology*, 36(3):488–494, 2015.

[201] M. M Higazi and E.A. Abdel-Gawad. Ct angiography collateral scoring: Correlation with dwi infarct size in proximal middle cerebral artery occlusion stroke within 12h onset. *The Egyptian Journal of Radiology and Nuclear Medicine*, 47(3):991–997, 2016.

[202] S. Kamalian, A. Kemmling, R.C. Borgie, L.T. Morais, S. Payabvash, A.M. Franceschi, S. Kamalian, A.J. Yoo, K.L. Furie, and M.H. Lev. Admission insular infarction> 25% is the strongest predictor of large mismatch loss in proximal middle cerebral artery stroke. *Stroke*, 44(11):3084–3089, 2013.

[203] J. H. Lee, Y. J. Kim, J. W. Choi, H. G. Roh, Y. I. Chun, H.-J. Cho, and H. Y. Kim. Multimodal ct: favorable outcome factors in acute middle cerebral artery stroke with large artery occlusion. *European neurology*, 69(6):366–374, 2013.

[204] F.O. Lima, K.L. Furie, G.S. Silva, M.H. Lev, É.C.S. Camargo, A.B. Singhal, G.J. Harris, E.F. Halpern, W.J. Koroshetz, W.S. Smith, et al. Prognosis of untreated strokes due to anterior circulation proximal intracranial arterial occlusions detected by use of computed tomography angiography. *JAMA neurology*, 71(2):151–157, 2014.

[205] N. Malik, Q. Hou, A. Vagal, J. Patrie, W. Xin, P. Michel, A. Eskandari, T. Jovin, and M. Wintermark. Demographic and clinical predictors of leptomeningeal collaterals in stroke patients. *Journal of Stroke and Cerebrovascular Diseases*, 23(8):2018–2022, 2014.

[206] O. Volny, P. Cimflova, and R. Mikulik. Ipsilateral sinus hypoplasia and poor leptomeningeal collaterals as midline shift predictors. *Journal of Stroke and Cerebrovascular Diseases*, 25(7):1792–1796, 2016.

[207] L.L.L. Yeo, P. Paliwal, H.L. Teoh, R.C. Seet, B.P. Chan, E. Ting, N. Venketasubramanian, W.K. Leow, B. Wakerley, Y. Kusama, et al. Assessment of intracranial collaterals on ct angiography in anterior circulation acute ischemic stroke. *American Journal of Neuroradiology*, 36(2):289–294, 2015.

[208] L.L.L. Yeo, W.Y. Kong, P. Paliwal, H.L. Teoh, R.C. Seet, D. Soon, R. Rathakrishnan, V. Ong, T.-H. Lee, H.-F. Wong, et al. Intravenous thrombolysis for acute ischemic stroke due to cervical internal carotid artery occlusion. *Journal of Stroke and Cerebrovascular Diseases*, 25(10):2423–2429, 2016.

[209] P. Yeo, L.L.L .and Paliwal, A.F. Low, E.L.W. Tay, A. Gopinathan, M. Nadarajah, E. Ting, N. Venketasubramanian, R.C.S. Seet, A. Ahmad, et al. How temporal evolution of intracranial collaterals in acute stroke affects clinical outcomes. *Neurology*, 86(5):434–441, 2016.

[210] B.K. Menon, E.E. Smith, S.B. Coutts, D.G. Welsh, J.E. Faber, M. Goyal, M.D. Hill, A.M. Demchuk, Z. Damani, K.-H. Cho, et al. Leptomeningeal collaterals are associated with modifiable metabolic risk factors. *Annals of neurology*, 74(2):241–248, 2013.

[211] V. Nambiar, S.I. Sohn, M.A. Almekhlafi, H.W. Chang, S. Mishra, E. Qazi, M. Eesa, A.M. Demchuk, M. Goyal, M.D. Hill, et al. Cta collateral status and response to recanalization in patients with acute ischemic stroke. *American Journal of Neuroradiology*, 35(5):884–890, 2014.

[212] E.M. Qazi, S.I. Sohn, S. Mishra, M.A. Almekhlafi, M. Eesa, C. D d'Esterre, A.A. Qazi, J. Puig, M. Goyal, A.M. Demchuk, et al. Thrombus characteristics

are related to collaterals and angioarchitecture in acute stroke. *Canadian Journal of Neurological Sciences*, 42(6):381–388, 2015.

[213] B.Y.-Q. Tan, W.-Y. Kong, J.N. Ngiam, H.-L. Teoh, V.K. Sharma, and L.L.-L. Yeo. The role of topographic collaterals in predicting functional outcome after thrombolysis in anterior circulation ischemic stroke. *Journal of Neuroimaging*, 27(2):217–220, 2017.

[214] L. von Baumgarten, K.M. Thierfelder, S.E. Beyer, A.B. Baumann, C. Bollwein, H. Janssen, M.F. Reiser, A. Straube, and W.H. Sommer. Early ct perfusion mismatch in acute stroke is not time-dependent but relies on collateralization grade. *Neuroradiology*, 58(4):357–365, 2016.

[215] A. Vagal, B.K. Menon, L.D. Foster, A. Livorine, S.D. Yeatts, E. Qazi, C. d'Esterre, J. Shi, A.M. Demchuk, M.D. Hill, et al. Association between ct angiogram collaterals and ct perfusion in the interventional management of stroke iii trial. *Stroke*, 47(2):535–538, 2015.

[216] A. García-Tornel, V. Carvalho, S. Boned, A. Flores, D. Rodríguez-Luna, J. Pagola, M. Muchada, E. Sanjuan, P. Coscojuela, J. Juega, et al. Improving the evaluation of collateral circulation by multiphase computed tomography angiography in acute stroke patients treated with endovascular reperfusion therapies. *Interventional neurology*, 5(3-4):209–217, 2016.

[217] F. Seker, A. Potreck, M. Möhlenbruch, M. Bendszus, and M. Pham. Comparison of four different collateral scores in acute ischemic stroke by ct angiography. *Journal of neurointerventional surgery*, 8(11):1116–1118, 2016.

[218] H. Nordmeyer, N. Webering, R. Chapot, J. Hadisurya, M. Heddier, P. Stracke, K. Berger, S. Isenmann, and R. Weber. The association between collateral status, recanalization and long term outcome in stroke patients treated with stent retrievers–are there indications not to perform thrombectomy based on ct angiography? *Journal of Neuroradiology*, 44(3):217–222, 2017.

[219] R. Parthasarathy, M. Kate, J.L. Rempel, D.S. Liebeskind, T. Jeerakathil, K.S. Butcher, and A. Shuaib. Prognostic evaluation based on cortical vein

score difference in stroke. *stroke*, 44(10):2748–2754, 2013.

[220] H. Zareie, D.A. Quain, M. Parsons, K.J. Inder, P. McElduff, F. Miteff, N.J. Spratt, and C. Levi. The influence of anterior cerebral artery flow diversion measured by transcranial doppler on acute infarct volume and clinical outcome in anterior circulation stroke. *International Journal of Stroke*, 8(4):228–234, 2013.

[221] S. Seeta Ramaiah, L. Churilov, P. Mitchell, R. Dowling, and B. Yan. The impact of arterial collateralization on outcome after intra-arterial therapy for acute ischemic stroke. *American Journal of Neuroradiology*, 35(4):667–672, 2014.

[222] I.N. Kaschka, S.P. Kloska, T. Struffert, T. Engelhorn, P. Gölitz, N. Kurka, M. Köhrmann, S. Schwab, and A. Doerfler. Clot burden and collaterals in anterior circulation stroke: differences between single-phase cta and multiphase 4d-cta. *Clinical neuroradiology*, 26(3):309–315, 2016.

[223] V. Rohan, J. Baxa, R. Tupy, L. Cerna, P. Sevcik, M. Friesl, J. Polivka, and J. Ferda. Length of occlusion predicts recanalization and outcome after intravenous thrombolysis in middle cerebral artery stroke. *Stroke*, 45(7):2010–2017, 2014.

[224] L. Elijovich, N. Goyal, S. Mainali, D. Hoit, A.S. Arthur, M. Whitehead, and A.F. Choudhri. Cta collateral score predicts infarct volume and clinical outcome after endovascular therapy for acute ischemic stroke: a retrospective chart review. *Journal of neurointerventional surgery*, pages neurintsurg–2015, 2015.

[225] N. Sillanpää, J.T. Saarinen, and H. Rusanen. Computed tomography angiography source images closely reflect the integrity of collateral circulation. *Journal of Neuroradiology*, 42(5):261–268, 2015.

[226] V.M. Timpone, M.H. Lev, S. Kamalian, L.T. Morais, A.M. Franceschi, L. Souza, and P.W. Schaefer. Percentage insula ribbon infarction of> 50%

identifies patients likely to have poor clinical outcome despite small dwi infarct volume. *American Journal of Neuroradiology*, 36(1):40–45, 2015.

[227] S. Agarwal, T. Matys, S.T. Marrapu, D.J. Scoffings, J. Mitchell, P.S. Jones, J.-C. Baron, and E.A. Warburton. Is ct-based perfusion and collateral imaging sensitive to time since stroke onset? *Frontiers in neurology*, 6, 2015.

[228] A. Angermaier, S. Langner, M. Kirsch, C. Kessler, N. Hosten, and A.V. Khaw. Ct-angiographic collateralization predicts final infarct volume after intra-arterial thrombolysis for acute anterior circulation ischemic stroke. *Cerebrovascular Diseases*, 31(2):177–184, 2011.

[229] A. Angermaier, P. Michel, A.V. Khaw, M. Kirsch, C. Kessler, and S. Langner. Intravenous thrombolysis and passes of thrombectomy as predictors for endovascular revascularization in ischemic stroke. *Journal of Stroke and Cerebrovascular Diseases*, 25(10):2488–2495, 2016.

[230] J. Aoki, Y. Tateishi, C.L. Cummings, E. Cheng-Ching, P. Ruggieri, M.S. Hussain, and K. Uchino. Collateral flow and brain changes on computed tomography angiography predict infarct volume on early diffusion-weighted imaging. *Journal of Stroke and Cerebrovascular Diseases*, 23(10):2845–2850, 2014.

[231] O.A. Berkhemer, I.G.H. Jansen, D. Beumer, P.S.S. Fransen, L.A. Van Den Berg, A.J. Yoo, H.F. Lingsma, M.E.S. Sprengers, S.F.M. Jenniskens, G.J.L. à Nijeholt, et al. Collateral status on baseline computed tomographic angiography and intra-arterial treatment effect in patients with proximal anterior circulation stroke. *Stroke*, 47(3):768–776, 2016.

[232] F. Brunner, B. Tomandl, K. Hanken, H. Hildebrandt, and A. Kastrup. Impact of collateral circulation on early outcome and risk of hemorrhagic complications after systemic thrombolysis. *International Journal of Stroke*, 9(8):992–998, 2014.

[233] E. Cheng-Ching, J.A. Frontera, S. Man, J. Aoki, Y. Tateishi, F.K. Hui, D. Wisco, P. Ruggieri, M.S. Hussain, and K. Uchino. Degree of collaterals

and not time is the determining factor of core infarct volume within 6 hours of stroke onset. *American Journal of Neuroradiology*, 36(7):1272–1276, 2015.

[234] S. Dehkharghani, R. Bammer, M. Straka, M. Bowen, J.W. Allen, S. Rangaraju, J. Kang, T. Gleason, C. Brasher, and F. Nahab. Performance of ct aspects and collateral score in risk stratification: can target perfusion profiles be predicted without perfusion imaging? *American Journal of Neuroradiology*, 37(8):1399–1404, 2016.

[235] D.W. Dippel, C.B. Majoie, Y.B. Roos, A. van der Lugt, R.J. van Oostenbrugge, W.H. van Zwam, H.F. Lingsma, P.J. Koudstaal, K.M. Treurniet, L.A. Van Den Berg, et al. Influence of device choice on the effect of intra-arterial treatment for acute ischemic stroke in mr clean (multicenter randomized clinical trial of endovascular treatment for acute ischemic stroke in the netherlands). *Stroke*, 47(10):2574–2581, 2016.

[236] A. Eilaghi, J. Brooks, C. d'Esterre, L. Zhang, R.H. Swartz, T.-Y. Lee, and R.I. Aviv. Reperfusion is a stronger predictor of good clinical outcome than recanalization in ischemic stroke. *Radiology*, 269(1):240–248, 2013.

[237] M. Espinosa de Rueda, G. Parrilla, S. Manzano-Fernández, B. García-Villalba, J. Zamarro, F. Hernández-Fernández, C. Sánchez-Vizcaino, E. Carreón, A. Morales, and A. Moreno. Combined multimodal computed tomography score correlates with futile recanalization after thrombectomy in patients with acute stroke. *Stroke*, 46(9):2517–2522, 2015.

[238] E.M. Fanou, J. Knight, R.I. Aviv, S.-P. Hojjat, S.P. Symons, L. Zhang, and M. Wintermark. Effect of collaterals on clinical presentation, baseline imaging, complications, and outcome in acute stroke. *American Journal of Neuroradiology*, 36(12):2285–2291, 2015.

[239] R. Grech, P.L. Galvin, S. Power, A. O'Hare, S. Looby, P. Brennan, and J. Thornton. Outcome prediction in acute stroke patients considered for endovascular treatment: a novel tool. *Interventional Neuroradiology*, 20(3):312–324, 2014.

[240] J. Hom, J.W. Dankbaar, B.P. Soares, T. Schneider, S.-C. Cheng, J. Bredno, B.C. Lau, W. Smith, W.P. Dillon, and M. Wintermark. Blood-brain barrier permeability assessed by perfusion ct predicts symptomatic hemorrhagic transformation and malignant edema in acute ischemic stroke. *American Journal of Neuroradiology*, 32(1):41–48, 2011.

[241] B.N. Huisa, W.P. Neil, R. Schrader, M. Maya, B. Pereira, N.T. Bruce, and P.D. Lyden. Clinical use of computed tomographic perfusion for the diagnosis and prediction of lesion growth in acute ischemic stroke. *Journal of Stroke and Cerebrovascular Diseases*, 23(1):114–122, 2014.

[242] M.M. Kawiorski, A. Vicente, D. Lourido, A. Muriel, E. Fandiño, J.C Méndez, V. Sánchez-González, A. Aguado, R. Álvarez-Velasco, and M.A. de Leciñana. Good clinical and radiological correlation from standard perfusion computed tomography accurately identifies salvageable tissue in ischemic stroke. *Journal of Stroke and Cerebrovascular Diseases*, 25(5):1062–1069, 2016.

[243] J.-T. Kim, M.-S. Park, K.-H. Choi, T.-S. Nam, S.-M. Choi, S.-H. Lee, B.-C. Kim, M.-K. Kim, and K.-H. Cho. The cbv-aspect score as a predictor of fatal stroke in a hyperacute state. *European neurology*, 63(6):357–363, 2010.

[244] H. Kim, S.T. Jin, Y.W. Kim, S.R. Kim, I.S. Park, and K.W. Jo. Predictors of malignant brain edema in middle cerebral artery infarction observed on ct angiography. *Journal of Clinical Neuroscience*, 22(3):554–560, 2015.

[245] K. Lin, W.E. Zink, A.J. Tsiouris, M. John, L. Tekchandani, and P.C. Sanelli. Risk assessment of hemorrhagic transformation of acute middle cerebral artery stroke using multimodal ct. *Journal of Neuroimaging*, 22(2):160–166, 2012.

[246] S. Man, J. Aoki, M.S. Hussain, D. Wisco, Y. Tateishi, G. Toth, F.K. Hui, and K. Uchino. Predictors of infarct growth after endovascular therapy for acute ischemic stroke. *Journal of Stroke and Cerebrovascular Diseases*, 24(2):401–407, 2015.

[247] A.M. Mortimer, D.H. Little, K.S. Minhas, E.R.J. Walton, S.A. Renowden, and M.D. Bradley. Thrombus length estimation in acute ischemic stroke: a potential role for delayed contrast enhanced ct. *Journal of neurointerventional surgery*, pages neurintsurg–2013, 2013.

[248] O. Ozkul-Wermester, E. Guegan-Massardier, A. Triquenot, A. Borden, G. Perot, and E. Gérardin. Increased blood-brain barrier permeability on perfusion computed tomography predicts hemorrhagic transformation in acute ischemic stroke. *European neurology*, 72(1-2):45–53, 2014.

[249] A. Renú, C. Laredo, R. Tudela, X. Urra, A. Lopez-Rueda, L. Llull, L. Oleaga, S. Amaro, and Á. Chamorro. Brain hemorrhage after endovascular reperfusion therapy of ischemic stroke: a threshold-finding whole-brain perfusion ct study. *Journal of Cerebral Blood Flow & Metabolism*, 37(1):153–165, 2017.

[250] B.P. Soares, E. Tong, J. Hom, S.-C. Cheng, J. Bredno, L. Boussel, W.S. Smith, and M. Wintermark. Reperfusion is a more accurate predictor of follow-up infarct volume than recanalization. *Stroke*, 41(1):e34–e40, 2010.

[251] X. Urra, L. San Román, F. Gil, M. Millán, D. Cánovas, J. Roquer, P. Cardona, M. Ribó, J. Martí-Fàbregas, S. Abilleira, et al. Medical and endovascular treatment of patients with large vessel occlusion presenting with mild symptoms: an observational multicenter study. *Cerebrovascular Diseases*, 38(6):418–424, 2014.

[252] T. van Seeters, G.J. Biessels, L.J. Kappelle, I.C. van der Schaaf, J.W. Dankbaar, A.D. Horsch, J.M. Niesten, M.J. Luitse, C.B. Majoie, J.A. Vos, et al. The prognostic value of ct angiography and ct perfusion in acute ischemic stroke. *Cerebrovascular diseases*, 40(5-6):258–269, 2015.

[253] T. van Seeters, G.J. Biessels, L.J. Kappelle, I.C. van der Schaaf, J.W. Dankbaar, A.D. Horsch, J.M. Niesten, M.J.A. Luitse, C.B.L.M. Majoie, J.A. Vos, et al. Ct angiography and ct perfusion improve prediction of infarct volume in patients with anterior circulation stroke. *Neuroradiology*, 58(4):327–337, 2016.

[254] T. van Seeters, G.J. Biessels, L.J. Kappelle, Y. van der Graaf, B.K. Velthuis, et al. Determinants of leptomeningeal collateral flow in stroke patients with a middle cerebral artery occlusion. *Neuroradiology*, 58(10):969–977, 2016.

[255] G. Zhu, P. Michel, A. Aghaebrahim, J.T. Patrie, W. Xin, A. Eskandari, W. Zhang, and M. Wintermark. Computed tomography workup of patients suspected of acute ischemic stroke. *Stroke*, 44(4):1049–1055, 2013.

[256] G. Zhu, P. Michel, A. Aghaebrahim, J.T. Patrie, W. Xin, A. Eskandari, W. Zhang, and M. Wintermark. Prediction of recanalization trumps prediction of tissue fate. *Stroke*, 44(4):1014–1019, 2013.

[257] G. Zhu, P. Michel, T. Jovin, J.T. Patrie, W. Xin, A. Eskandari, W. Zhang, and M. Wintermark. Prediction of recanalization in acute stroke patients receiving intravenous and endovascular revascularization therapy. *International Journal of Stroke*, 10(1):28–36, 2015.

[258] A.J. Yoo, R. Hu, R. Hakimelahi, M.H. Lev, R.G. Nogueira, J.A. Hirsch, R.G. González, and P.W. Schaefer. Ct angiography source images acquired with a fast-acquisition protocol overestimate infarct core on diffusion weighted images in acute ischemic stroke. *Journal of Neuroimaging*, 22(4):329–335, 2011.

[259] S.H. Ahn, C.D. d'Esterre, E.M. Qazi, M. Najm, M. Rubiera, E. Fainardi, M.D. Hill, M. Goyal, A.M. Demchuk, T.Y. Lee, et al. Occult anterograde flow is an under-recognized but crucial predictor of early recanalization with intravenous tissue-type plasminogen activator. *Stroke*, pages STROKEAHA–114, 2015.

[260] R. Blanc, S. Pistocchi, D. Babic, B. Bartolini, M. Obadia, S. Alamowitch, and M. Piotin. Intravenous flat-detector ct angiography in acute ischemic stroke management. *Neuroradiology*, 54(4):383–391, 2012.

[261] E. Cortijo, A.I. Calleja, P. García-Bermejo, P. Mulero, S. Pérez-Fernández, J. Reyes, M. Fe Muñoz, M. Martínez-Galdámez, and J.F. Arenillas. Relative cerebral blood volume as a marker of durable tissue-at-risk viability in hyperacute ischemic stroke. *Stroke*, 45(1):113–118, 2014.

[262] I.N. Kaschka, S.P. Kloska, T. Struffert, T. Engelhorn, P. Gölitz, N. Kurka, M. Köhrmann, S. Schwab, and A. Doerfler. Clinical and radiological outcome after mechanical thrombectomy in acute ischemic stroke: What matters? *The neuroradiology journal*, 29(2):99–105, 2016.

[263] S.-L. Jung, Y.-J. Lee, K.-J. Ahn, Y.-I. Kim, K.-S. Lee, Y.-S. Shin, K.-S. Lee, and B.-S. Kim. Assessment of collateral flow with multi-phasic ct: Correlation with diffusion weighted mri in mca occlusion. *Journal of Neuroimaging*, 21(3):225–228, 2011.

[264] S.-W. Chang, Y.-C. Huang, L.-C. Lin, J.-T. Yang, H.-H. Weng, Y.-H. Tsai, and T.-H. Lee. Effect of dehydration on the development of collaterals in acute middle cerebral artery occlusion. *European journal of neurology*, 23(3):494–500, 2016.

[265] Z.-H. Cho, Y.-B. Lee, C.-K. Kang, J.-W. Yang, I.-H. Jung, C.-A. Park, C.-W. Park, and Y.-B. Kim. Microvascular imaging of asymptomatic mca steno-occlusive patients using ultra-high-field 7t mri. *Journal of neurology*, 260(1):144–150, 2013.

[266] S. Ruland, A. Ahmed, K. Thomas, M. Zhao, S. Amin-Hanjani, X. Du, and F.T. Charbel. Leptomeningeal collateral volume flow assessed by quantitative magnetic resonance angiography in large-vessel cerebrovascular disease. *Journal of Neuroimaging*, 19(1):27–30, 2009.

[267] D. Hong, H.S. Seo, Y.H. Lee, K.J. Kim, S.-il Suh, and J.-M. Jung. Leptomeningeal enhancement on magnetic resonance imaging as a predictor of hemodynamic insufficiency. *Journal of computer assisted tomography*, 39(3):307–312, 2015.

[268] A. Förster, H. Wenz, H.U. Kerl, M. Al-Zghloul, S. Habich, and C. Groden. Flair vascular hyperintensities and dynamic 4d angiograms for the estimation of collateral blood flow in posterior circulation occlusion. *Neuroradiology*, 56(9):697–707, 2014.

[269] A. Förster, B. Mürle, H.U. Kerl, H. Wenz, M. Al-Zghloul, S. Habich, and C. Groden. Sparing of the hippocampus indicates better collateral blood flow in acute posterior cerebral artery occlusion. *International Journal of Stroke*, 10(8):1287–1293, 2015.

[270] B.C.V. Campbell, S. Christensen, B.M. Tress, L. Churilov, P.M. Desmond, M.W. Parsons, P.A. Barber, C.R. Levi, C. Bladin, G.A. Donnan, et al. Failure of collateral blood flow is associated with infarct growth in ischemic stroke. *Journal of Cerebral Blood Flow & Metabolism*, 33(8):1168–1172, 2013.

[271] A. Wouters, P. Dupont, S. Christensen, B. Norrving, R. Laage, G. Thomalla, G. Albers, V. Thijs, and R. Lemmens. Association between time from stroke onset and fluid-attenuated inversion recovery lesion intensity is modified by status of collateral circulation. *Stroke*, 47(4):1018–1022, 2016.

[272] F. Nicoli, P.L. de Micheaux, and N. Girard. Perfusion-weighted imaging–derived collateral flow index is a predictor of mca m1 recanalization after iv thrombolysis. *American Journal of Neuroradiology*, 34(1):107–114, 2013.

[273] D.C. Haussen, S. Koch, E. Saraf-Lavi, T. Shang, S. Dharmadhikari, and D.R. Yavagal. Flair distal hyperintense vessels as a marker of perfusion-diffusion mismatch in acute stroke. *Journal of Neuroimaging*, 23(3):397–400, 2013.

[274] K. Villringer, R. Serrano-Sandoval, U. Grittner, I. Galinovic, A. Schneider, A.-C. Ostwaldt, P. Brunecker, A. Rocco, and J.B. Fiebach. Subtracted dynamic MR perfusion source images (sMRP-SI) provide collateral blood flow assessment in MCA occlusions and predict tissue fate. *European radiology*, 26(5):1396, 2016.

[275] K.Y. Lee, L.L. Latour, M. Luby, A.W. Hsia, J.G. Merino, and S. Warach. Distal hyperintense vessels on flair an mri marker for collateral circulation in acute stroke? *Neurology*, 72(13):1134–1139, 2009.

[276] M. Gawlitza, J. Böhme, M. Maros, D. Lobsien, D. Michalski, C. Groden, K.-T. Hoffmann, and A. Förster. Flair vascular hyperintensities and 4d mr

angiograms for the estimation of collateral blood flow in anterior cerebral artery ischemia. *PloS one*, 12(2):e0172570, 2017.

[277] M. Gawlitza, J. Gragert, U. Quäschling, and K.T. Hoffmann. Flair-hyperintense vessel sign, diffusion-perfusion mismatch and infarct growth in acute ischemic stroke without vascular recanalisation therapy. *Journal of Neuroradiology*, 41(4):227–233, 2014.

[278] I. Mourand, D. Milhaud, C. Arquizan, K. Lobotesis, R. Schaub, P. Machi, X. Ayrignac, O.F. Eker, A. Bonafé, and V. Costalat. Favorable bridging therapy based on dwi-flair mismatch in patients with unclear-onset stroke. *American Journal of Neuroradiology*, 37(1):88–93, 2016.

[279] M. Hernández-Pérez, J. Puig, G. Blasco, N.P. de la Ossa, L. Dorado, A. Dávalos, and J. Munuera. Dynamic magnetic resonance angiography provides collateral circulation and hemodynamic information in acute ischemic stroke. *Stroke*, pages STROKEAHA–115, 2015.

[280] M. Ichijo, K. Miki, S. Ishibashi, M. Tomita, T. Kamata, H. Fujigasaki, and H. Mizusawa. Posterior cerebral artery laterality on magnetic resonance angiography predicts long-term functional outcome in middle cerebral artery occlusion. *Stroke*, 44(2):512–515, 2013.

[281] J.P. Son, M.J. Lee, S.J. Kim, J.-W. Chung, J. Cha, G.-M. Kim, C.-S. Chung, K.H. Lee, and O.Y. Bang. Impact of slow blood filling via collaterals on infarct growth: Comparison of mismatch and collateral status. *Journal of stroke*, 19(1):88, 2017.

[282] X. Lou, S. Yu, F. Scalzo, S. Starkman, L.K. Ali, D. Kim, N.M. Rao, J.D. Hinman, P.M. Vespa, R. Jahan, et al. Multi-delay asl can identify leptomeningeal collateral perfusion in endovascular therapy of ischemic stroke. *Oncotarget*, 8(2):2437, 2017.

[283] C.J. Maurer, K. Egger, A.-K. Dempfle, M. Reinhard, S. Meckel, and H. Urbach. Facing the time window in acute ischemic stroke: the infarct core. *Clinical neuroradiology*, 26(2):153–158, 2016.

[284] S. Olindo, N. Chausson, J. Joux, M. Saint-Vil, A. Signate, M. Edimonana-Kaptue, S. Jeannin, M. Mejdoubi, M. Aveillan, P. Cabre, et al. Fluid-attenuated inversion recovery vascular hyperintensity: an early predictor of clinical outcome in proximal middle cerebral artery occlusion. *Archives of neurology*, 69(11):1462–1468, 2012.

[285] X.-E. Wei, J. Zhou, W.-B. Li, Y.-W. Zhao, M.-H. Li, and Y.-H. Li. Mri based thrombolysis for flair-negative stroke patients within 4.5–6h after symptom onset. *Journal of the neurological sciences*, 372:421–427, 2017.

[286] N. Yamamoto, J. Satomi, Y. Izumi, Y. Yamamoto, I. Yamaguchi, T. Furukawa, S. Nagahiro, and R. Kaji. Predictors of a favorable outcome after recanalization in patients with cerebral major vessel occlusion. *Journal of Stroke and Cerebrovascular Diseases*, 24(12):2793–2799, 2015.

[287] M. Goyal, B.K. Menon, and C.P. Derdeyn. Perfusion imaging in acute ischemic stroke: let us improve the science before changing clinical practice. *Radiology*, 266(1):16–21, 2013.

[288] O. Y. Bang, M. Goyal, and D. S. Liebeskind. Collateral circulation in ischemic stroke. *Stroke*, 46(11):3302–3309, 2015.

[289] J.M. Wardlaw, K.W. Muir, M.-J. Macleod, C. Weir, F. McVerry, T. Carpenter, K. Shuler, et al. Clinical relevance and practical implications of trials of perfusion and angiographic imaging in patients with acute ischaemic stroke: a multicentre cohort imaging study. *J Neurol Neurosurg Psychiatry*, pages jnnp–2012, 2013.

[290] N.J.J. MacDougall, F. McVerry, X. Huang, A. Welch, R. Fulton, and K.W. Muir. Post-stroke hyperglycaemia is associated with adverse evolution of acute ischaemic injury. In *Cerebrovascular diseases*, volume 37, pages 267–267. KARGER ALLSCHWILERSTRASSE 10, CH-4009 BASEL, SWITZERLAND, 2014.

[291] X. Huang, B.K. Cheripelli, S.M. Lloyd, D. Kalladka, F.C. Moreton, A. Siddiqui, I. Ford, and K.W. Muir. Alteplase versus tenecteplase for thrombolysis

after ischaemic stroke (attest): a phase 2, randomised, open-label, blinded endpoint study. *The Lancet Neurology*, 14(4):368–376, 2015.

[292] Apollo Medical Imaging Technology Pty Ltd. Mistar, 2001. https://www.apollomit.com/index.html (accessed September 30, 2019).

[293] A. Fedorov, R. Beichel, J. Kalpathy-Cramer, J. Finet, J.-C. Fillion-Robin, S. Pujol, C. Bauer, D. Jennings, F. Fennessy, M. Sonka, et al. 3d slicer as an image computing platform for the quantitative imaging network. *Magnetic resonance imaging*, 30(9):1323–1341, 2012.

[294] M. Parsons, N. Spratt, A. Bivard, B. Campbell, K. Chung, F. Miteff, B. O'Brien, C. Bladin, P. McElduff, C. Allen, et al. A randomized trial of tenecteplase versus alteplase for acute ischemic stroke. *New England Journal of Medicine*, 366(12):1099–1107, 2012.

[295] F. McVerry. Multimodal CT imaging in acute ischemic stroke, 2014.